Development of Advanced Water Treatment Technology Using Microbubbles

October 2006

Pan Li

Abstract

Microbubbles with diameters on the order of 10 μm have their unique characteristics which are often called size effect. Their amazing effectiveness for closed-water purification pushes them into limelight in the field of water treatment. However, except for the several successful cases, there is few fundamental and specific research data reported. Moreover, the present microbubble generation methods all have their own merits and demerits and they need to be improved to meet the requirement for water treatment. In this study, the author firstly evaluates the characteristics of a newly-developed microbubble generator, and then makes some attempts to improve its microbubble generation efficiency. The improved microbubble generation system is then introduced to the advanced water treatment processes and examined for the effectiveness. The applications to advanced water treatment studied in the present research include air flotation and ozone oxidation.

Air flotation is widely used as an alternative to sedimentation in the field of water treatment to remove algae from nutrient-rich stored water or to treat low turbidity, high colored water at low temperature. The most popular type of air flotation, Dissolved air flotation (DAF), has its inherent disadvantages, such as high electrical power requirement, complex system and higher service cost. The author tried three different microbubble generation methods to develop an efficient Induce Air Flotation (IAF) system. Kaolin suspension with low concentration was used as the model water. The best performance occurred in the improved method where gas and water were simultaneously induced and mixed by the pump, and dispersed through the rotating-flow microbubble generator.

Ozone is a popular oxidant and disinfectant in advanced water treatment. However, the

application of ozone has been limited by its low utilization efficiency because the ozone mass transfer rate from the gas phase to the liquid phase is relatively low. Microbubbles, with high specific interfacial area, large residence time and high inner pressure, are thought to be excellent in ozone gas mass transfer. However, the lack of knowledge about mass transfer using microbubbles causes many difficulties in the ozone reactor design. The author evaluates the mass transfer efficiency of microbubbles under different conditions. The volumetric mass transfer coefficient increases with increasing both induced-gas and water flow rates. The $k_{L,O_3}a$ obtained in the present study was also compared to those from other researchers. A similar level of $k_{L,O_3}a$ was achieved at low gas flow rates when microbubbles were employed.

A further research on the removal of organic contaminants in water was carried out. Demethyle Sulfoxide (DMSO) was selected as the model contaminant because it makes much odor trouble for the traditional waste water treatment. Experimental results indicate that the ozonation of DMSO is a first-order mass-transfer controlled reaction. Ozone utilization ratio increases with a decrease in gas flow rate. The ratio of DMSO removed to ozone dissolved can be raised to as high as 0.8 or higher with proper gas and water flow rates. It was also proved that no free radicals were yield by air microbubbles in the microbubble generation system.

It is expected that the specific data in the present study could provide valuable information for the design of water treatment processes using microbubbles.

CONTENTS

CHAPTER 1

Introduction

1.1 Background

Along with the increase in population worldwide, the quantity of water supply for domestic and industrial uses increases, and so does that of wastewater produced. However, the capacity of the rivers, lakes and oceans to assimilate the waste is finite. For this reason, water pollution occurs when the addition of contaminants to the water excesses its capacity. In fact, it has become a serious problem in the global context, especially in the developing countries, with the economic development.

In my mother country, China, the population has been rapidly growing from the 1950s and now reached to about 1.3 billion, accounting for about 20% of the world's total (http://www.cpirc.org.cn/index.asp). Meanwhile, the economy is also rapidly growing and now China plays a major role in world trade. However, a harmful by-product of its extraordinary economic growth has been severe environmental pollution problems, including acid rain, thick smog, toxic waste, water pollution, and carbon dioxide emissions, etc. Especially, water pollution and the consequent water shortage are critical problems in China. Along with the economic growth in the recent decade, the production of wastewater (industrial, municipal and agricultural) has been rapidly and steadily increasing. The volume of wastewater increased by 27.8% from 1981 to 1995, with an average annual increase of 1.65% (Wu *et al.*, 1999). However, in most cities of China, the construction of urban drainage, sewage and wastewater treatment has lagged far behind the economic development and environmental requirements for many years. Until 1996, only 5% of municipal wastewater and 17% of industrial discharge received any treatment before being discharged into lakes, rivers, irrigation ditches, or the coastal waters (Wu *et al.*, 1999). As a result, these river systems cannot endure the overload of contaminants

and water pollution takes place. Quoting 2004 report on the state of environment from China's State Environmental Protection Administration, 74.5% of river systems do not meet Grade II requirements, which are the government standards for primary drinking water supplies, and 27.9% of river systems are unsuitable even for agricultural purposes (http://www.zhb.gov.cn/eic/649368311779295232/index.shtml). However, in fact, most of these contaminated water systems are currently used in society as irrigation for farmlands and personal water consumption, which has been leading to more and more environmental and health problems. In China, liver and stomach cancer deaths have doubled since the 1970s, and are now the leading causes of cancer mortality in the country of China (Changhua *et al.*, 1998). China now has the highest liver cancer death rate in the world. These phenomenal increases are believed to have direct link with water pollution. Meanwhile, water shortage is another critical issue resulting from water pollution. China's per capita water reserves of 2,500 m^3 are one-fourth the global average and more than 100 of China's 660 cities are facing extreme water shortage.

Government regulations in most countries are being enhanced with the growing of public awareness and concern for controlling water pollution. In the United States, National Interim Primary Drinking Water Regulations for bacteria, turbidity, 10 inorganic chemicals, 6 pesticides, and radionuclides became effective on June 24, 1977. It was amended in 1977 to regulate thrihalomethanes (THMs), chlorine-disinfection by-products, and again in 1989 to regulate additional 83 contaminants (Craun, 1991). In China, the present drinking water standard has only 35 basic items. A new drinking water standard which is more stringent is to be adopt in 2006. The new standard includes 106 items mainly about organic pollutants and toxic substances.

It is clear that the traditional treatment processes cannot meet the more and more stringent standards for drinking water and discharging wastewater. A schematic of traditional water treatment plants is shown in **Fig. 1-1(a)** (Sincero, 1996). The basic conventional treatment is performed by two unit operations, namely, settling and filtration and the unit process of disinfection. The traditional treatment can remove almost all of the solid material and most of dissolved materials in raw water. **Fig. 1-1(b)** shows a schematic diagram of typical wastewater treatment systems (Sincero, 1996). In general,

the removal of organic pollutants may be divided into two stages: primary treatment which involves the removal of the wastewater solids, and secondary treatment which involves the removal of colloids and dissolved organic matter. Chorine has been widely used as disinfectant to prevent the waterborne transmission of infectious disease in the traditional water and wastewater treatment. However, it has been proved to be the largest source of trihalomethanes (THMs) (Meier *et al.*, 1986; Noot *et al.*, 1989; Yang *et al*., 2005; Hua *et al.*, 2006). Moreover, the traditional technology seems ineffective for the contol of micropolutants such as pesticides and other dissolved organic substances.

Advanced water treatment systems then emerged as an effective way to keep essential resources available and suitable for use and have become an area of global focus. For drinking water treatment, biological stabilization incorporating ozone prior to granular activated carbon (GAC) filtration is recognized as an efficient process for dissolved organics removal (Arslan-Alaton, 2004; Jung *et al.*, 2004) and disinfection by-product (DBP) control (Chaiket *et al.*, 2002; Chang *et al.*, 2002). For wastewater treatment, after the primary and secondary treatments, additional treatment steps such as membrane separation (Ray *et al*., 1986; Marinas, 1991), ozone oxidation (Ergas, 2006; Fontanier *et al*., 2006; Jardim, 2006), denitrification (Cui and Jahng, 2004) and biological phosphorus removal (Lopez *et al.*, 2006), have been added to provide for removal of nutrients and toxic materials. **Fig. 1-2** shows one example for advanced water treatment, where ozone treatment was applied as an alternative of chlorination and an oxidizer of contaminants.

As compared to the advanced water treatment technologies mentioned above, microbubble technology is less known though promising. In fact, microbubble technology was introduced to water and wastewater treatment in the 1920s, to take particles away from water as used in the air flotation process (Kiuri, 2001). However, its application had almost been restricted within the flotation separation prior to 1990. With the recent discovery of its bioactivity in fish culture and water purification (Onari *et al*., 1997, 1999, 2002a, 2002b), the microbubble technology is attracting more and more attention due to the unique characteristics, such as slow rise velocity, negative zeta-potential, etc. The interest in this research is its application to water and wastewater treatment. Firstly, an introduction about characteristics, generation methods, and

applications of microbubbles will be made in the following sections 1.2 and 1.3.

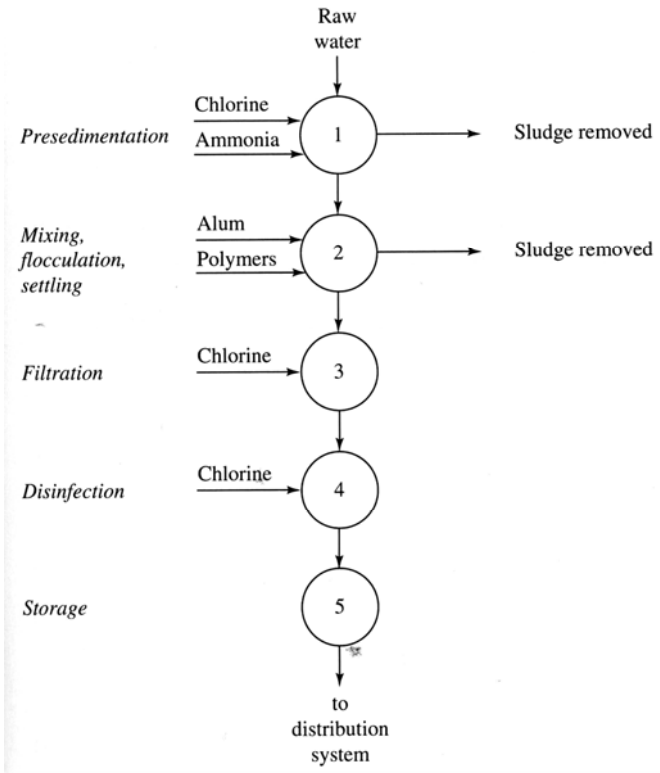

(a) Traditional drinking water treatment process

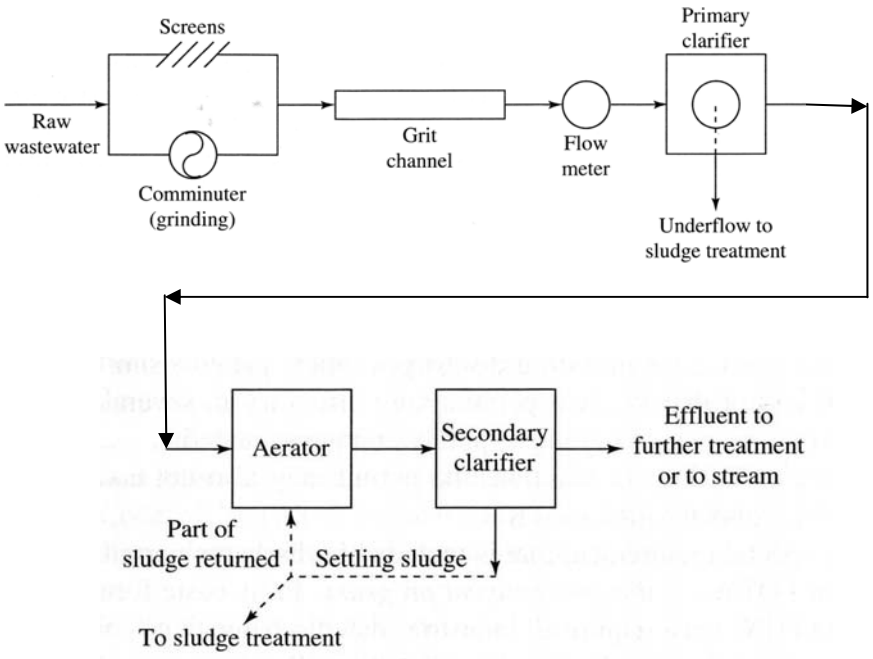

(b) Traditional wastewater treatment process

Fig. 1-1 Traditional water and wastewater treatment processes (Sincero, 1996)

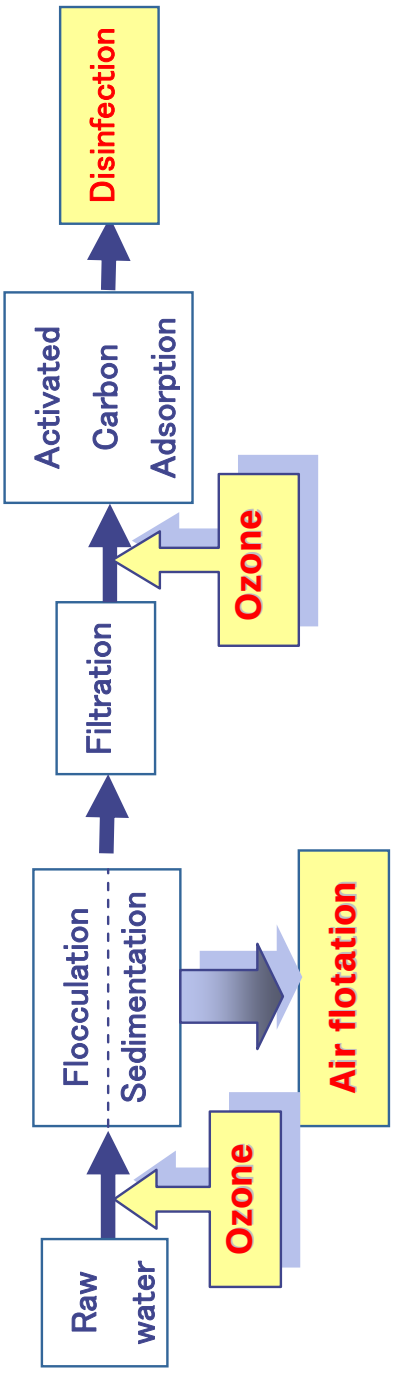

Fig. 1-2 Advanced water treatment processes

1.2 Characteristics of microbubbles

Microbubble is defined as an extremely small bubble, usually a few hundred micrometers in diameters, that can be uniformly suspended in liquid such as blood (The American Heritage® Dictionary of the English Language: Fourth Edition, 2000)). Some other researchers refer to bubbles with diameters on the order of 10μm as microbubbles (Ohnari, 2002a). Researchers have not reached agreement on the definition of microbubbles. Overall, the suitable microbubble sizes are different in the various fields of application (Tsuge and Li, 2006).

As compared to milli-bubbles which have diameters on the order of millimeters, microbubbles have many different characteristics resulted from their small sizes:

1.2.1 High specific interfacial area

Microbubbles have very high specific interfacial area. The specific interfacial area (interfacial surface area per unit volume of dispersion), a [m^{-1}], for spherical bubbles is expressed by the following equation

$$a = \frac{6\varepsilon_G}{d_{b,32}} \qquad \textbf{(1-1)}$$

where ε_G [-] is the gas holdup which is defined as the fraction of gas in a gas-in-liquid dispersion and $d_{b,32}$ [m] is the Sauter mean bubble diameter.

For a given gas holdup, the decrease of bubble size obviously results in the increase of specific interfacial area. For example, if there are 1.9×10^5 milli-bubbles with the diameter of 1mm in 1 L water with the gas holdup of 0.1, the specific interfacial area is 6.0×10^2 m^{-1}; If 10 μm microbubbles are used, the number of bubbles increases by 10^6 times and a increases to 6.0×10^4 m^{-1}.

1.2.2 Slow rise velocity

Terminal rise velocity of microbubbles is very slow. After formation, a bubble rapidly accelerates to its terminal velocity, u_b [m/s]. For small and spherical bubbles (Re<0.1), the value of u_b can be calculated using the Stoke's law

$$u_b=\rho g d_b^2/18\mu \quad \textbf{(1-2)}$$

where ρ [kg/m^3] is the liquid density, g [=9.8 m/s^2] is the gravity acceleration, μ [Pa·s] is the liquid viscosity. Stoke's law is only applicable to small bubbles with immobile surface. For the clear case where the bubble has a mobile surface, the following Hadamard-Rybczynski equation is often used

$$u_b=\rho g d_b^2/12\mu \quad \textbf{(1-3)}$$

A plot of the variation of rising velocity with radius for bubbles in purified and contaminated water is shown in **Fig. 1-3** (Ohnari, 2005; Takemura, 2004; Tsuge, 1982; Ueyama and Miyamoto, 2006). The presence of contaminants e.g. surfactants makes bubble surface immobile, which results in slower rise velocity. The terminal rise velocity, u_b, is proportional to the square of bubble diameter, d_b^2. A microbubble with the radius of 10 μm rises with the velocity of about 50 μm/s, in another word, 3 mm per minute. Such slow rising velocity leads to larger residence time and, therefore, higher gas holdup which is associated with larger specific interfacial area. Larger bubbles have higher rise velocities and exit as ellipsoids (1 to 10 mm) or spherical caps (>10 mm).

1.2.3 High inner pressure

The inside-outside pressure difference of a microbubble is very high.

Gas pressure inside a bubble is greater than that of outside due to the surface tension. The magnitude of the pressure difference, ΔP, can be predicted according to the Young-Laplace Equation as follows,

$$\Delta P = 4\sigma / d_b \quad \textbf{(1-4)}$$

where σ [N/m] is the surface tension of liquid. The smaller the bubble is, the higher the pressure inside it is. For instance, the Laplace pressure of a 10 μm bubble is about 2.9×10^4 Pa at 25 ºC, about 0.3 times the atmospheric pressure, while for a 1 μm bubble, ΔP is 2.9×10^5 Pa, 3 times the atmospheric pressure.

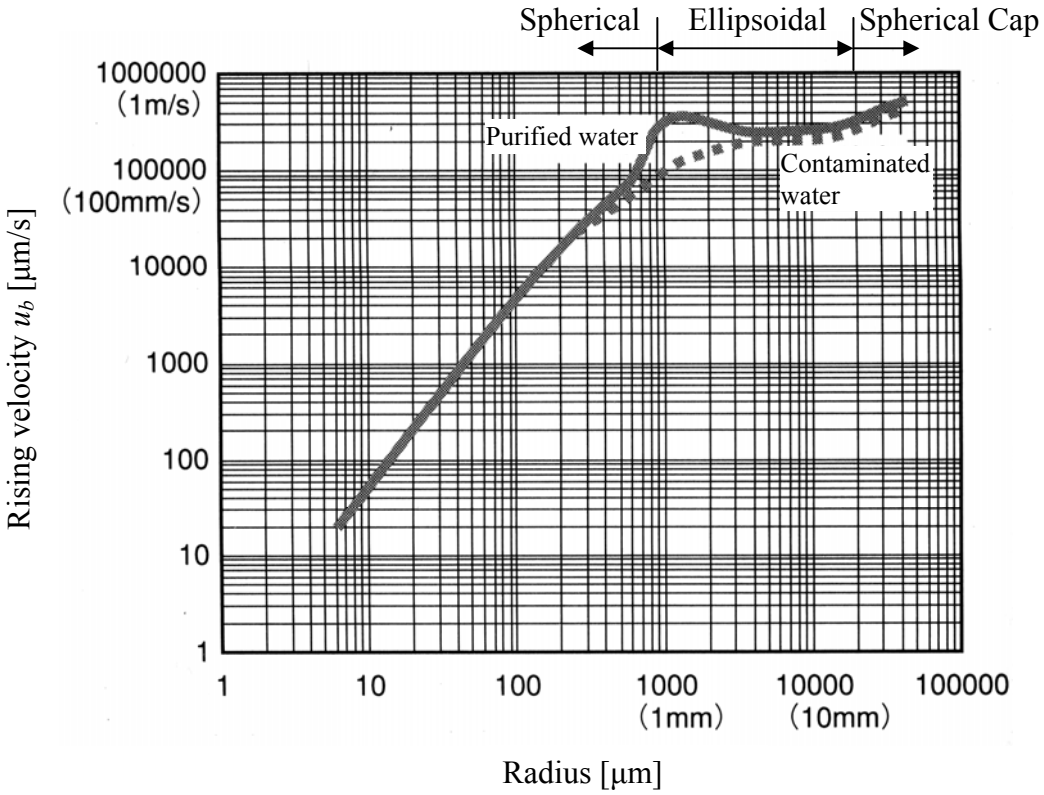

Fig. 1-3 Bubble rising velocity vs. bubble radius (Ohnari, 2005; Takemura, 2004; Tsuge, 1982; Ueyama and Miyamoto, 2006)

1.3 Microbubble generating methods

For conventional bubble generation, nozzles or orifices (Tadaki and Maeda, 1963; Takahashi and Miyahara, 1979; Tsuge and Hibino, 1979; Tsuge, 1986; Terasaka and Tsuge, 1990) are often used. Fine bubbles are usually produced using porous media (Koide *et al.*, 1968; Miyahara and Tanaka, 1997), constant flow nozzles (Terasaka and Tsuge, 1993), membrane (Yazawa *et al*., 1988), or gas spargers combined with mixers e.g. impellers (Forrester, *et al.*, 1998; Johnson, *et al.*, 1982). However, it is hard to generate microbubbles using these techniques mentioned above due to the difficulty in preventing bubble coalescence. For this reason, microbubbles are often generated by different ways that can be divided into three types in terms of their mechanism: pressurization type, cavitation type and rotating-flow type.

1.3.1 Pressurization type

The pressurization type of microbubble generating system is based on the Henry's law. This physical law states that the dissolved concentration of a solute gas in a liquid at saturation, C^*, is proportional to the partial pressure of that gas above the liquid, P, at a given temperature, provided no chemical reaction takes place between the gas and the liquid. Following this law, much more gas can dissolve into liquid at an elevated pressure. In the pressurization type, high pressurized water is saturated with gas and then injected into normal environment with atmospheric pressure through a nozzle. Microbubbles are formed during the sudden pressure drop.

This kind of microbubble generation method has been applied to water and wastewater treatment, known as dissolved air flotation (DAF), where air is dissolved into water at elevated pressures of 0.4–0.5 MPa and then released through decompression nozzles to a flotation tank. The theoretical specific volume of released air per unit pressure difference is listed in **Table 1-1** (Tanbo *et al.*, 1984) under varied temperatures. The pressure difference applied in most DAF systems is at or lower than 0.4 MPa. Therefore, the volume concentration of air microbubbles released from saturated water is restricted to be

lower than 1/13 at 20 ºC through theoretical calculation.

Measurements of bubble sizes for the pressurization type indicate that microbubbles maintain a steady size range of 10 to 100 μm with an average diameter between 40 and 80 μm (Edzwald, 1995; Fukushi *et al.*, 1998; Han *et al.*, 2002a and 2002b; Vlyssides *et al.*, 2004). Moreover, the average bubble size decreases as the saturator pressure increases, but increasing the pressure has a small effect on bubble size above 0.5 MPa (De Rijk *et al.*, 1994; Han *et al.*, 2002a).

1.3.2 Cavitation type

When the local ambient pressure at a point in a liquid falls below the liquid's vapor pressure at the local ambient temperature, the liquid can undergo a phase change, creating largely empty voids termed cavitation bubbles. Cavitaion occurs in pumps, propellers, and impellers, which is often undesirable in those cases. However, some researchers make use of this phenomenon to generate microbubbles. Venturi tube is one example (Takemura, 2003; Fujiwara *et al*., 2003). As shown in Fig. 1-4 **(a)**, the venturi tube has a conic shape (Fujiwara, 2006). If a pump forces a fluid flowing into the venture tube, an increase in velocity occurs in the constricted part simultaneously with the decrease in pressure which leads to gases (e.g. air) being sucked in through the tube. When the pressure recover takes places further downstream, the sucked gas bubbles collapse yielding small bubbles as shown in Fig. 1-4 **(b)**. However, fine bubbles are tending to coalesce into large bubbles in the vicinity of the veturi tube. Surfactants are often used to avoid that. Fujiwara (2006) found that bubbles generated with a venture tube by adding pentanol at the concentration of 50 ppm have a mode diameter of about 100 μm and a sauter diameter of about 250 μm.

1.3.3 Rotating-flow type

A typical design of the rotating-flow type of microbubble bubble generator is shown **Fig. 1-5(a)** (Tatsumi, 2004)**.** It also has a conic shape. Microbubble generation is initiated by pumping water from the tangential direction into it. The fluid flows in a rotating motion along the inner wall to form a vortex. The center of the vortex is a low-pressure area because of centrifugal force, which makes gas (e.g. air) drawn into it. When the fluid

takes air out of the generator with very high rotating velocity, air can be sheared into microbubbles.

The rotating-flow type of microbubble generator (**Fig. 1-5(b)**) was improved by Ohnari (2000) in recent years. Its inner structure is not clear but the microbubble generation principle described by the inventor seems to be similar with that in the typical one (Ohnari *et al*., 1999; Ohnari, 2000). The biggest difference between them is the relative position of gas induction and water input points. In the new type developed by Ohnari (2000), water input point is apart from the gas induction point while they are at the same end of the generator in the typical one. When water flows into the one end of the improved generator, the major part of fluid circulates inside the generator before leaving out of it as shown in Fig. 1-5(b). Air is aspirated from the other end into the vacuum zone along the axis. It is sheared by the rotating flow and then the input flow just before leaving the generator, which results in better microbubble generating efficiency.

Table 1-1 Theoretical specific volume of released-air in water (Tanbo *et al.*, 1984)

Temperature	Density of water	Density of air	Henry's constant	air released per unit pressure difference	
[ºC]	[kg/m^3]	[kg/m^3]	[atm/mole frac]	per atm	
				[$\times 10^{-3}$kg/m^3]	[m^3/m^3]
15	999.13	1.2255	60700	26.5	0.0216
16	998.97	1.2213	61800	26.0	0.0213
17	998.80	1.2170	62900	25.5	0.0210
18	998.62	1.2129	64100	25.0	0.0206
19	998.43	1.2087	65200	24.6	0.0204
20	998.23	1.2046	66400	24.2	0.0201
21	998.02	1.2004	67700	23.7	0.0197
22	997.80	1.1964	68700	23.3	0.0195
23	997.56	1.1923	69800	23.0	0.0193
24	997.32	1.1883	70800	22.6	0.0191
25	997.07	1.1843	72000	22.3	0.0188

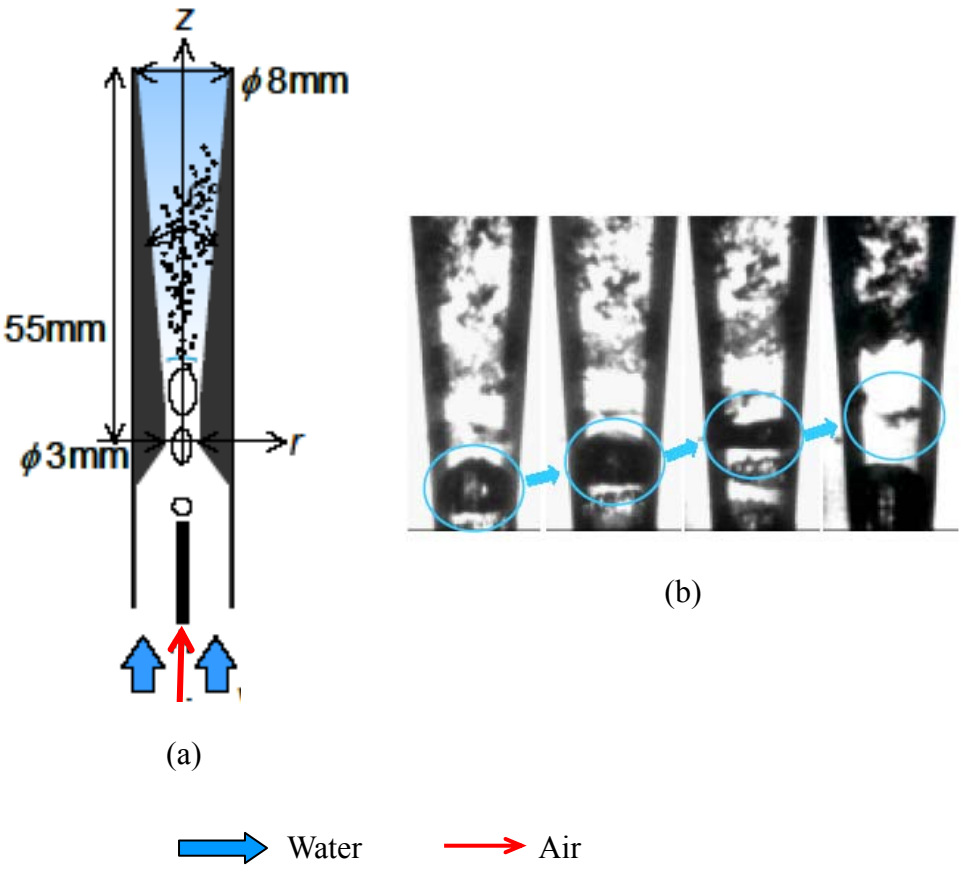

Fig. 1-4 Venturi tube microbubble generator (Fujihara, 2006)

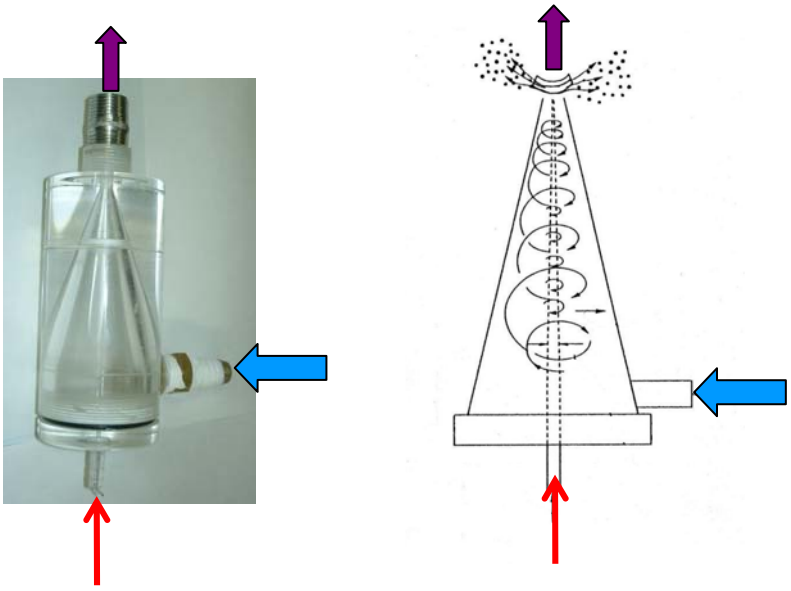

(a) Typical one (Tatsumi, 2004)

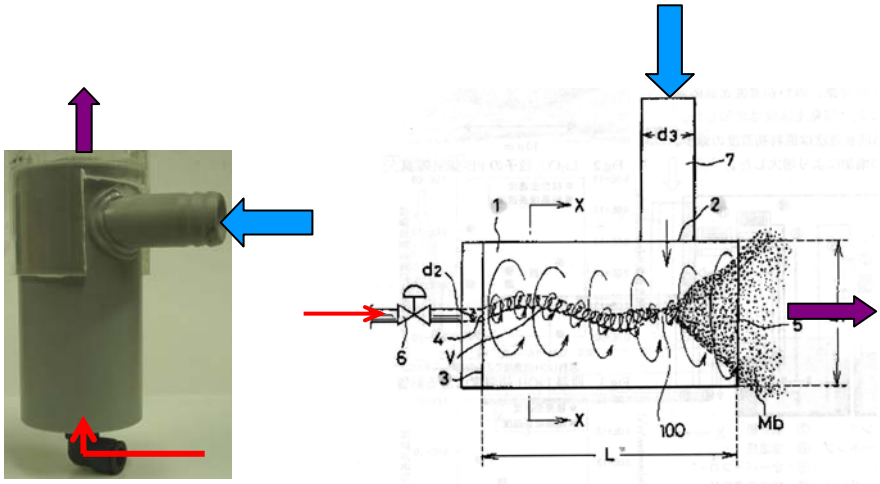

(b) Improved one by Ohnari (2000)

Water Air Bubbly water

Fig. 1-5 Rotating flow microbubble generators

1.4 Applications of microbubbles

Microbubbles, due to its extremely small size and these associated characteristics, are gaining more and more attention in various fields, such as fish and shellfish culture, medicine, water purification, etc.

1.4.1 Water and wastewater treatment

The main applications of microbubbles in water and wastewater treatment can be divided into two categories: air flotation and oxygen supplying.

(1) Air flotation

Flotation is a separation process where air bubbles capture partially hydrophobic solid particles and carry them to the surface for separation or removal. The flotation separation was applied to mineral processing in the beginning, where it enables a selective classification of ore constituents (Kitchener, 1984), and recently it has gained attention in water and wastewater treatment for water clarification (Kiuru, 2001; Schofield, 2001).

Air flotation is used as the alternative of sedimentation to remove particles, when treating low turbidity, high colored water at low temperatures, or when removing algae from nutrient-rich stored water (Edzwald *et al.*, 1994;). It is because that in these cases, the floc particles produced during the flocculation treatment have such low density that they have a tendency to settle very slowly or to float in sedimentation tank. The use of flotation is, therefore, proposed as an alternative to gravity settling in these cases.

(2) Oxygen supplying

Nutrient enrichment, elevated concentration of nitrogen and phosphorous is a serious ecological problem, which often occurs in lakes. The overgrowth of algae and aquatic plants as a consequence of excessive nutrient will decrease the dissolved oxygen concentration, and even result in oxygen “dead zones” in the deep part of water. Some field experiments on supplying oxygen to the deep part using microbubbles were carried

out (Morimoto *et al.*, 1996; Onari *et al.*, 1999; Mastuo *et al.*, 2005). As referred to Mastuo *et al*. (2005), dissolved oxygen concentration of the lower layer in the dam lake rapidly increased after providing pure oxygen microbubbles. A little increase of turbidity also occurred in the lower part, but it did not affect the turbidity in the middle and surface layers. Yamada and Minagawa (2005) did a pilot experiment and proposed a model for their oxygen supplying system using microbubbles. They found that the oxygen concentration increased with decreasing bubble size.

1.4.2 Fish and shellfish culture

In recent years, the application of microbubbles to fish and shellfish culture draws much interest (Ohanari, 1999, 2002 and 2003; Takahashi, 2004). Field experiments with microbubbles were conducted in the oyster beds in Hiroshima as reported on Yomiuri Shinbun issued on July 22, 1999. It was proved that microbubbles increased both the growth rate of the cultured oysters and the size of the shucked meats. Ohnari (2002) carried out studies on its mechanism. It seems that the increase of dissolved oxygen concentration with the microbubble injection is playing an important role in the growth promotion. They also showed that the mean blood flux in the heart of shellfishes increased by 2.0-2.5 times with microbubble supply. Moreover, the Coliform bacteria count in the body of oysters was decreased below the standard for raw eating after blowing air microbubble for only 15 min. Generally, the oysters must be disinfected by ozone, chloride or ultra-violet for 48 hours to meet the standard.

1.4.3 Medicine

Microbubbles have been utilized as a contrast agent, together with ultrasound, in the field of medicine for a long time (Takegami, 2005). Some latest researches show that microbubbles also have clinical applications, such as, targeted delivery of drugs and genes, “blusting” blood clots and even noninvasive assessment of organ inflammnation and tumors’ metastatic potential.

1.4.4 Others

There are also many other researches on microbubble application. Goto *et al.* (2006) proposed a system using microbubbles to separate oil from oil-polluted soil. McCormick and Bhattacharyya (1970) first found that the presence of microbubbles could reduce the frictional resistance between ship and water during navigation. Weber and Agblevor (2005) used a microbubble dispersion (MBD) generator to supply oxygen in viscous fungal fermentation. They found that the cell mass productivity increased about twice when MBD was used instead of the conventional sparging.

1.5 Purpose of the Present Study

Microbubbles, as small as colloid particles and cells, have their unique characteristics, often called size effect. Their amazing effect for closed-water purification pushes them into limelight in the field of water treatment. However, except for several successful cases on the application for closed-water purification, there is few fundamental and specific research data reported. Moreover, the present microbubble generation methods all have their own merits and demerits and they need to be improved to meet the requirement for water treatment. In this study, the author firstly evaluates the characteristics of a newly-developed microbubble generator, and then makes some attempts to improve its microbubble generation efficiency in **CHAPTER 2**.

The improved microbubble generation system is then introduced to the advanced water treatment processes and examined for the effectiveness. The applications to advanced water treatment studied in the present research include air flotation and ozone oxidation.

In fact, the earliest application of microbubbles on water treatment originated from air flotation. Microbubbles in the air flotation process are produced by the way of pressurization or cavitations. The former type of air flotation is known as dissolved air flotation (DAF). Fine and uniform microbubbles generated in DAF can efficiently catch fine waste particles in water. But high electrical power requirement, complex system and higher service cost are its inherent disadvantages. Moreover, the microbubble generation efficiency in DAF is determined by the Henry's law and therefore cannot be increased

over the theoretical value. On the other hand, the air flotation using the cavitation way to produce microbubbles is called dispersed air flotation or induced air flotation (IAF). It is usually simple and cost-effective. However, large bubbles generated in the dispersed air flotation lead to poor bubble-particle collision efficiency which is one of the most important factors in particle removal. Moreover, high shear in conventional mechanical flotation cell usually results in breakage of the fragile particles (Jameson, 1999; Zabel, 1992). The author strives to develop an efficient IAF system with the improved microbubble generation method and examine its suitability under various conditions, which will be described in **CHAPTER 3**.

The rotating-flow microbubble generator is chosen for the present study due to its simple structure and comparatively better microbubble generation efficiency. But two problems emerge when it is applied to air flotation. One is the high turbulence during bubble generation, and the other is insufficient microbubbles generation rate. To overcome these problems, the author tries to separate the high-shear region where microbubbles are generated from the flotation zone where bubble-particle agglomerates rise to the water surface. This separated flotation system will be introduced in Section 3.2.

We are not satisfied with the separated flotation system because it seems so complex and hard to operate. Our other attempt is to design a one-cell flotation system where microbubble generation and flotation are set in the same zone. In Section 3.3, the preliminary experiments were carried out in order to search for an appropriate polymeric flocculant which could produce stronger floc particles and to develop a bubble generation method which could form microbubbles with high concentrations. After that, in Section 3.4, the properties of the developed one-cell flotation system were checked for particle removal under various conditions.

In the last two chapters, ozonation with microbubbles is discussed. Ozone is a popular oxidant and disinfectant in advanced water treatment. However, the application of ozone has been limited by its low utilization efficiency because the ozone mass transfer rate from gas phase to liquid phase is relatively low. Microbubbles, with high specific interfacial area, large residence time and high inner pressure, are thought to be excellent

in ozone gas mass transfer. However, the lack of knowledge about mass transfer using microbubbles causes many difficulties in the ozone reactor design. The author evaluates the mass transfer efficiency of microbubbles in **CHAPTER 4**. The microbubble generation system developed in CHAPTER 2 is also applied to mass transfer and compared with the normal ones.

A further research on the removal of organic contaminants in water with ozone is carried out in **CHAPTER 5**. Demethyle Sulfoxide (DMSO), which is mainly found in the wastewater from the manufacture of semiconductors and liquid crystal displays, is selected as the model contaminant because it makes much odor trouble for the traditional waste water treatment. It is proved to be an effective way to oxidize DMSO with hydroxyl radicals before the biological treatment for the control of odor problems. Firstly, the author verifies whether air microbubbles have the ability to oxidize DMSO by yielding free radicals through microbubble collapse. Then ozone is applied to the oxidation of DMSO.

A summary of this study is given in **CHAPTER 6.** The author evaluates the microbubble generation efficiency for the rotating-flow microbubble generator and makes an effort to improve it. The possibility for the improved system to be applied in the advanced water treatment is examined especially for the air flotation and gas mass transfer.

Nomenclature

a	specific interfacial area	[m^{-1}]
C^*	dissolved concentration of a solute gas in a liquid at saturation	[mol/L]
d_b	bubble diameter	[m]
$d_{b,32}$	Sauter mean bubble diameter	[m]
g	gravity acceleration	[m/s^2]
u_b	bubble rise velocity	[m/s]
P	Pressure	[Pa]
ΔP	Laplace pressure	[Pa]
ε_G	gas holdup	[—]
ρ	liquid density	[kg/m^3]
μ	liquid viscosity	[Pa·s]
σ	surface tension of liquid	[N/m]

Literature cited

Arslan-Alaton, I.; "Granular Activated-Carbon Assisted Ozonation of Biotreated Dyehouse Effluent," *AATCC Review,* **4,** 21-24 (2004)

Chaiket, T., P. C. Singer, A. Miles *et al.*; "Effectiveness of Coagulation, Ozonation, and Biofiltration in Controlling DBPs," *J. Am. Water Works Assoc.,* **94,** 81-95 (2002)

Chang, E. E., C. H. Liang, Y. W. Ko *et al.*; "Effect of-Ozone Dosage for Removal of Model Compounds by Ozone/GAC Treatment," *Ozone Sci. Eng.,* **24**, 357-367 (2002)

Changhua, W, M. Gottlieb, D. Davis; "China's environment and health," In: World Resources 1998-1999. Washington, DC: World Resources Institute, 120-122 (1998)

Craun, G. F.; "Epidemiologic Studies of Organic Micropollutants in Drinking Water," O. Hutzinger, *The Handbook of Environ. Chemistry*, **5** (Part A) 8-9 (1991)

Cui, R., D. Jahng; "Nitrogen control in AO Process with Recirculation of Solubilized Excess Sludge," *Water Research,* **38,** 1159-1172 (2004)

De Rijk, S. E., Van der Graaf, J. H. J. M. and Den Blanken J. G.; "Bubble Size in Flotation Thickening," *Water Research.*, **28**, 465-473 (1994)

Edzwald, J. K., D. Q. Bunker, Jr. J. Dahlquist, L. Gillberg and T. Hedberg; "Dissolved Air Flotation: Pretreatment and Comparisons to Sedimentation," Chemical Water and Wastewater Treatment III, Springer-Verlag Berlin Heidelberg, pp.3-18 (1994)

Edzwald, J. K.; "Principle and Applications of Dissolved Air Flotation," *Wat. Sci. Tech.*, **31**, 1-23 (1995)

Ergas, S. J., B. M. Therriault and D. A.Reckhow; "Evaluation of water reuse technologies for the textile industry," *J. Environ. Eng.-ASCE,* **132,** 315-323 (2006)

Forrester, S. E., C. D. Rielly and K. J. Carpenter; "Gas-Inducing Impeller Design and Performance Characteristics," *Chem. Eng. Sci*., **53**, 603-615 (1998)

Fontanier, V., V. Farines, J. Albet *et al.*; "Study of catalyzed ozonation for advanced treatment of pulp and paper mill effluents," *Water Research,* **40,** 303-310 (2006)

Fukushi, K., Y. Matsui and N. Tambo; "Dissolved Air Flotation: Experiments and Kinetic

Analysis," *J. Water SRT-Aqua*, 47, 76-86 (1998)

Fujiwara, A.; "Microbubble generation Using Venturi Tube," *ECO Industry*, **11**, 27-30 (2006) (In Japanese)

Fujiwara, A., S. Takagi, K. Watanabe and Y. Matsumoto; "Experimental Study on the New Micro-Bubble Generator and its Application to Water Purification System," 4th Proceeding of the ASME/JSME, Honolulu, United States (2003)

Goto, Y., A. Serizawa, T. Eguchi, H. Tanaka and M. Izumi; *Japanese J. Multiphase Flow,* **20**, 39 (2006)

Han, M., Y. Park, J. Lee and J. Shim; "Effect of Pressure on Bubble Size in Dissolved Air Flotation," *Water Sci. & Tech.: Water Supply*, **2**, 41-46 (2002a)

Han, M., Y. Park and T. J. Yu; "Development of A New Method of Measuring Bubble Size," *Water Sci. & Tech.: Water Supply*, **2**, 77-83 (2002b)

Hua, G. H., D. A. Reckhow and J. Kim; "Effect of Bromide and Iiodide Ions on the Formation and Speciation of Disinfection Byproducts during Chlorination," *Environ. Sci. & Tech.*, **40**, 3050-3056 (2006)

Jameson, G. J.; "Hydrophobicity and Floc Density in Induced-Air Flotation for water treatment," *Colloids Surfaces A: Physicochem. Eng. Aspects,* **151**, 269-281 (1999)

Jardim, W. F.; "Trends and Strategies of Ozone Application in Environmental Problems," *Quim. Nova.*, **29**, 310-317 (2006)

Johnson, B. D., R.M. Gershey, R.C. Cooke and W. H. Jr. Sutcliffe; "A Theoretical Model for Bubble Formation at a Frit Surface in a Shear Field," *Sep. Sci. Technol.* **17**, 1027-1039 (1982)

Jung, S.W., K.H. Baek, M. J. Yu; "Treatment of taste and odor material by oxidation and adsorption," *Water Sci. & Tech.,* **49,** 289-295 (2004)

Kitchener, J. A.; "The Froth Flotation Process: Past, Present and Future," The Scientific Basis of Flotation, Martinus Nijhoff Publishers, Netherlands, pp.3-52 (1984)

Kiuru, H. J.; "Development of Dissolved Air Flotation Technology from the First Generation to the Newest (Third) One (DAF in Turbulent Flow Conditions)," *Water Science and Technology,* **43**, 1-7 (2001)

Koide, K., S. Kato, H. Tanaka and H. Kubota; "Bubble Generated from Porous Plate," *J.*

Chem. Eng. Japan, **1**, 51-56 (1968)

Lopez, C., M. N. Pons and E. Morgenroth; "Endogenous Processes during Long-Term Starvation in Activated Sludge Performing Enhanced Biological Phosphorus Removal," *Water Research*, **40**, 1519-1530 (2006)

Marinas, B. J.; "REVERSE-OSMOSIS TECHNOLOGY FOR WASTE-WATER REUSE," *Water Sci. & Tech.,* **24** 215-227 (1991)

Matsuo, K., K. Maeda and H. Ohnari; "Water purification of a dam lake using micro bubble technology," Japanese Society for Multiphase Flow Annual Meeting, Tokyo, Japan, August, 346-348 (2005)

Meier, J. R., H. P. Ringhand and W. E. Coleman *et al.*; *Environ. Health Perpect*., **69**, 101 (1986)

McCormick, M. E. and R. Bhattacharyya; *Naval Eng. J.*, **85**, 11 (1973)

Miyahara, T. and A. Tanaka; "Size of Bubbles Generated from Porous Plates," *J. Chem. Eng. Japan*, **30**, 353-355 (1997)

Morimoto, M. *et al*.; "A Development of Waste Water Purification Technique in Closed Water Area," *Journals of the Japan Society of Civil Engineers*, **553**, 33-40 (1996)

Noot, D. K. , W. B. Anderson and S. A. Daignault *et al.*; *J. Am. Water Works Assoc.,* **81**, 87 (1989)

Ohnari, H.; "Waste Water Purification in Wide Water Area by Use of Micro-Bubble Techniques," *Japanese J. Mutiphase Flow*, **11**, 263-266 (1997)

Ohnari, H., T. Saga, K. Watanabe, K. Maeda and K. Matsuo; "High Functional Characteristics of Micro-bubbles and Water Purification," *Resources Processing*, **46**, 238-244 (1999)

Ohnari, H.; "Swirling Type Micro-Bubble Generating System," Japan Patent, **2000-618002** (2000)

Ohnari, H.; "Water Purification of Ocean Environment and Revival of Fisheries Cultivation Using Micro Bubble Technology," The 21st Symposium on Multiphase Flow, Nagoya, Japan, July (2002)

Ohnari, H.; "Application of microbubble technology to fishery," *Chemical Engineering*, **67**, 130-141 (2003) (In Japanese)

Ohnari, H.; “A Grounding in Microbubble Technology,” Concepts in Basic Bubble and Foam Engineering, Techno-System Co., pp.427 (2006)

Ray, R. J., J. Kuceragienger and S. Retzlaff; “Membrane-Based Hybrid Processes for Energy-Efficient Waste-Water-Treatment,” *J. Membrane Science,* **28,** 87-106 (1986)

Sincero, A. P. and G. A. Sincero; “Environmental Engineering: A Design Approach,” *Prentice-Hall, Inc., USA*, 227, 302 (1996)

Schofield, T.; “Dissolved Air Flotation in Drinking Water Production,” *Water Sci. & Tech.,* **43**, 9-18 (2001)

Tadaki, T. and S. Maeda; “The Size of Bubbles from Single Orifices,” *Kagaku Kogaku Ronbunshu*, **27**, 147-155 (1963)

Takahashi, M.; “Tiny Bubbles for Industry and Science,” *Japanese J. Multiphase Flow*, **18**, 324-331 (2004)

Takahashi, T. and T. Miyahara; “Bubble Volume Formed at Submerged Orifices,” *Kagaku Kogaku Ronbunshu*, **5**, 453-456 (1979)

Takegami, K., Y. Kaneko, T. Watanabe *et al.*; “Comparison of Option and MRX-133 Microbubble Contrast Agent in Improving Heating and Coagulation Volume Efficiency of High Intensity Focused Ultrasound,” *Radiology*, **237**, 132-136 (2005)

Takemura, F. and Y. Matsumoto; “Apparatus and Method for Fine Bubble Generation,” Japan Patent, 2003-230824

Takemara F.; Course of Characteristics and Application of Microbubble, Technical Information Center (2004) (In Japanese)

Tatsumi, K.; “Water treatment technology and facility in the future,” *Kagaku Soti*, **1**, 71-80 (2004) (In Japanese)

Tambo, N., K. Fukushi and S. Ohata; “Comparison between Dissolved Air Flotation and Sedimentation,” *J. JWWA*, **603**, 1984

Terasaka, K. and H. Tsuge; “Bubble Formation at a Single Orifice in Highly Viscous Liquids,” *J. Chem. Eng. Japan*, **23**, 160-165(1990)

Terasaka, K. and H. Tsuge; “Bubble Formation under Constant-Flow Condition,” *Chem.*

Eng. Sci., **48**, 3417-3422 (1993)

Tsuge, H.; "Improvement of Chemical Engineering-Bubble & Drop & Dispersion Engineering," The Society of Chemical Engineering/Maki Shoten, pp.4 (1982)

Tsuge, H.; "Hydrodynamics of Bubble Formation from Submerged Orifices," Engcyclopedia of Fluid Mechanics, Gulf Publishing Company, pp.191-232 (1986)

Tsuge, H., P. Li; "Water purification using microbubbles, *ECO Industry*, **11**, 53-57 (2006) (In Japanese)

Tsuge, H. and S. Hibino; "Effect of Column Diameter on the Volume of Bubble Formed from a Submerged Single Orifice," *Kagaku Kogaku Ronbunshu*, **5**, 361-365 (1979)

Tsuge, H. and H. Unno; "Bubble technology," Kogyo Chosakai Publishing, pp.120 (2004) (In Japanese)

Ueyama, S. and M. Miyamoto; "The World of Microbubbles," Kogyo Chosakai Publishing, pp.58 (2006) (In Japanese)

Vlyssides, A. G., S. T. Mai and E. M. P. Barampouti; "Bubble Size Distribution Formed by Depressurizing Air-Saturated Water," *Ind. Eng. Chem. Res.*, **43**, 2775-2780 (2004)

Weber, J. and F. A. Agblevor; "Microbubble Fermentation of *Trichoderma Reesei* for Cellulose Production," *Process Biochemistry*, **40**, 669-676 (2005)

Wu, C. H., C. Maurer and Y. Wang *et al.*; "Water Pollution and Human Health in China," *Environmental Health Perspectives,* **107**, 251-256 (1999)

Yamada, S. and H. Minagawa; "A Study for Oxygen Supplying to Deep Part with Microbubbles," *Japanese Society for Multiphase Flow Annual Meeting*, Tokyo, Japan, August 1-3, 345-346 (2005)

Yang, X, C. Shang and J. C. Huang; "DBP formation in breakpoint chlorination of wastewater," *Water Research*, **39,** 4755-4767 (2005)

Yazawa, T., H. Nakamichi, H. Tanaka and K. Eguchi; "Permeation of Liquid through Porous Glass Membrane with Surface Modification," *J. Ceram. Soc. Japan*, **96**, 18-23 (1988)

Zabel, Th. F.; "Flotation in Water Treatment," Innovations in Flotation Technology, Kluwer Academic Publishers, Netherlands, pp.431-454 (1992)

CHAPTER 2

Microbubble generation

2.1 Background

In this study, we adopted the rotating-flow microbubble generator (RFMG) which was developed by Ohnari (2000). This newly developed microbubble generator is very simple and easy to operate. Its effectiveness for shellfish growth promotion (Ohnari *et al*., 1999) and water purification (Ohnari, 1997) also attracted our interest.

A schematic diagram is illustrated in **Fig. 2-1** and the dimensions of the two types (M2-M and M2-LM, Nanoplanet Research Institute Co.) used in this study are also shown in it. The generator has a cylindrical configuration with the diameter of 45~50 mm and the height of 80~100 mm. There are only two entrances set in its each end without any moving parts. The one in the upper part along the tangential direction is for water, while the other one in the middle of the bottom along the axis is for gas. The exit for the mixture of water and gas is set in the center of top.

The special inner design provides its high microbubble generation efficiency than that of the typical one. However, when the RFMG is used under surfactant free or low solute conditions in practice, the gas/liquid ratio for microbubble generation was found relatively low (Okamoto *et al.*, 2005). It is believed that both size and concentration of microbubbles are of considerable importance in the application of microbubbles. For example, air microbubbles generated in the air flotation have an average diameter of 40~80 μm. For average bubble size of about 60 μm, the typical number concentration of air microbubbles is between 44 and 88 × 10^6 bubbles per liter and the typical volume concentration is between 5,000 and 10,000 ppm (Haarhoff and Edzwald, 2004).

We checked the microbubble generation characteristics of the RFMG in this chapter. In addition, a new method of using the RFMG was proposed to improve the microbubble generation efficiency. Bubble size distribution and gas holdup were measured and used as evaluation indexes.

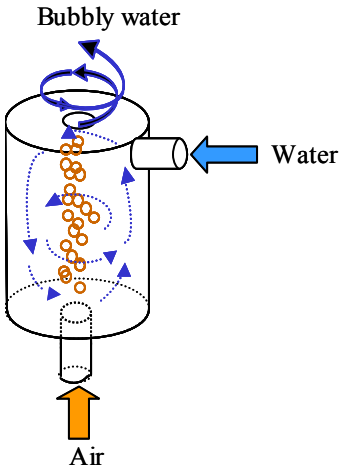

(a) Schematic diagram and flow pattern inside it

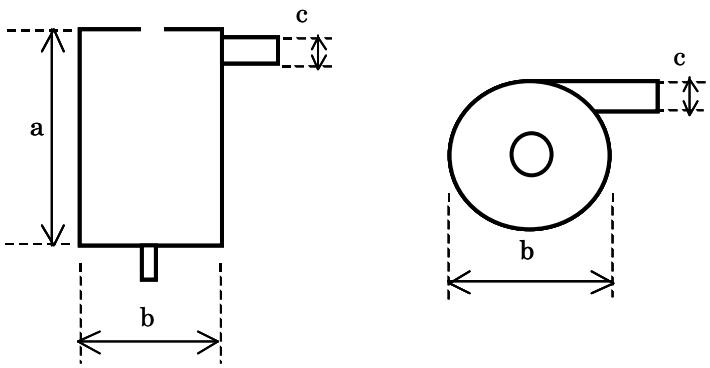

Type	a [mm]	b [mm]	c [mm]
M2-M	80	45	15
M2-LM	100	50	25

(b) Dimensions

Fig. 2-1 Schematic diagram and dimensions of rotating-flow microbubble generator

2.2 Microbubble generation methods

2.2.1 Normal method (a): gas suction by generator

The general method for using rotating-flow microbubble generator (RFMG) is illustrated in **Fig. 2-2(a),** where the RFMG is set in a tank connected with a pump and a gas induction pipeline. As described in Section 1.3.1, microbubble generation is started by pumping water into the generator. A rotating flow is formed along the inner wall of the generator, which results in a negative pressure zone along its axis. Gas is aspirated by the negative pressure and sheared by the rotating flow. Microbubbles are generated when the mixture of water and gas is spouted out with high rotating velocity (Onari *et al*., 1999; Onari, 2000; Tsuge and Unno, 2004).

2.2.2 Improved method (b): gas suction by cavitation pump with generator

Fig. 2-2(b) shows an improved method where, by contrast, gas suction by the generator is stopped. A centrifugal pump (20KED04s, Nikuni Co.) is used to induce gas instead.

Generally, gas ingestion into the suction pipe connected with a centrifugal pump is detrimental because the consequent cavitations can degrade its performance and even destruct pump's internal components. However, the kind of centrifugal pump used in this study is especially designed for the operation under cavitations. A normal centrifugal pump can handle only 0.5% gas by volume, while the specially-designed cavitation pump can operate under the gas/liquid ratio of 1/10.

The cavitation pump was originally developed for gas dissolution in the dissolved air flotation systems. As shown in **Fig. 2-3**, gas and liquid are simultaneously induced by the pump and mixed in it. The mixture of gas and liquid is pumped into a saturation tank where liquid is saturated with gas at about 0.4 MPa and the excess air is released out. It can be seen that the system is complicated. Moreover, if the gas to be dissolved is toxic or expensive, the excess gas from the separator should be recycled instead of being released to the environment. In this study, we simplified the system as shown in **Fig. 2-3** by eliminating the air separator tank which often takes large place. In addition, the

RFMG was set in the outflow line as shown in **Fig. 2-2(b)**.

2.2.3 Method (c) for comparison: gas suction by cavitation pump with single dispersing nozzle

Additionally, the RFMG in the improved method (b) was replaced with a single dispersing nozzle (see **Fig. 2-2(c)**). **Fig. 2-4** is a schematic diagram of the single dispersing nozzle which has an inner diameter of 16 mm. There are 8 dispersing orifice with the diameter of 5 mm distributed the nozzle. We will compare method (c) with (b) to check whether the generator in the method (b) has an effect on bubble generation or not.

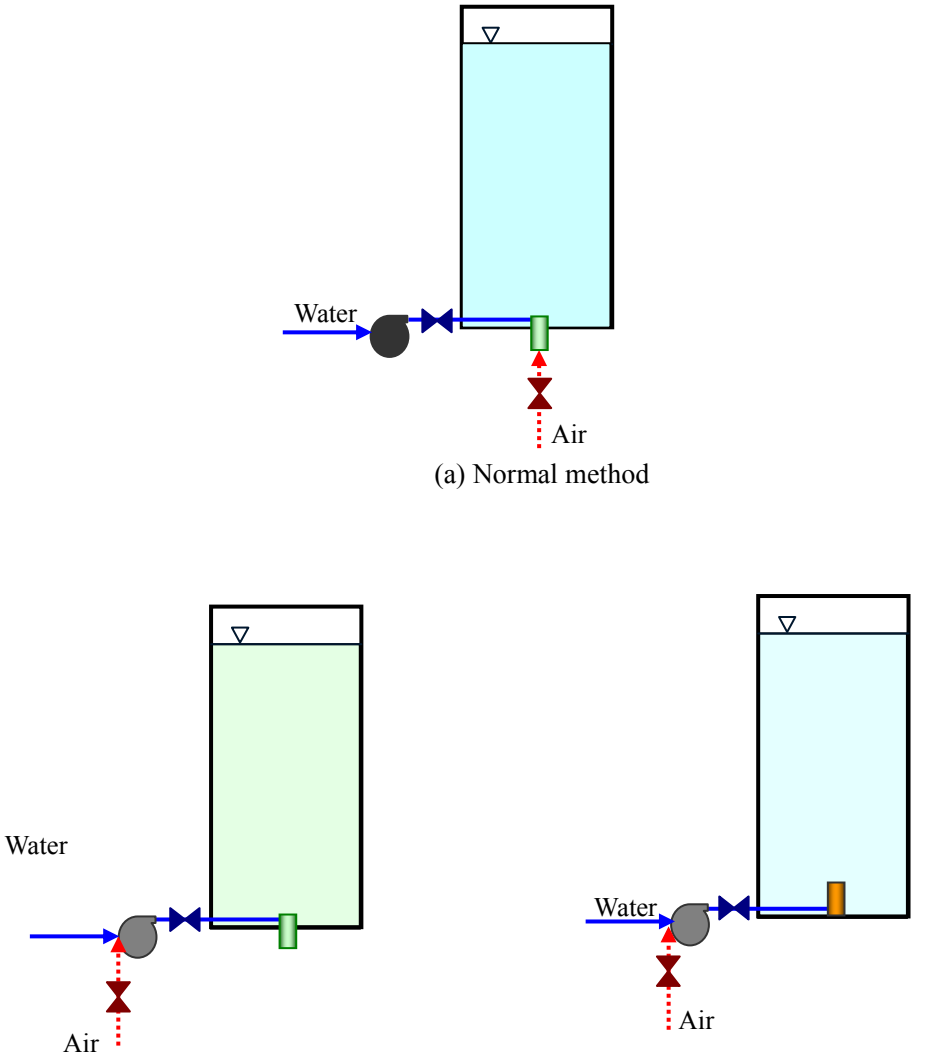

Fig. 2-2 Microbubble generation methods

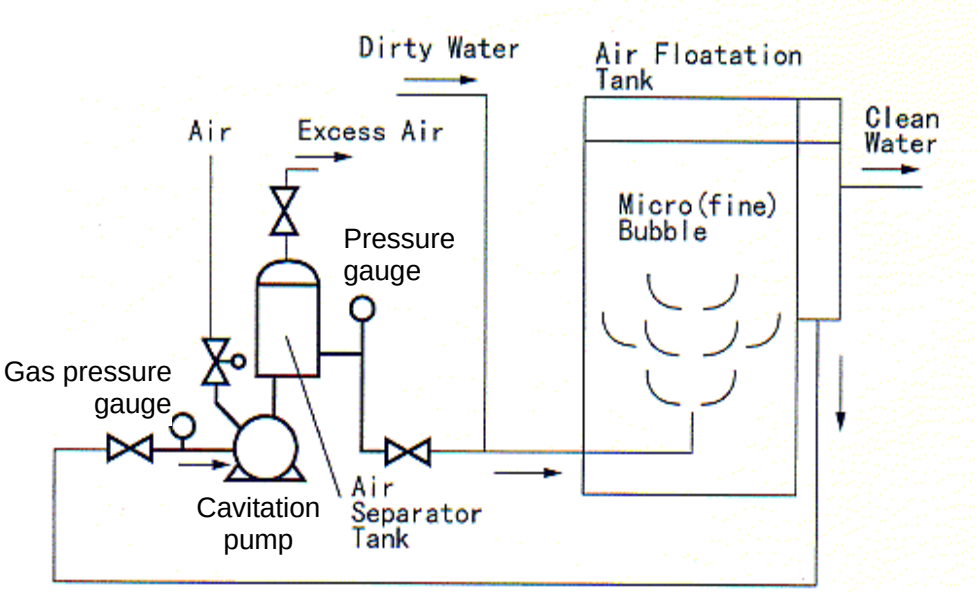

Fig. 2-3 Dissolved air flotation system using the cavitation pump

(http://www.nikuni.co.jp/english/DAFPump/DAFPump.html)

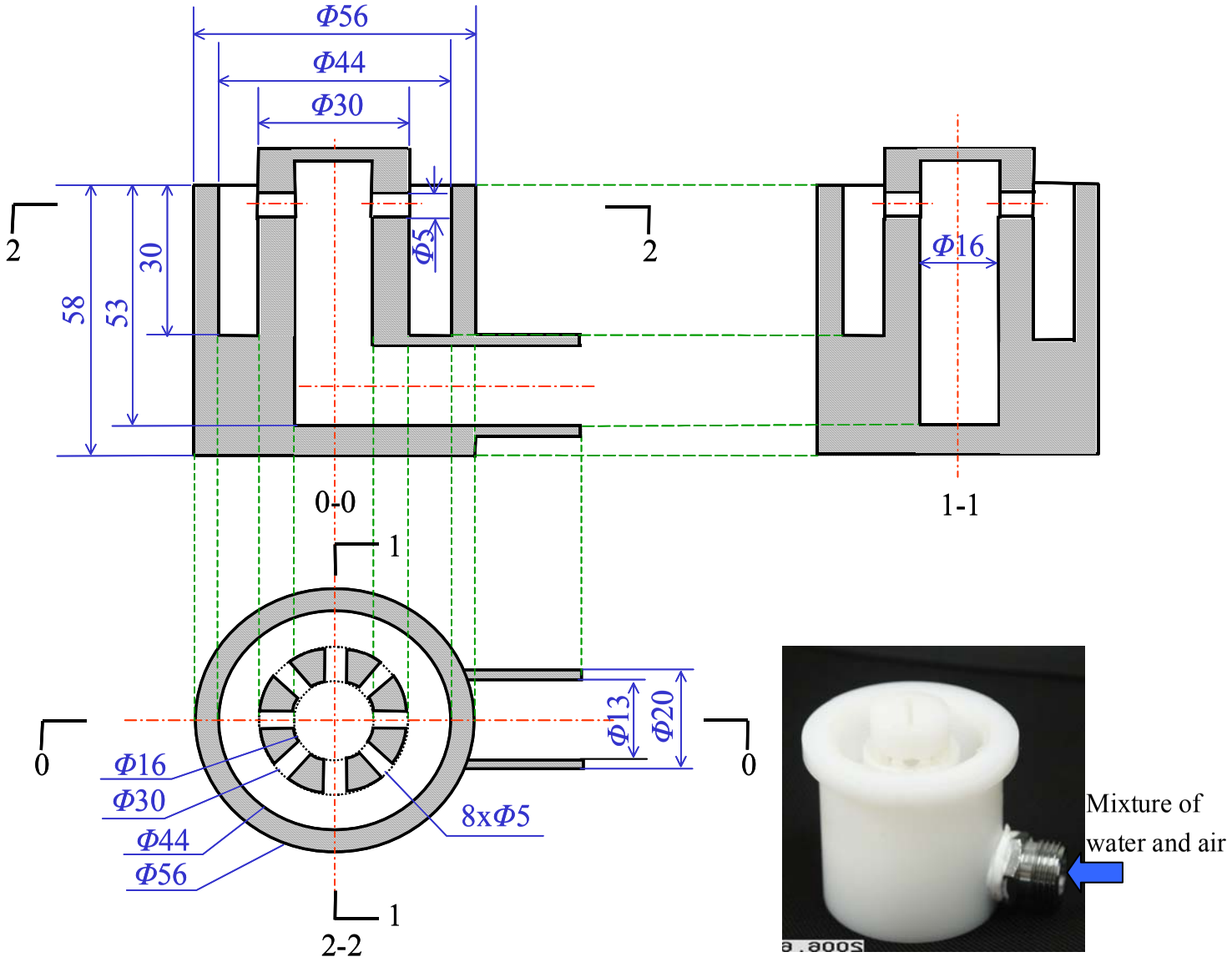

Fig. 2-4 A schematic diagram and a picture of the single nozzle used in method (c)

2.3 Experimental setup

Fig. 2-5 shows the experimental setup which consists of a bubble generation system, a size measurement system and a gas holdup measurement system.

The main part of the bubble generation system is a cylindrical bubble column which is made of acrylic resin with an inner diameter of 0.20m. The rotating-flow microbubble generator (M2-M, Nanoplanet Research Institute Co.) or the dispersing single nozzle was set in the middle of column bottom. Gas was allowed to be induced either by the generator or by the centrifugal pump. A backflow prevention valve was connected between the gas flow meter 8 and the valve 10 or 11.

The bubble size measurement system includes a viewing chamber, a microscope, a high-speed camera, and a monitor. Microbubbles were generated in a bubble column with a height of 60 cm under a flow-through pattern. Bubbly water in the bubble column was introduced through an adjustable valve 14 into the rectangular viewing chamber of 1m×100mm×250mm (height). The high-speed camera (Motionscope8000, NIPPON ROPER Co., Ltd.) was equipped with a VH-Z450 macro lens (KEYENCE, Co.), an X-Y-Z positioning stage and a 12V/100W halogen light source. A micrometer scale with the accuracy of 1 μm was used as a standard scale. The recorded video was reproduced and captured into images with free software named AVI cutter (Version 0.4.2, MTD). Size of microbubbles was obtained by processing the images with PopImaging (Version 3.4.0.0, Digital being kids Co., Ltd). It took us much time to get a size distribution at one condition because not fewer than 300 microbubbles were measured. Therefore, we searched for another time-efficiency measurement technique, that is, laser diffraction particle size analyzer. Sato (2005) compared bubble size distributions obtained from the particle size analyzer (LS230, Beckman Counter, Inc.) with that from the image analysis. She found that they agreed with each other very well with a deviation less than 10 μm. In the method with the laser size analyzer, microbubble sample was taken by a beaker. A surfactant, sodium dodecylbenzenesulfonate solution was added into the sample and quietly mixed with a glass rod. Sato (2005) found that the surfactant addition into

samples make the analysis results more stable. After surfactant addition, samples were poured slowly into the measuring cell where 750nm laser was irradiated and the strength of diffracted/scattered laser was measured. Microbubble size was calculated with an optical module based on both the Fraunhofer and Mie theories of light scattering. The real part of refraction ratio used in the optical module was 1.0 while the imaginary part of it was zero.

Gas holdup was measured to evaluate overall bubble volume concentration. Microbubbles were generated in a bubble column with a height of 1.15m under a circulation pattern. During gas holdup measurement, water circulation was firstly started by switching on the pump without any air suction. After the water surface height got stable, the valve 10 or 11 in the air suction line was then opened and microbubbles were generated. The water surface heights before and during microbubble generation were online measured every 10 seconds with an ultrasonic displacement sensor (UC-500, Keyence Co.), and used to calculate the gas holdup, ε_G, by the following expression,

$$\varepsilon_G = \frac{H_2 - H_1}{H_2} \tag{2-1}$$

where H_1 is the average of stable liquid surface heights [m] before bubbling and H_2 is the average of liquid surface heights [m] in the last 5 minutes of 15 minutes' bubbling.

In general, flow regimes in bubble columns can be divided into homogeneous flow and heterogeneous flow depending on the gas flow rate (Schumpe and Grund, 1986; Deckwer, 1992). At low gas velocities homogeneous flow prevails, i.e. the bubbles have almost uniform small sizes and rise velocities. At higher gas throughputs bubbles coalesce and large bubbles with higher rise velocity than small bubbles are also formed. This flow regime is termed heterogeneous referring to the much different bubble sizes. It is found that the flow regime in bubble columns has a great effect on the gas/liquid mass transfer in chemical industries. Therefore, the flow regime in the bubble column using microbubbles was investigated when gas and water flow rates were changed in wide ranges.

Tap water and air were used as the liquid phase and the dissolving gas, respectively, in all the experiments of this chapter. Water temperature was about 19~25℃.

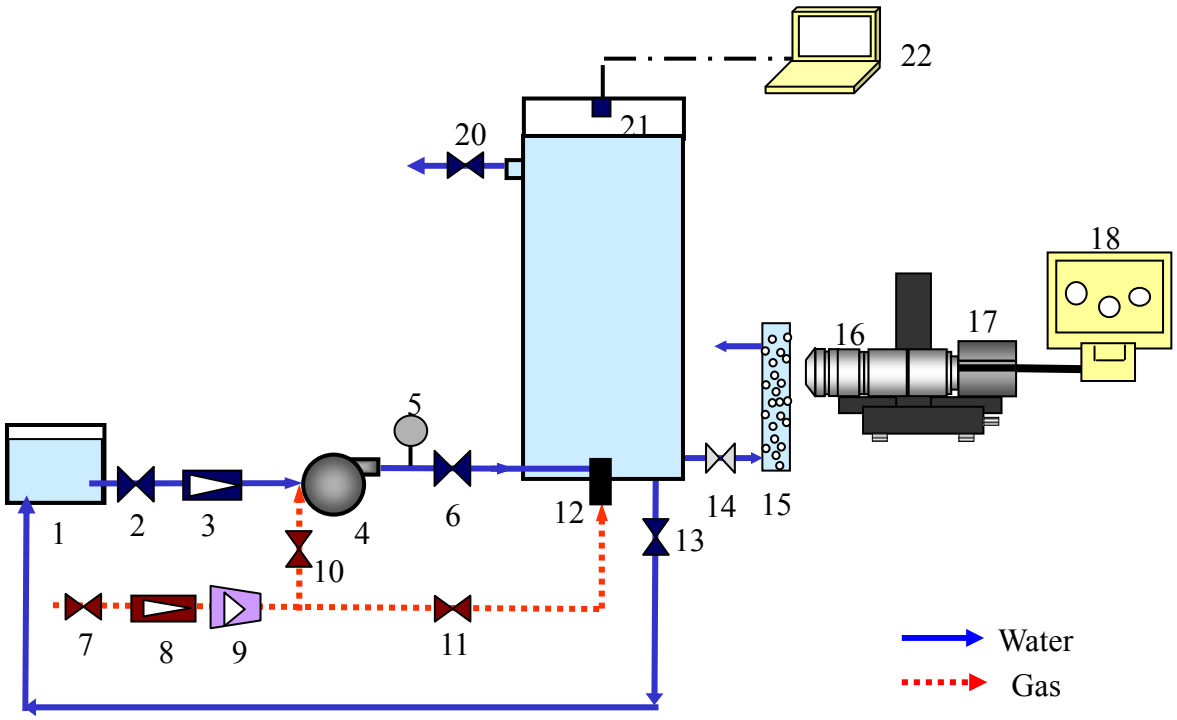

1. Buffer tank
2, 6, 7, 10, 11, 13, 14, 20. Valves
3. Gas flow meter
4. Centrifugal pump
5. Pressure gauge
8. Gas flow meter
9. Backflow prevention valve
12. Microbubble generator or dispersing nozzle
15. Viewing cell
16. Microscope
17. High-speed video camera
18. Video recorder
19. Bubble column
21. Ultrasonic displacement sensor
22. PC

Fig. 2-5 Experimental setup of bubble generation system

2.4 Results and discussion

2.4.1 Microbubble generation conditions

Bubble generation conditions for Type M2-M are illustrated in **Fig. 2-6** where the normal method (a) (Fig. 2-2(a)) was employed (Sato, 2005). At lower gas flow rate, there were only microbubbles generated and water in the bubble column looks like milk; With increasing the gas flow rate, a little amount of milli-bubbles were seen rising to the water surface of bubble column, though they could not be seen from the side of the bubble column; A further increase in gas flow rate resulted in more milli-bubbles which coalesce with microbubbles leading to the increase of transparence in the bubble column, therefore, milli-bubbles could be seen from the side of the bubble column; Much more increase in gas flow rate just increase the quantity of milli-bubbles generated. Water in the bubble column became almost transparent and milli-bubbles were seen jetted from the generator.

As compared with water flow rate, air flow rate seems a little more important for microbubble generation. At the water flow rate, Q_W, of 13.6 L/min, air flow rate, Q_A, should be controlled at least lower than about 0.3 L/min in order to obtain only microbubbles. Microbubbles prevail until the air flow rate reaches 0.7 L/min. On the other hand, for the air flow rate of 0.5 L/min, microbubbles are mainly generated as long as the water flow rate is controlled to be higher than 10 L/min.

Based on these observations, the author concludes that making gas flow rate lower or water flow rate higher than a critical value is necessary for microbubble generation. However, the decrease of gas flow rate results in low microbubble concentration. Meanwhile, it is not recommended to increase the water flow rate too high for yielding fine microbubbles from the view of running cost.

2.4.2 Comparison of microbubble size in the different generation methods

The size distributions of microbubbles produced by the three methods are compared in

Fig. 2-7 at the gas flow rate of 0.5L/min and the water flow rate of 12L/min. **Fig. 2-7(a)** shows the volumetric frequency at each diameter range while **Fig. 2-7(b)** shows the numerical one. Bubble generated by three methods under the present condition were mainly distributed in the range of 20~200 μm. Much smaller microbubbles were formed by the improved method (b) as compared to the normal method (a). Microbubbles generated by the method (c) have the broadest distribution and the largest mode diameter.

The average diameter and standard deviation are listed in **Table 2-1**. Microbubbles generated in the improved method (b) have the smallest average diameter of 50 μm and standard deviation of 23μm. The average diameters in method (a) and (c) are 55 μm and 67 μm, respectively.

2.4.3 Comparison of gas holdup in different microbubble generation methods

The variation of water surface height is shown in **Fig. 2-8** where microbubbles were generated with the normal method (a) at different gas flow rates. Water circulation was started at t=0 but no air was drawn in, therefore, the water surface level kept constant in the first few minutes. When the valve in the air suction line was opened, a sudden rise in the water surface height was observed at each gas flow rate. After that, the water surface approximately approached at a constant level. When the pump was switched off with cutting off air suction at the same time, microbubble generation was finished. After that, the water level dropped because of the disengagement of bubbles remaining in the bubble column. The disengagement profiles at different gas flow rates were obviously different. The water level gradually dropped after stopping bubble generation at the gas flow rate of 0.5 L/min (**Fig. 2-8(a)**). On the other hand, at higher gas flow rates of 1.0 and 1.5 L/min, the drops of the water surface height were very fast right after stopping bubble generation, and then became slow as shown in Fig. 2-8 (b) and (c).

Because bubble rise velocity depends on bubble size (Fig. 1-3), the dropping rate of water surface height is also determined by the bubble size. Therefore, the characteristics of disengagement indicated that bubbles generated at Q_A=0.5 L/min had uniform and small bubble size while those at Q_A=1.0 L/min and Q_A=1.5 L/min have two distinct size classes, that is milli-bubbles and microbubbles. The bubble generation conditions as

shown in Fig. 2-6 agree with the information obtained from the gas holdup as well.

Fig. 2-9 shows the change of water surface heights with time in the improved method (b). As same as that observed in the method (a), the water level raised fast till it reached an almost constant value. However, the water level suddenly went up rather than dropped down right after stopping microbubble generation. After arriving at a peak, the water surface went down with a gradually decreasing rate. The increase of water surface height after stopping microbubble generation was due to the sudden pressure drop in the pump. During microbubble generation, air was pressurized and partly dissolved into water by the pump. The volume of air was recovered after being released from the generator due to its compressibility, which resulted in the increase of water surface height after switch off the pump.

Fig. 2-10 shows how the water level varied in the method (c). As compared to the method (b), the water surface height fluctuated more intensely. It was investigated that many milli-bubbles were formed during bubble generation and their burst on the water surface made the surface fluctuate much more. The comparison of disengagement profile with method (b) shows that water levels dropped more quickly in method (c) after stopping bubble generation, which suggests that bubbles generated in method (c) had larger size than that in method (b).

The gas holdups obtained in three methods are calculated using Eq. (2-1) and compared in **Fig. 2-11**. The highest gas holdup was achieved for the method (b), where gas is aspirated by the pump with the microbubble generator. However, when the gas was allowed to be induced by the generator (Fig. 2-2 (a)) or the generator was changed to the dispersing nozzle (Fig. 2-2 (c)), the gas holdup greatly decreased by 30-60%. Water in the bubble column seemed like milk during microbubble generation by the method (b), while it was almost transparent and milli-bubbles were investigated when methods (a) and (c) were applied.

It is suggested that the rotating-flow microbubble generator in the improved method (b) play an important role, that is, the prevention of microbubble coalescence. As the microbubble generator is not allowed to induce gas, it just works like an injection nozzle. When water is pumped into it, a two-phase flow with very high rotation velocity occurs,

which prevents the released bubbles from coalescing. On the other hand, the undissolved part of induced air is sheared by the rotating flow and spouted out as microbubbles. Therefore, much more microbubbles can be generated in the method (b).

2.5 Conclusions

Smaller microbubbles and higher gas holdup relating higher microbubble volume concentration were achieved in the improved method (b), where the rotating-flow microbubble generation was combined with the cavitation pump. It is expected that the novel microbubble generation system could show good performance when applied to the advanced water and wastewater treatment. The following three chapters will give some discussion on its applications.

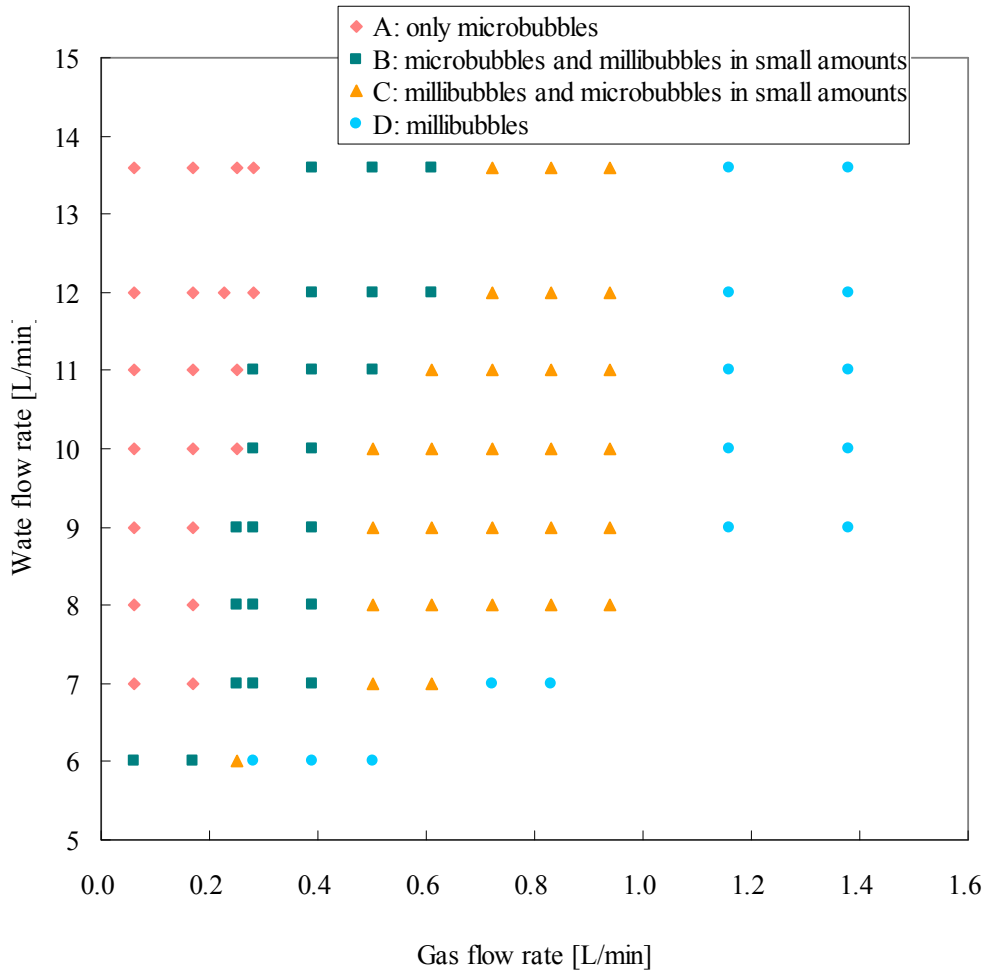

Fig. 2-6 Bubble generating conditions of the rotating-flow microbubble generator M2-M (Sato, 2005)

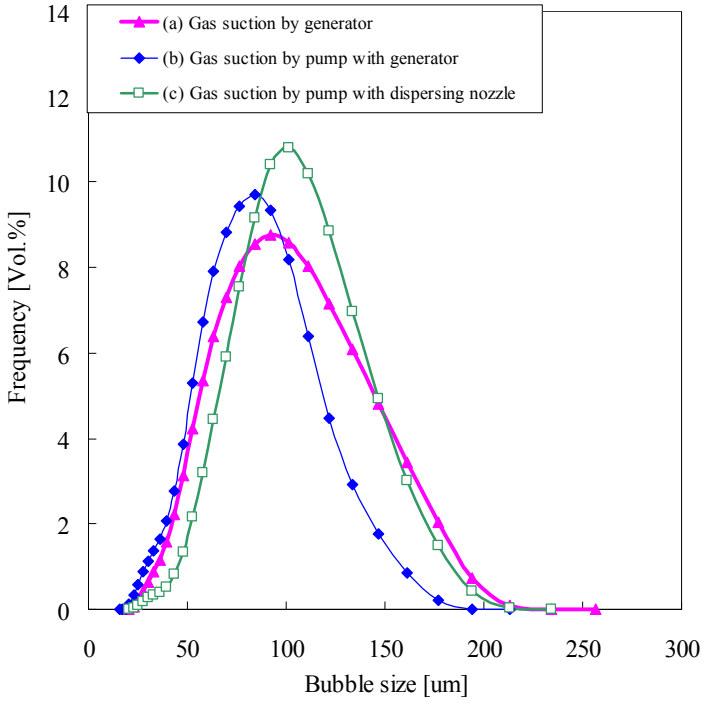

(a)

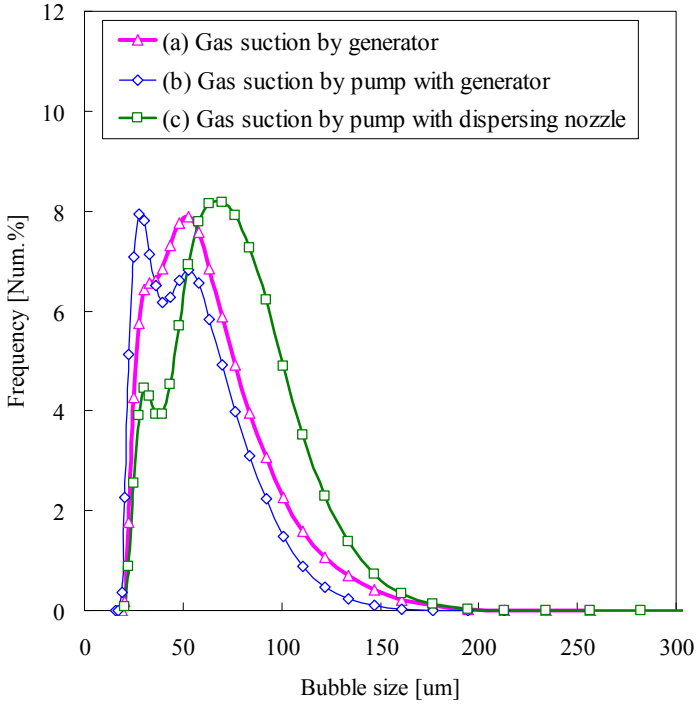

(b)

Fig. 2-7 Comparison of microbubble size distributions in different generation methods (M2-M; Q_W: 12L/min; Q_A: 0.5L/min)

Table 2-1 Comparison of microbubbles generated in different methods

Method	Average diameter	Standard deviation
	μm	μm
(a)	55	26
(b)	50	23
(c)	67	29

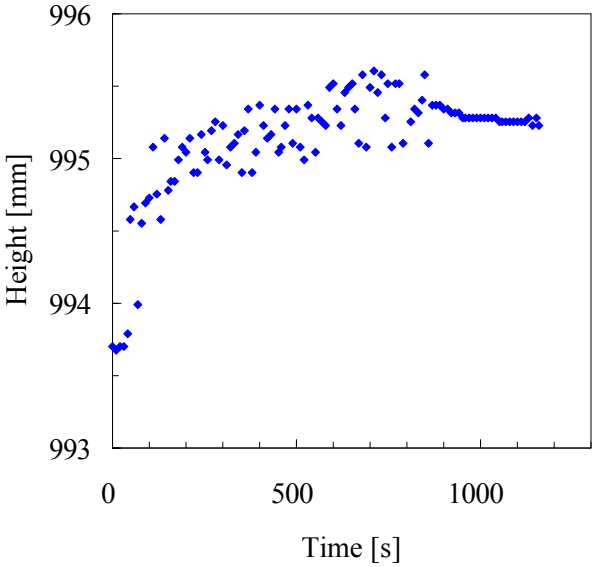

(a) Q_W: 12 L/min Q_A: 0.5L/min

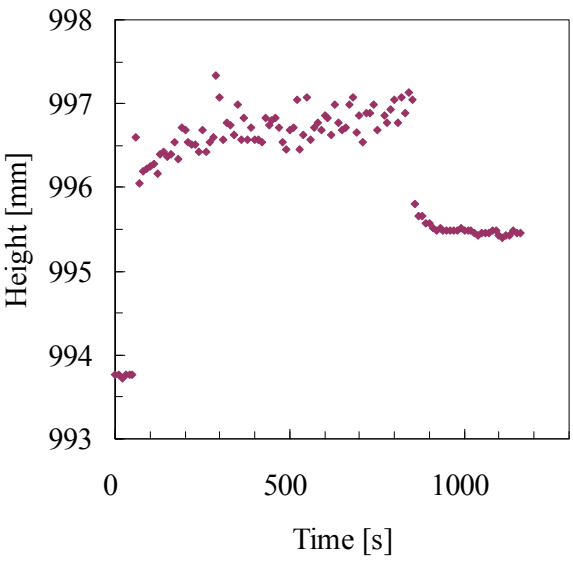

(b) Q_W: 12 L/min Q_A: 1.0 L/min

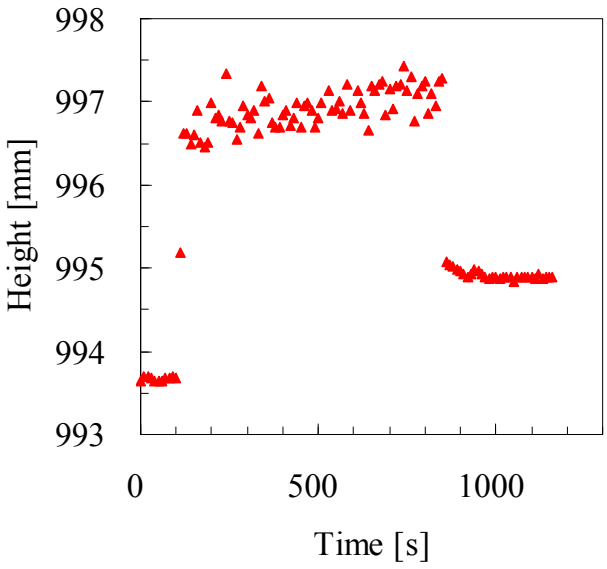

(c) Q_W: 12 L/min Q_A: 1.5L/min

Fig. 2-8 Variation of water surface height in the normal method (a)
(Gas suction by generator)

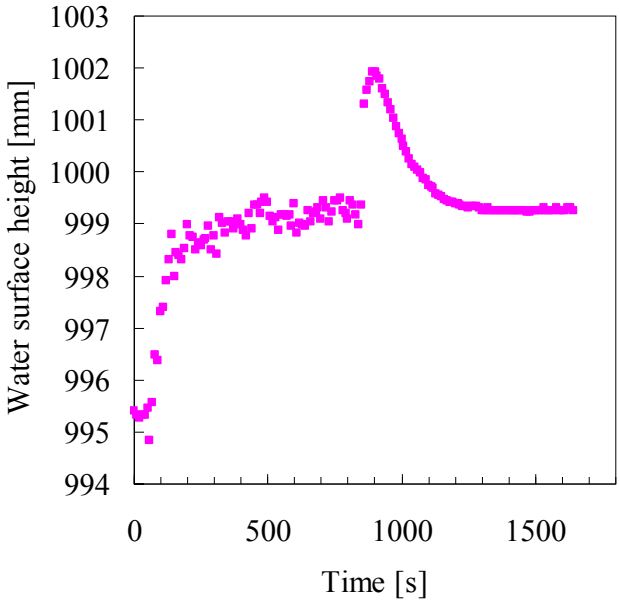

(a) Q_W: 12 L/min Q_A: 0.5L/min

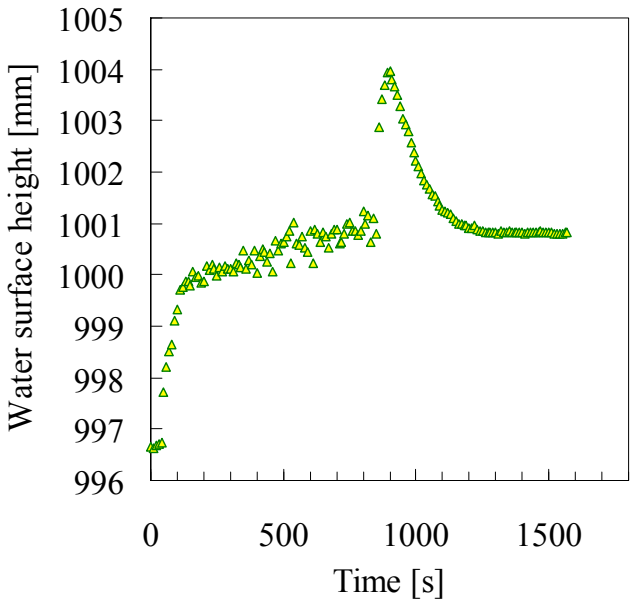

(b) Q_W: 12 L/min Q_A: 1.0 L/min

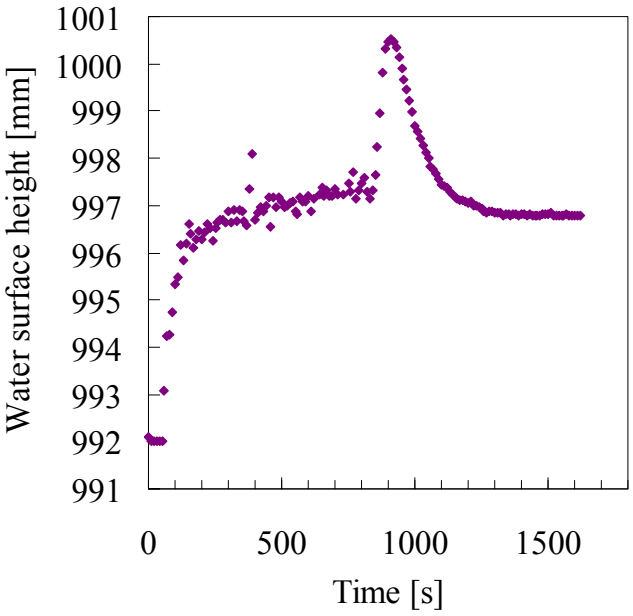

(c) Q_W: 12 L/min Q_A: 1.5L/min

Fig. 2-9 Variation of water surface height in the normal method (b)

(Gas suction by pump through generator)

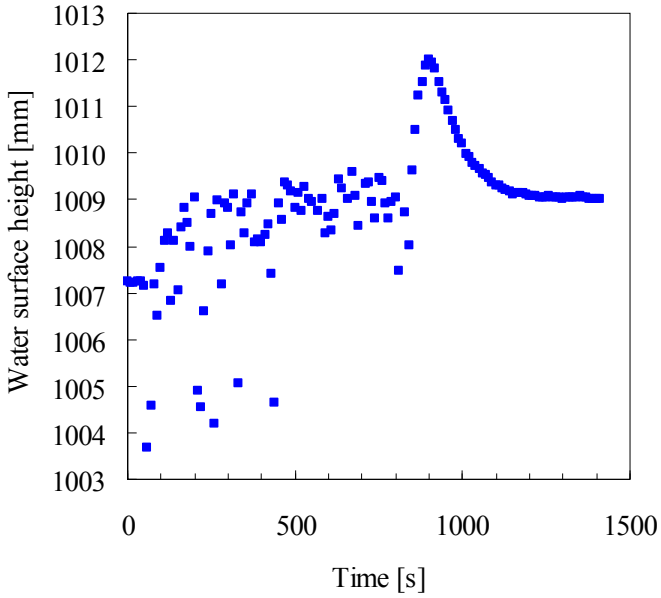

(a) Q_W: 12 L/min Q_A: 0.5L/min

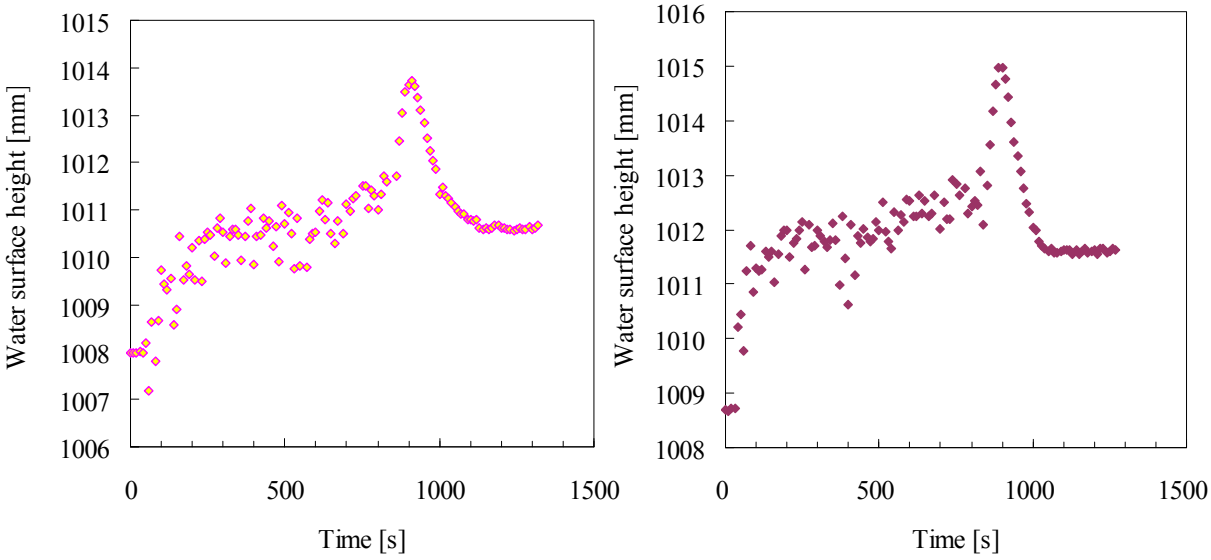

(a) Q_W: 12 L/min Q_A: 1.0 L/min

(c) Q_W: 12 L/min Q_A: 1.5L/min

Fig. 2-10 Variation of water surface height in the normal method (c)

(Gas suction by pump through dispersing nozzle)

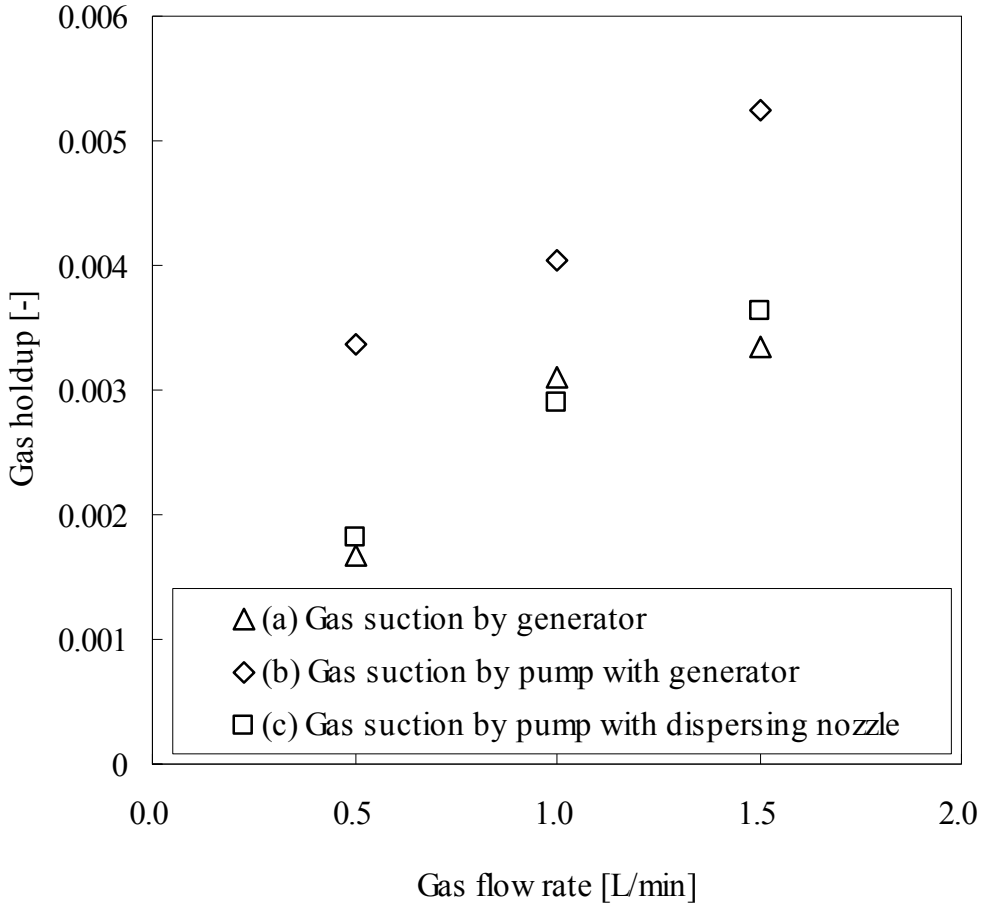

Fig. 2-11 Effect of microbubble generating method on gas holdup (Q_W: 12L/min)

Nomenclature

H_1	average of stable liquid surface heights before bubbling	[m]
H_2	average of liquid surface heights in the last 5 minutes of 15 minutes' bubbling	[m]
Q_A	air flow rate	[L/min]
Q_W	water flow rate	[L/min]
t	time	[min]
ε_G	gas holdup	[—]

Literature cited

Deckwer, W. D.; "Bubble Column Reactors," John Wiley & Sons Ltd, West Sussex, England, pp.3-4 (1992)

Haarhoff, J. and J. K. Edzwald; "Dissolved Air Flotation Modelling: Insights and Shortcomings," *J. Water Supply: Research & Technology-AQUA*, **53**, 127-150 (2004)

Okamoto, R., H. Takeda, H. Shakutsui and H. Ohnari; "Performance of Micro-Bubble Generators," *Japanese Society for Multiphase Flow Annual Meeting*, Tokyo, Japan, August (2005) (in Japanese)

Ohnari, H., T. Saga, K. Watanabe, K. Maeda and K. Matsuo; "High Functional Characteristics of Micro-bubbles and Water Purification," *Resources Processing*, **46**, 238-244 (1999) (in Japanese)

Ohnari, H.; "Swirling Type Micro-Bubble Generating System," Japanese Patent, 2000-618002 (2002)

Sato, U.; "Effects of factors on microbubble generation," Bachelor's thesis, Keio University, pp.35 (2005) (In Japanese)

Schumpe, A. and G. Grund; "The Gas Disengagement Technique for Studying Gas Holdup Structure in Bubble Columns," *Can. J. Chem. Eng.,* **64**, 891-896 (1986)

CHAPTER 3

Induced air flotation using microbubbles

3.1 Introduction

As introduced in Section 1.4.1, the flotation recently gains much interest in water and wastewater treatment due to its high throughput and efficiency. The general process of flotation separation can be divided into two types in terms of bubble generation methods, that is, Dissolved Air Flotation (DAF), and dispersed air flotation which is often known as Induced Air Flotation (IAF).

3.1.1 Dissolved Air Flotation

The schematic diagram of a water treatment system using Dissolved Air flotation (DAF) is shown in **Fig. 3-1.** Raw water is introduced into the water treatment plant. The fine particles in raw water are flocculated producing flocs in the pretreatment process which involves two steps: particle destabilization and particle flocculation. Particle destabilization takes place after dosing chemical coagulant in the flash mixer, where the coagulant is dispersed uniformly and quickly by a high-speed stirrer. On the other hand, particle flocculation and growth of aggregates occur during the slow mixing stage in the flocculator.

In the major component of DAF process, part of purified water is recycled and saturated up to 70~80% with air at elevated pressure in the range of 0.4~0.5MPa. The pressurized water is then decompressed via injection nozzles in the flotation cell. The released gas bubbles readily adhere to the surface of floc particles forming bubble-particle agglomerates and rise to the liquid surface where a layer of sludge forms, which can be removed over a beach (Zlokarnik, 1998; Jameson, 1999; Shawwa and Smith, 2000).

Microbubbles in DAF has an average diameter d_b of 40-80μm (Han *et al*., 2002b; Haarhoff and Edzwald, 2004). The use of such small bubbles improves the bubble-particle collision efficiency which is one of the most important factors in particle removal. However, the DAF process has a number of inherent disadvantages, that is, high electrical power requirement, complex system including a compressor, a saturator and a separate flotation tank and higher service costs (Schofield, 2001). Moreover, because the bubble generation principle in DAF is based on the Henry's law, the amount of air dissolved into water at a given pressure and temperature is limited and relatively low. The maximum value of air/water ratio is about 1/17-1/13 under normal conditions, as mentioned in Chapter 1.

3.1.2 Induced Air Flotation

Induce Air Flotation (IAF) is occasionally found in wastewater treatment, where relatively large bubbles with diameters of several hundreds micrometers are formed by mechanical agitation or sparger air injection (Evans *et al*., 1992; Heindel and Bloom, 2002). Many researchers suggested that the large bubbles in IAF have correspondingly large terminal velocities leading to much more compact flotation systems. They tried to use the IAF as an alternative to the DAF in water treatment. Zlokarnik (1982 and 1998) developed IAF with a specially designed self-aspirating and radically discharging funnel-shaped nozzle. Jameson (1999), Yan and Jameson (2004) utilized a confined plunging jet flotation cell, also known as a Jameson cell, to remove oils and fats from dairy and abattoir wastes, and blue-green algae from natural waters and maturation ponds.

However, the bubble size also has an effect on the efficiency of bubble-particle collision. Large bubbles lead to poor collision efficiency (Shawwa *et al.*, 2000). Moreover, high shear in conventional mechanical flotation cell usually results in breakage of the fragile particles (Jameson, 1999; Zabel, 1992). These disadvantages are usually overcome by dosing some surfactants to produce smaller bubble and impart hydrophobicity to hydrophilic flocs (Jameson, 1999). The addition of surfactant is obviously not a good idea, because that will cause additional treatment for the sludge and

complex operation system.

3.1.3 Purpose in this chapter

It is necessary to search for a simple and energy saving method which can successfully generate numerous microbubbles, and meanwhile will avoid high shear rates to obviate the destruction of the aggregates.

In this chapter, we focused on developing a new form of IAF with the rotating-flow microbubble generator for water treatment. To approach to the goal, we have to overcome its disadvantages, that is, high turbulence during microbubble generation and low microbubble concentration. In the preliminary stage, we attempted designing a **separated flotation system** in Section 3.2. The high-shear region in the liquid where microbubbles are produced is separated from the relatively quiescent zone where flotation takes place in the separated flotation system. After that, we tried to develop a more simple system, **one-cell flotation system,** in Section 3.4 by searching for an appropriate polymeric flocculant and increasing the microbubble concentration with the improved microbubble generation system.

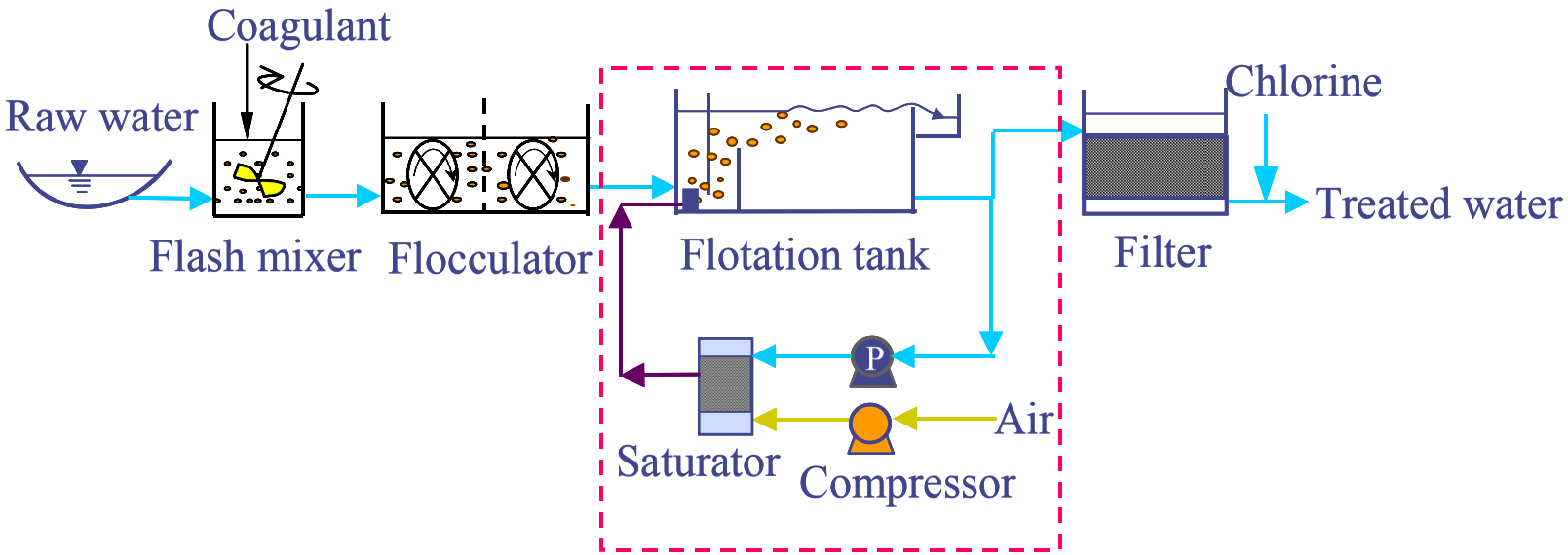

Fig. 3-1 Schematic diagram of dissolved air flotation (DAF) process

3.2 Separated flotation system

3.2.1 Experimental setup

The experimental setup as shown in **Fig. 3-2** consists of three units: microbubble generation unit, batch flotation unit and bubble size measurement unit. The objects that we separate the microbubble generation zone from the flotation zone are: (1) to avoid the destruction of fragile flocs by the turbulent during bubble generation; (2) to obtain a stable and high microbubble concentration.

The normal method (Fig. 2-2(a)) was employed in the microbubble generation unit, where a rotating-flow microbubble generator (M2-M, Nanoplanet Research Institute Co.) was set in the middle of a cylindrical acrylic tank with the dimensions of Φ20×55 cm (height). Tap water in the buffer tank was pumped by a centrifugal pump (WPS401, Iwaya Electric MFG Co., Ltd.) to the microbubble generator by which gas, at the same time, was aspirated. The tap water used to generate microbubbles is called as recycle water, because in water treatment plant it is recycled from the treated water as shown in Fig. 3-1.

Kaolin suspension (10 mg kaolin in 1 L tap water) was prepared as simulated raw water because such kind of suspended matters as kaolin are the major impurities in water and wastewater. The initial turbidity of the sample water was maintained near 8 NTU in each experiment.

Kaolin particles in water are characteristically very small and they tend to suspend in water due to both their small size and to the electrical charge between particles (typically negative). Coagulants are always used to neutralize the repulsive electrical charges surrounding particles allowing them to “stick together” creating flocs. Alum ($Al_2(SO_4)_3$) is the most common coagulant used in water treatment, and it was utilized in the present experiments in Section 3.2. Standard jar testers using different alum dosages and flocculation times were carried out to determine the optimum flocculation conditions.

The main part in the batch flotation unit is the flotation tank which is a cylinder made

of acrylic resin, whose inner diameter was 10cm with the height of 26cm.

The flotation experimental procedures are as follows: (1) kaolin suspension with volume of V_0 was filled into the flotation tank; (2) alum was injected into the kaolin suspension and rapidly mixed with it for 5min at a rotating rate of 150rpm so that it was distributed as evenly as possible in the suspension; (3) then the rotating rate was slowed down to 40 rpm in order to enhance contact between floc particles and colloidal particles as well as floc particles themselves, which allowed the floc particles to grow up in size. The time for slow mixing which was called flocculation time was varied in the range of 0~20 minutes; (4) after the slow mixing was finished, bubbly water (volume V_r) in the microbubble generation tank was induced into the flotation tank; (5) microbubbles collided with the kaolin particles and carried them to the surface without any mixing. During this flotation period, samples were taken from the bottom every 5 minutes for 20 minutes; (6) turbidities of samples were measured with a turbidimeter (TN-100, Eutech Instruments Pte. Ltd.) to examine the weight concentration of kaolin particles and video images were taken with a high-speed video camera (Motionscope800, Nipponpoper Co., Ltd.) to study the attachment of bubbles and floc particles. The pH (HM-40S, DKK-TOA Co.) of the initial sample water was 7.51~7.60 and subsequently varied in the range of 6.90~7.11 after the addition of the coagulant.

As the bubbly water was added into the flotation tank, the kaolin suspension was diluted according the dilution ratio, $r(=V_r/V_0)$. Therefore, the initial concentration of kaolin should be revised as follows,

$$C_0^{'} = \frac{C_0 V_0 + C_r V_r}{V_0 + V_r} = \frac{C_0 + C_r (V_r / V_0)}{1 + V_r / V_0} = \frac{C_0 + r \cdot C_r}{1 + r} \qquad \textbf{(3- 1)}$$

where C_0 is the turbidity of raw kaolin suspension [NTU], C_r is the turbidity of bubbly water from the microbubble generation tank, r is the dilution ratio which is also referred to as recycle ratio (r was kept 10% in all experiments in Section 3.2). Because the tap water with a turbidity of zero was used to generate microbubbles (C_r=0), the revised initial concentration can be reduced to,

$$C_0^{'} = \frac{C_0}{1 + r} \qquad \textbf{(3- 2)}$$

The particle removal efficiency, R [%], in the batch flotation experiments is defined by the following equation,

$$R = \frac{C_0^{'} - C}{C_0^{'}} \times 100 \qquad \textbf{(3- 3)}$$

where C is the turbidity of treated kaolin suspension [NTU]. Substituting Eq. (3-2) into Eq. (3-3) gives the expression of the particle removal efficiency, R, as follows,

$$R = \frac{C_0 - (1+r) \cdot C}{C_0} \times 100 \qquad \textbf{(3- 4)}$$

It has been found that the most important parameter in the air flotation system is the surface characteristics (zeta potential) of both bubbles and particles, and the next is the sizes of the bubbles and the particles (Han, 2002b). In the present experiments, the size and zeta potential of floc particles were varied by changing the flocculation time and coagulant dosage. The sizes of microbubbles were controlled by changing flow rates of recycle water and induced air, while the zeta potential of microbubbles was not controlled.

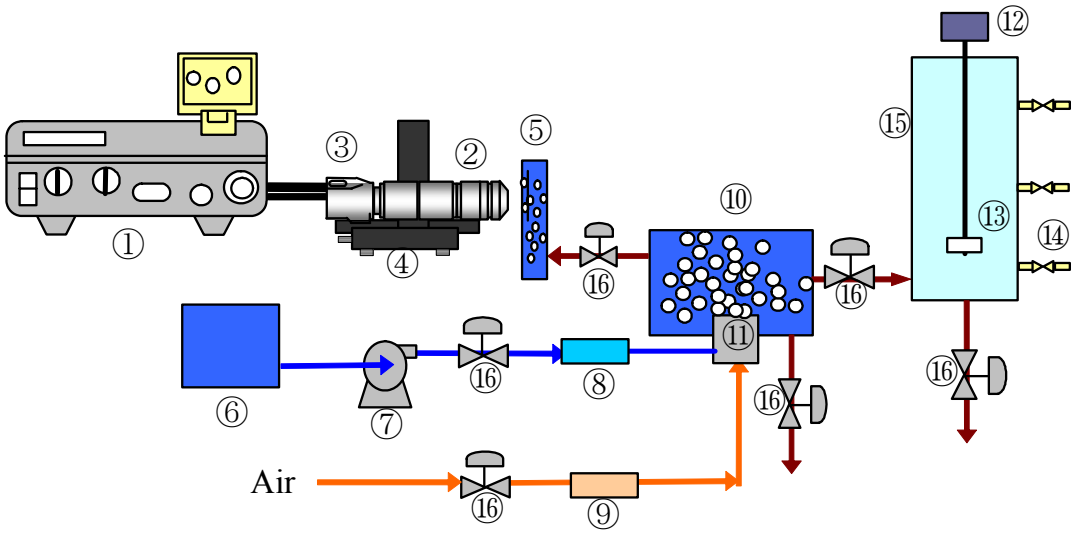

① Monitor and controller
② Microscope
③ CCD Camera
④ Adjustable microscope support
⑤ Viewing chamber
⑥ Buffer tank
⑦ Pump
⑧ Water flow meter
⑨ Gas flow meter
⑩ Microbubble generation tank
⑪ Microbubble generator
⑫ Variable speed Motor
⑬ Impellor
⑭ Sampling tap
⑮ Flotation tank
⑯ Valve

Fig. 3-2 Experimental setup for separate flotation

3.2.2 Results and discussion

(1) Effect of coagulant dosage on particle removal efficiency

The effect of alum dosage on the particle removal efficiency is illustrated in **Fig. 3-3 (a) and (b).** Flotation time, that is, sampling time, means the period when microbubbles adhered to floc particles and carried them to the water surface. The alum dosage was varied from 0.56mg/L to 4.0mg/L and the flocculation time was kept 10 minutes. Microbubbles were generated under the water flow rate of 6.67 L/min and the induced air flow rate of 0.6 L/min.

The removal efficiency increased when the flotation time increased from 0-15 minutes, but did not change so much when it got longer than 15 minutes as shown in **Fig. 3-3(a)**. When the alum dosage increased from 0.56 mg-Al/L to 1.0 mg-Al/L, the particle removal efficiency after 15 minutes' flotation increased from 52% to 85%. However, it gradually decreased when the alum dosage was over 2.5 mg-Al/L as shown in **Fig. 3-3(b)**. The optimum dosage range of alum is between 1.0 to 2.5 mg-Al/L.

Air bubbles are negatively charged the same as kaolin suspension (Okada and Akagi, 1987; Okada *et al.*, 1990). The kaolin zeta potential becomes less negative with the addition of alum, and reaches zero and even positive as the dosage increases (Han *et al.*, 1999; Han *et al.*, 2001). Therefore, the collision between the negatively charged bubbles and the floc particles become much better as the zeta potential of floc particles increases linearly with alum dosage. As a result, higher removal efficiency occurs when the magnitude of positive charge is greater. However, too much over dosage will decrease the zeta potential of floc particles as referred by Han *et al.* (1999), therefore, the particle removal efficiency decreased.

(2) Effect of flocculation time on particle removal efficiency

Fig. 3-4 (a) and (b) show the particle removal efficiency at various flocculation times. Flocculation time is the slow mixing time after the addition of alum. Fine kaolin particles

grow up to flocs during the slow mixing. Microbubbles were generated at the water flow rate of 13.7 L/min and the induced air flow rate of 0.6 L/min. The alum dosage was 1.0 mg-Al/L, while flocculation time, slow mixing time after initial rapid mixing, was varied from 5 min to 20 minutes.

When the flocculation time was zero, that is to say, no slow mixing was performed, the particle removal efficiency is as low as about 15% as shown in **Fig. 3-4 (a)**. As it was increased to 5 minutes, the removal efficiency increased suddenly. After that, the highest removal occurred when the flocculation time exceeded 10 minutes as shown in **Fig. 3-4 (b).**

The flocs gradually grew up during the slow mixing. For the sedimentation process large flocs are required. But flotation does not require large floc particles. In fact, floc particle densities less than water are required and are achieved by attachment of air bubbles to floc particles. Consequently, the use of longer flocculation times is not economically feasible in practice. This result coincides with the design and operation of DAF, where shorter flocculation times are preferred.

(3) Effect of air flow rate on particle removal efficiency

Fig. 3-5 (a) and **(b)** show the effect of flow rate of induced air on the particle removal efficiency. Microbubbles were generated under the water flow rate of 13.6 L/min and the induced air flow rate of 0.38 L/min, 0.60 L/min, 0.72 L/min and 0.95 L/min. The alum dosage was 1.0 mg/L and the flocculation time after rapid mixing was 10 minutes. Better particle removal efficiency was achieved at lower air flow rate as shown in **Fig. 3-5 (b)**.

From the bubble generation map in Fig. 2-6, we can see that much more microbubbles are generated at low gas flow rate for a given water flow rate. The occurrence of milli-bubbles at high gas flow rats leads to the bubble coalescence which results in the decrease of microbubble concentration in the generation tank. Therefore, the particle removal efficiency was decreased with increasing the air flow rate.

(4) Effect of recycle water flow rate on particle removal efficiency

Fig. 3-6 (a) and **(b)** show the effect of water flow rate on particle removal efficiency. The alum dosage was 1.0mg/L and the flocculation time was 10min. The water flow rate during microbubble generation was varied to be 6.7L/min, 10.0L/min, and 13.7 L/min, and the induced air flow rate was at a constant value of 0.60 L/min. The particle removal efficiency at various water flow rates reaches to a similar level as shown in **Fig. 3-6 (b)**. However, the removal efficiency reached 76% right after 5 minutes' flotation at the water flow rate of 6.7 L/min, while it was only 40% obtained at Q_W=13.6 L/min.

It has been proved that the bubble size decreases with the increase of water flow rate (Sato, 2006). Smaller microbubbles generated at Q_W=13.6 L/min have low rise velocity. Therefore, it took much longer time for these smaller bubbles to carry the flocs to the water surface.

3.2.3 Conclusions

A separated Induced Air Flotation (IAF) system was developed in this section, where the bubble generation zone was separated from the flotation. Microbubbles generated in the IAF are distributed in the size range of 20–200 μm and the average size is around 70 μm. To examine its suitability for removal of particles from water, the particle removal efficiency at various operational conditions was measured in batch IAF experiments of a kaolin suspension system. The IAF has the ability to remove particles by 80~90% from water with kaolin particles at the concentration of 10 mg/L.

The results of removal efficiency in the batch experiments also show that the chemical pretreatment is critical to IAF performance. Lower flocculation time and alum dosage could be employed in IAF. Microbubbles were generated at various flow rates of recycle water and induced air. Low air flow rates performed a little better particle removal, because more microbubbles were generated at low air flow rate. On the other hand, low water flow rates shortened the flotation time, because big microbubbles generated at low water flow rates could rise more quickly. In another word, not only the microbubble concentration but also the bubble size is very importance for the IAF.

The results from the batch experiments in the separate flotation system give valuable basic knowledge. But the separate flotation system seems too complex to be used in

practice. Much simpler system should be developed.

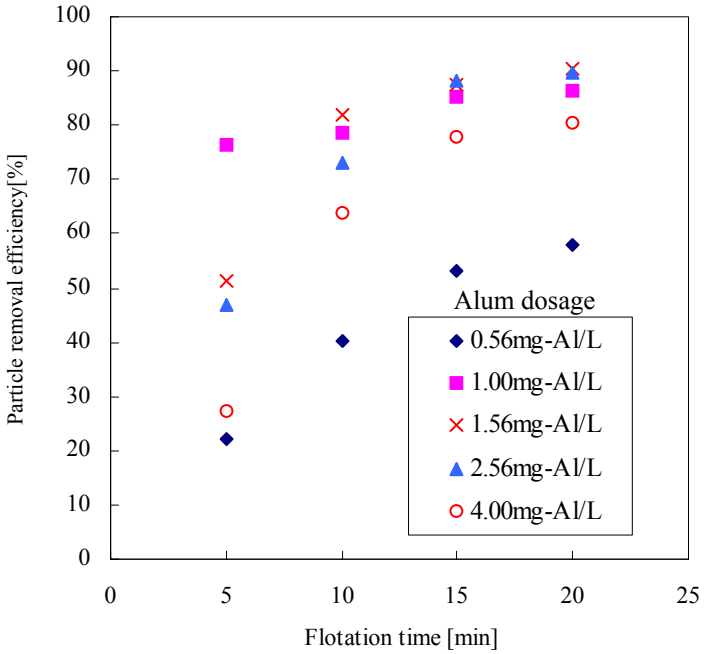

(a)

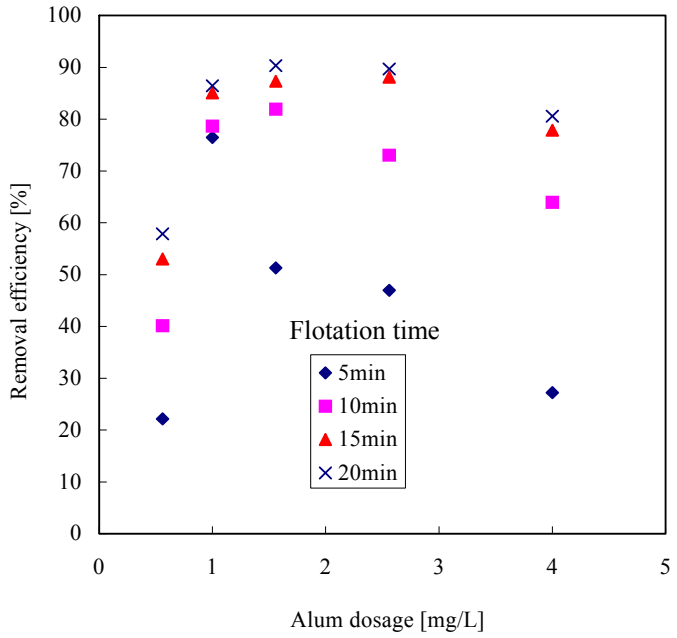

(b)

Fig. 3-3 Effect of alum dosage on particle removal efficiency

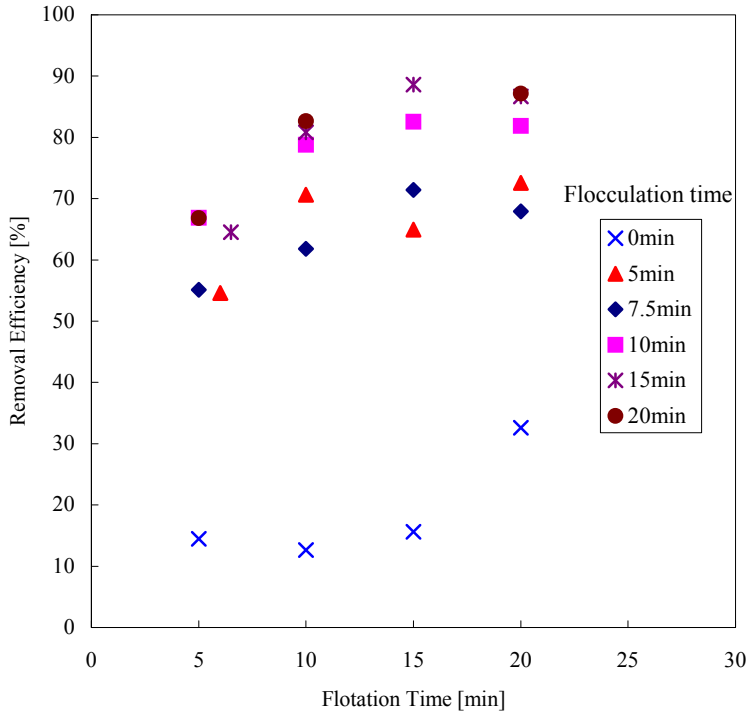

(a)

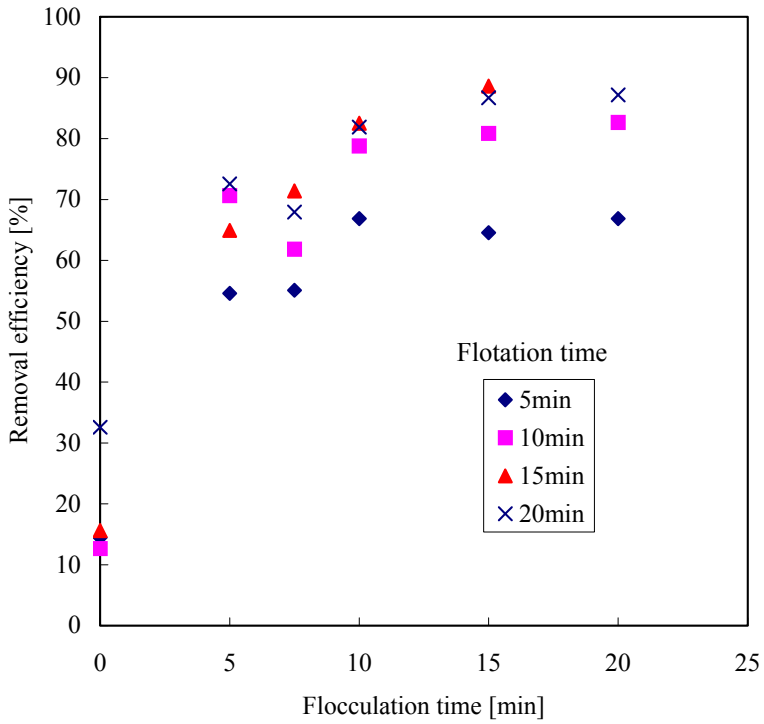

(b)

Fig. 3-4 Effect of flocculation time on particle removal efficiency

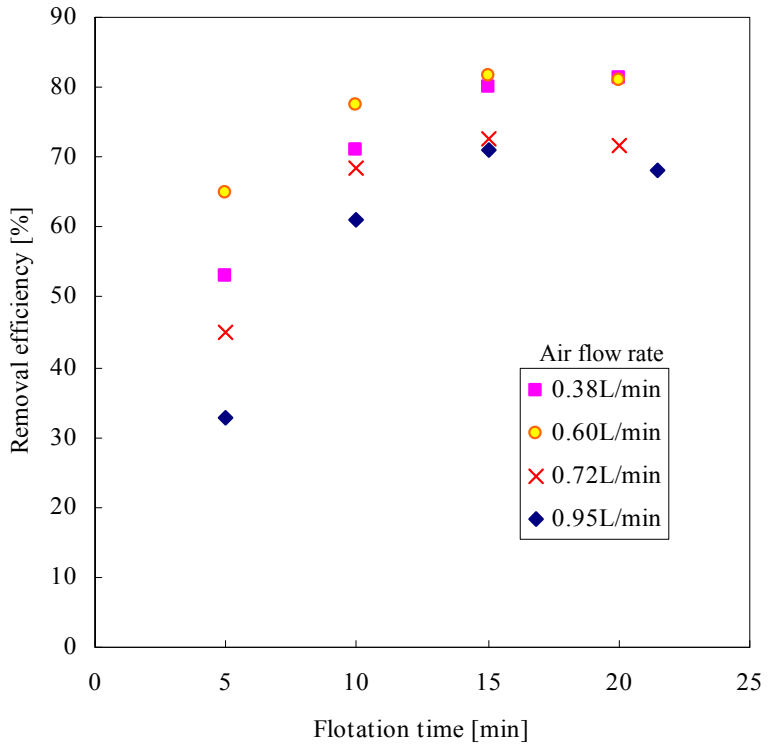

(a)

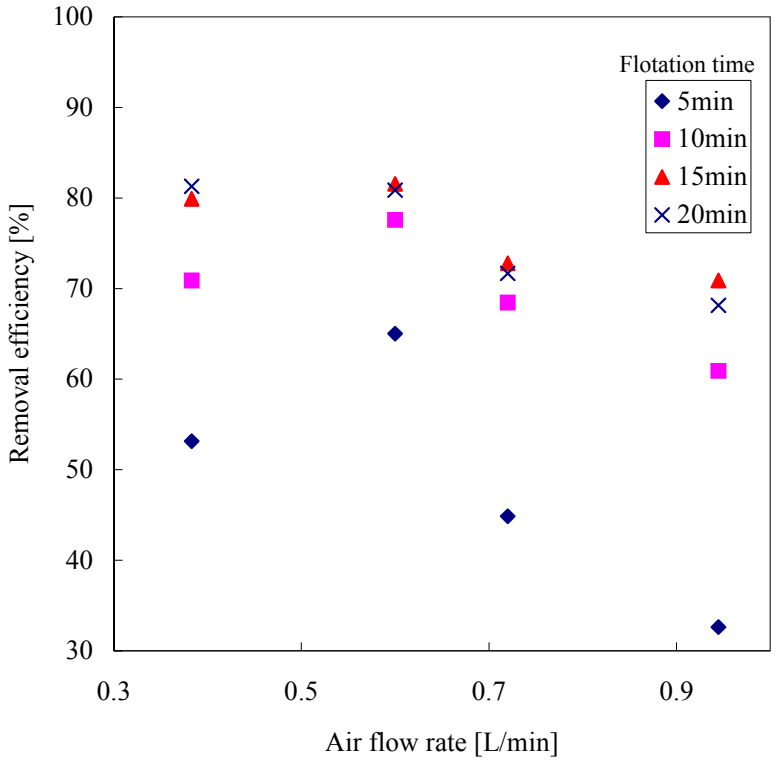

(b)

Fig. 3-5 Effect of air flow rate on particle removal efficiency

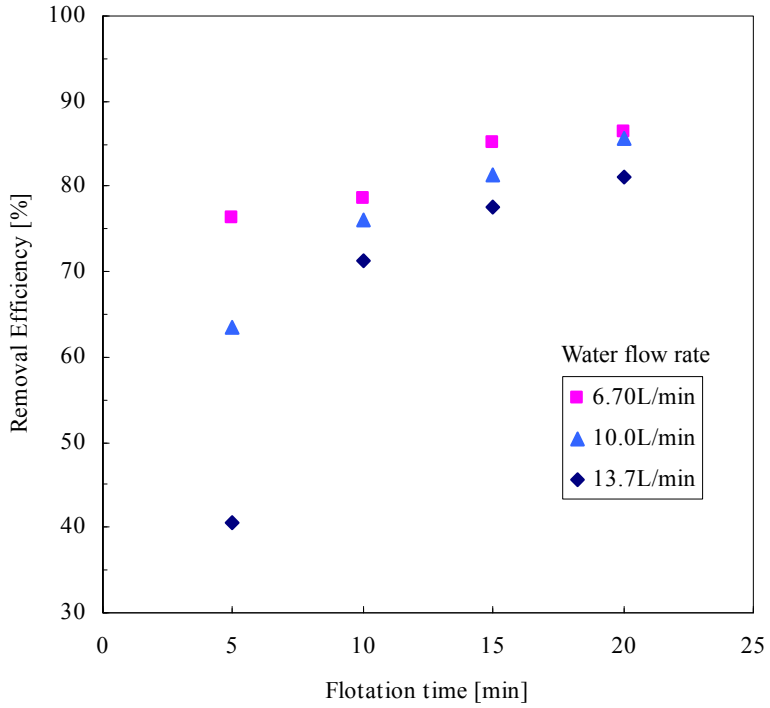

(a)

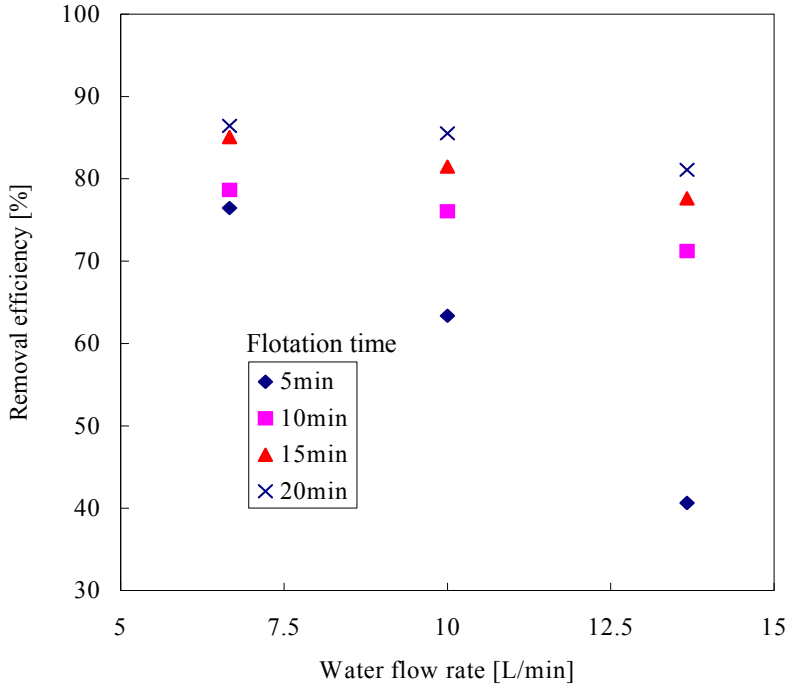

(b)

Fig. 3-6 Effect of water flow rate on particle removal efficiency

3.3 Preliminary experiments for one-cell flotation

When we set the microbubble generation zone with the flotation zone in one-cell flotation system**,** there are two problems: the turbulence during bubble generation and the low microbubble concentration. In the preliminary experiments for the one-cell flotation, we will search for an appropriate polymeric flocculant to produce stronger flocs and develop a microbubble generating method to obtain microbubbles with higher concentration.

3.3.1 Experimental setup

The experimental setup for one-cell flotation is shown in Fig. 3-7. The rotating-type microbubble generator (M2-M/PVC, Nanoplanet Research Institute Co.) is directly set at the middle of the bottom of the flotation tank which was a cylinder made of acrylic resin and has an inner diameter of 20cm and a height of 100cm.

Kaolin suspension (10mg kaolin in 1L tap water) was prepared as the raw water, and the initial turbidity was maintained near 8 NTU in each experiment.

For the coagulant, polyhydroxy aluminum chloride ($Al1_3(OH)_{20}(SO_4)_2Cl_{15}$, PAC) was used and compared with aluminum sulfate ($Al_2(SO_4)_3$, alum). PAC is a partially hydrolyzed aluminum chloride solution which has been reported to provide stronger flocs than alum (Gregory and Rossi, 2001; McCurdy et al., 2004; Zouboulis and Traskas, 2005). Edzwald *et al.* (1994) also reported that PAC was quicker to react than alum, especially in cold waters and required shorter flocculation times. A decade of large scale experience in dissolved air flotation reported by Kempeneers *et al.* (2001) indicates that when using PAC the aluminum dosage could be halved as compared to alum while maintaining a similar effluent turbidity.

For the microbubble generation, we applied the centrifugal pump (20KED04s, Nikuni Co., Ltd.) which can be operated under cavitation conditions. The maximum gas/liquid ratio is supposed to be 1/10. During microbubble generation, air is aspirated by the pump

and the generator simultaneously. Backflow prevention valves are installed in the gas pipe lines, connecting the pump or the generator with the gas flow meters.

Kaolin suspension (10mg kaolin in 1L tap water) was mixed rapidly for 5min at a rotating rate of 300rpm after the coagulant injection, and then mixed slowly at a rotating rate of 70 rpm for 15 minutes. Microbubbles were directly produced in the flotation tank by pumping water into the generator and inducing air from the pump and the generator simultaneously. Microbubbles were allowed to collide with the kaolin particles and to carry them to the surface without any mixing. During this period, samples were taken from the bottom every 5 minutes for 20 minutes. Turbidities of the treated water were measured to calculate the particle removal efficiency with Eq. (3-1). Water flow rate during microbubble generation was 12 L/min while flow rates of air induced by the pump, Q_{A1}, and generator, $Q_{A2,}$ were controlled in the range of 0.17~0.60 L/min.

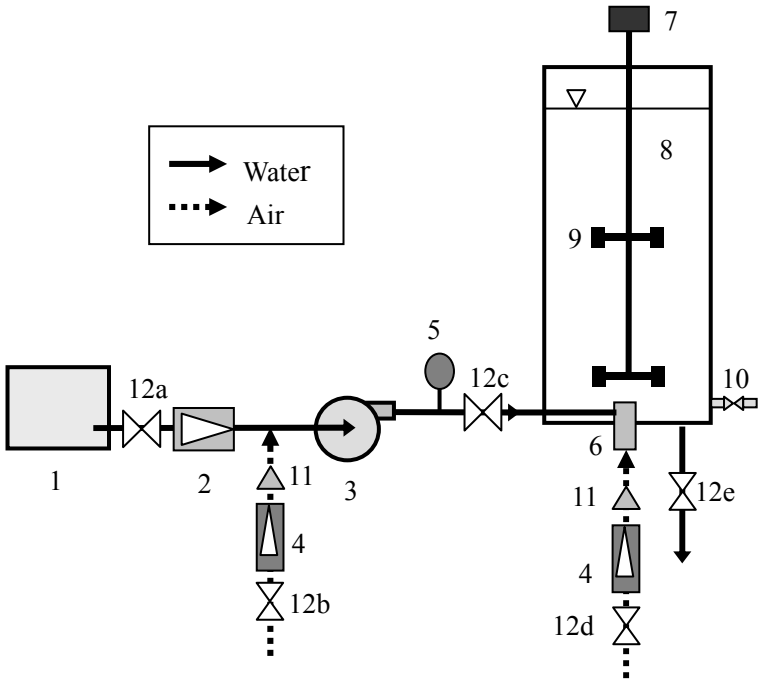

1. Buffer tank
2. Water flow meter
3. Centrifugal pump
4. Gas flow meter
5. Pressure gauge
6. Microbubble generator or dispersing nozzle
7. Variable speed Motor
8. Flotation tank
9. Impellor
10. Sampling tap
11. Backflow prevention valve

12a-e. Valve

Fig. 3-7 Experimental setup for one-cell flotation

3.3.2 Results and discussion

(1) Comparison of PAC with alum

The particle removal efficiencies using PAC and alum as the coagulant are compared in **Fig. 3-8**. Water flow rate for microbubble generation was kept 13.6 L/min. Air was induced by the pump at a flow rate of 0.5 L/min while air aspiration by the generator was stopped. Recycle ratio was 20%. The particle removal efficiency was increased by 10% when PAC was used as coagulant. Compared with alum, PAC has lower hydrophilicity and is able to form stronger flocs that will resist fracture during bubble generation (McCurdy et al., 2004; Zouboulis and Traskas, 2005).

(2) Effect of gas suction way to particle removal efficiency

Fig. 3-9 (a), (b) and **(c)** show the effect of flow rate of air induced by the centrifugal pump, Q_{A1}, on particle removal efficiency. Q_{A1} is varied for 0.28, 0.50 and 0.70 L/min, while the flow rate of air induced by the generator, Q_{A2}, was changed for 0, 0.17 and 0.28 L/min. Water flow rate was kept at 13.6 L/min. The particle removal efficiency was greatly increased with increasing Q_{A1} at any Q_{A2}. The additional gas suction by the centrifugal pump could increase the microbubble concentration.

The data in Fig. 3-9 was rearranged and shown in **Fig. 3-10 (a), (b)** and **(c)** which show the effect of flow rate of air induced by the generator, Q_{A2}, on particle removal efficiency. The highest particle removal efficiency was achieved when there was no air induced by the generator (Q_{A2}=0). Increasing Q_{A2} reduced the particle removal efficiency. In another word, the generator should not be allowed inducing any air when the centrifugal pump aspirates air.

3.3.3 Conclusions

There are two problems with the rotating-flow microbubble generator for the

application to one-cell flotation, that is, high turbulence and low microbubble concentration during bubble generation.

To overcome the first problem, the author selected ployaluminum chloride (PAC) as coagulant because it can produce more robust flocs. The increase of bubble removal efficiency indicates that PAC is a suitable coagulant for the one-cell flotation.

The second problem was overcome by changing the gas suction way. The author utilized a centrifugal pump and combined it with the rotating-flow microbubble generator. Air was allowed to be induced both by the pump and by the generator in the improved system. The air flow rates and water flow rate are varied and their effects on the particle removal efficiency were examined. Experimental results show that the particle removal efficiency increases with the increase of pump-induced air flow rate, but is inversely proportional to the generator-induced air flow rate. Thus, it is recommended that the air should be induced only by the centrifugal pump, but not by the generator.

In the next section, a one-cell IAF system will be proposed using the improved microbubble generating system and compared with the normal one.

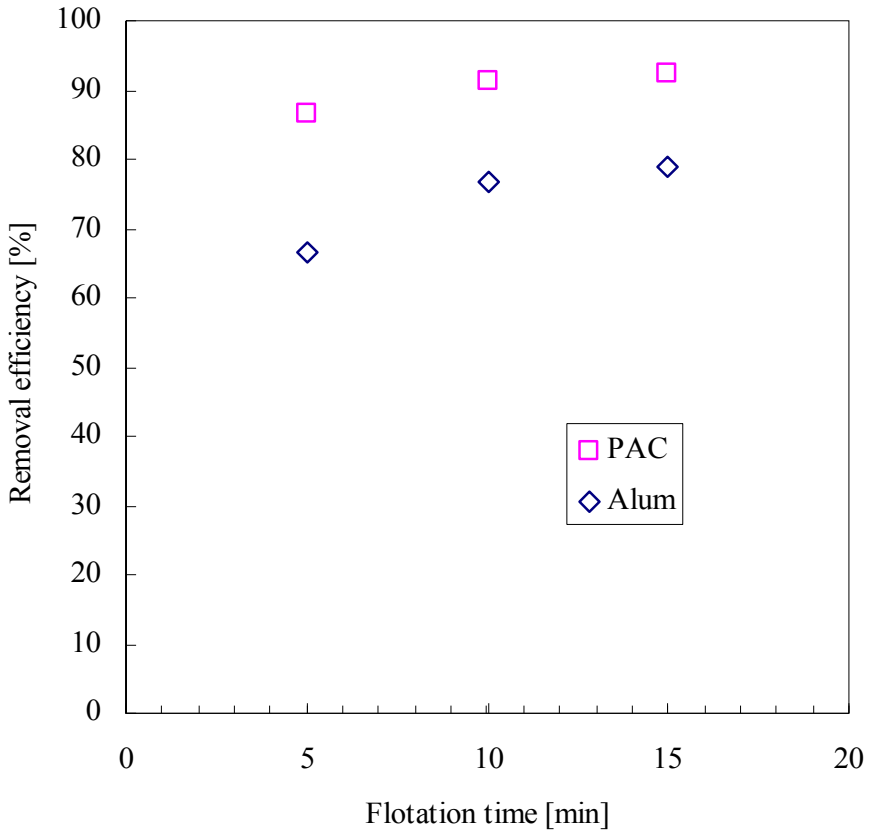

Fig. 3-8 Comparison of PAC with alum

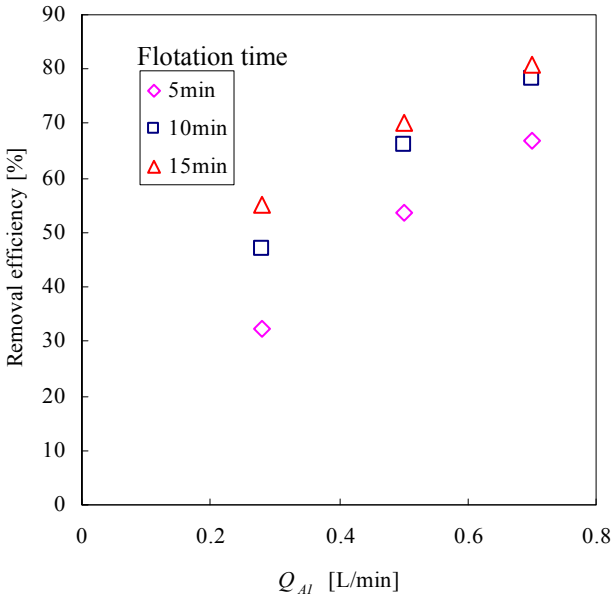

(a) Q_{A2}=0 L/min

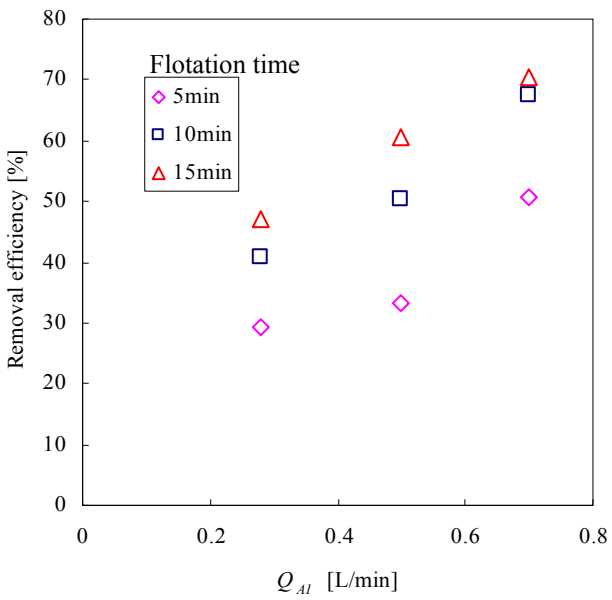

(b) Q_{A2}=0.17 L/min

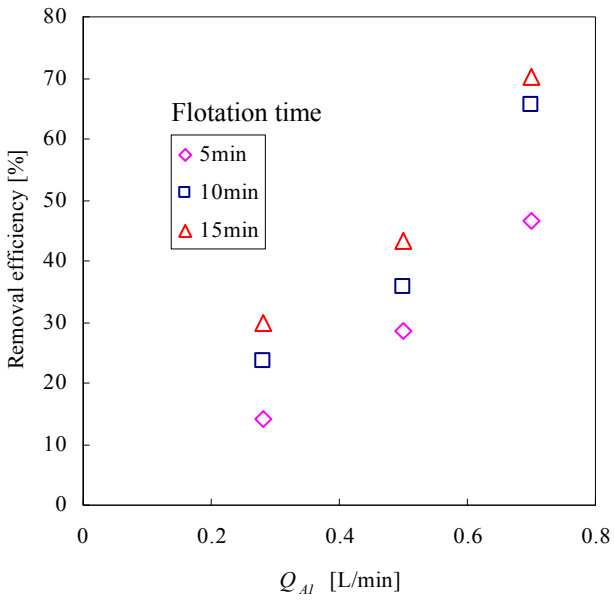

(c) Q_{A2}=0.28 L/min

Fig. 3-9 Effect of flow rate of air induced by the centrifugal pump

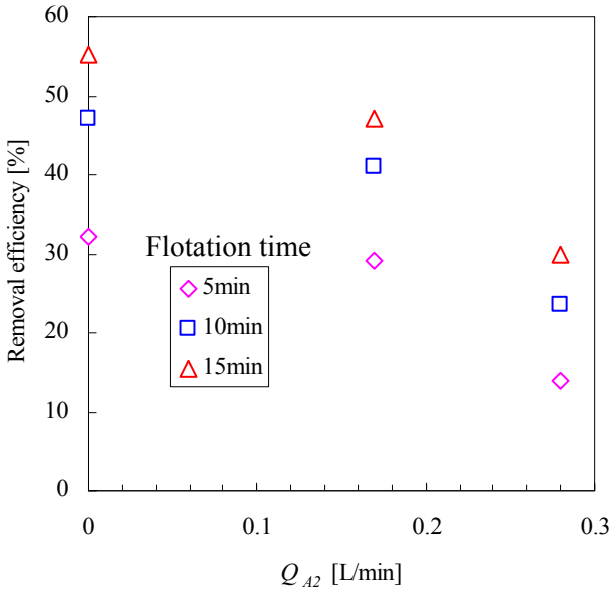

(a) Q_{A1}=0.28 L/min

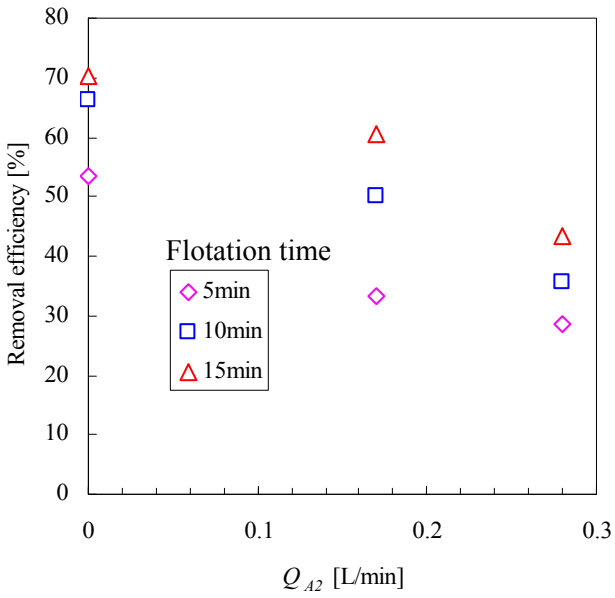

(b) Q_{A1}=0.50 L/min

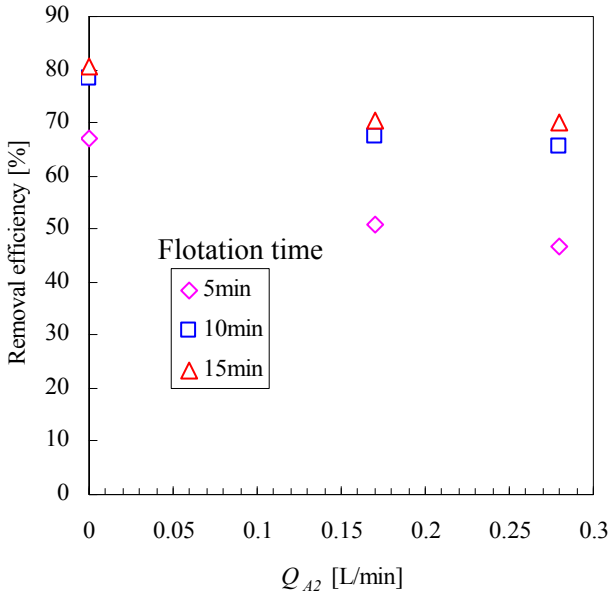

(c) Q_{A1}=0.70 L/min

Fig. 3-10 Effect of flow rate of air induced by the generator

3.4 One-cell flotation

3.4.1 Experimental setup

The experimental setup for the one-cell flotation is shown in Fig. 3-7**.** The cylindrical flotation tank made of acrylic resin has an inner diameter of 20 cm and a height of 65 cm. Polyhydroxy aluminum chloride (PAC) was used as the coagulant. The batch flotation experiments were performed by the same procedures as the preliminary experiments were done. The experimental conditions are shown in **Table 3-1. T**he particle removal efficiencies were compared with regard to microbubble generation methods as shown in Fig. 2-2.

Table 3-1 Experimental conditions in one-cell flotation

Coagulation	Rapid mixing rate	[rpm]	200
	Rapid mixing time	[min]	1~3
Flocculation	Slow mixing rate	[rpm]	40
	Slow mixing time	[min]	0~15
Flotation	Water flow rate, Q_W	[L/min]	10~14
	Air flow rate, Q_A	[L/min]	0.50~1.50
	Recycle ratio, r	[%]	5~20

3.4.2 Results and discussion

(1) Comparison of microbubble generating methods

Particle removal efficiencies of the three methods were compared and results are illustrated in **Fig. 3-11**. The removal efficiency significantly increases when air is induced by the pump with the microbubble generator as shown in Fig. 2-2 (b). However, the removal efficiency decreases as low as 50-80 %, when air is induced by the generator

(Fig. 2-2 (a)) or by the pump with the dispersing nozzle (Fig. 2-2 (c)). In fact, sedimentation of flocs was observed in the methods (a) and (c), because microbubbles were insufficient to collect all of particles.

The kinetic rate of particle removal in a batch flotation is considered to be a first-order reaction,

$$\frac{dN_p}{dt} = -kN_p \qquad \textbf{(3- 5)}$$

where N_p is the particle number concentration, k is the rate constant given by the following equation (Edzwald, 1995 and 2004),

$$k = (3/2)\alpha_{pb}\eta_T(\varphi_b / d_b) \qquad \textbf{(3- 6)}$$

where α_{pb} is the particle-bubble collision efficiency which is changed through coagulation and flocculation; η_T is the total single collector efficiency which is dependent on microbubble size according to d_b^{-2} and particle size (over 1 μm) according to d_p^2, φ_b is the microbubble volume concentration and d_b is the microbubble diameter. Consequently, it is suggested that smaller microbubbles with higher volume concentration improve flotation.

Bubble volume concentration can also be described as gas holdup. The comparison of gas holdups in Fig. 2-11 and bubble size distributions in Fig. 2-7 shows the smallest microbubbles with the highest gas holdup were formed in the method (b). The smaller and higher gas holdup relating higher microbubble volume concentration result in better particle removal performance achieved in the method (b).

(2) Effect of flocculation and flotation conditions on particle removal in the improved IAF system

The improved microbubble generation method was then introduced to the IAF system. Its performance to remove particles should be examined under various conditions.

① Effect of coagulant dosage

The effect of coagulant dosage on particle removal efficiency is shown in **Fig. 3-12** for

water flow rates Q_W of 12 and 14 L/min. The removal efficiency increases with the increase of PAC dosage for both water flow rates. While the jar-test-determined optimum dosage for sedimentation was 1.5 mg-Al/L, a little overdose shows better efficiency in IAF. This tendency agrees with that shown in the separated flotation system (Fig. 3-3). However, too much over dosage will cause the decrease of removal efficiency.

② Effect of flocculation time

In practice, flocculation time and mixing conditions are controlled to change the floc size. The rapid mixing is to dissolve the coagulant which can destabilize kaolin particles. The destabilized particles agglomerate together and grow up to flocs during the slow mixing period. Their effects on the particle removal efficiency in the batch flotation experiments are shown in **Fig. 3-13**. For rapid mixing of 1 minute, the removal efficiency is only about 20-30 %. As the rapid mixing time increases to 3 min, it increases suddenly to 80-90 %. But, much longer flocculation time just shows a little effect on the removal efficiency. It indicates that longer flocculation time is not necessary in this IAF process, which coincides with the design and operation of DAF, where shorter flocculation times are preferred (Edzwald, 1995; Haarhoff and Edzwald, 2004). Actually, longer flocculation time is not economically feasible in practice.

③ Effect of air and water flow rates

The effects of air and water flow rates on particle removal efficiency are illustrated in **Fig. 3-14.** The removal efficiency is increased from about 85% to about 90% when water flow rate decreases from14 L/min to 12 L/min. But it is not improved much further when Q_W is decreased from 12 L/min to 10 L/min. The bubble size and bubble number concentration for different water flow rates are shown in **Table 3-2.** As the water flow rate Q_W increased from 12 to 14L/min, the bubble number concentration decreased from 4.6×10^4 to 2.5×10^4 bubbles mL^{-1} but the average bubble size increased from 52 to 62μm. Consequently, the particle removal rate constant k in Eqs. (3-5,6) decreases with increasing Q_W due to the increase of bubble size and decrease of bubble concentration.

Moreover, the high turbulence resulted from high water flow rate may destruct the fragile flocs, which can further degrade the particle removal performance of the flotation.

Water flow rate was controlled by adjusting the valve 12c in Fig. 3-7 in the experiments. Water flow rate of 14 L/min was obtained with the valve 12c full open. Closing the valve resulted in a decrease in the water flow rate accompanied by an increase in the pressure of the pump outflow. The pressure of the outflow then dropped again as the fluid flowed through the generator. The lower the water flow rate, the greater the pressure drop. When the water flow rate decreased from 14 to 12 and then 10 L/min, the pressure drop increased from 0.3 MPa to 0.4 MPa, and much higher to 0.5 MPa. In the dissolved air flotation, it is found that smaller bubble can be generated at higher saturation pressure as long as the pressure is lower than a critical value (about 3.5 atmospheres) (Han *et al*., 2002b). Bubble size shown in **Table 3-2** indicated a similar tendency. The average size of bubbles decreased when the pressure drop increased from 0.3 MPa (at Q_W=14 L/min) to 0.4 MPa (at Q_W=12 L/min). The average size of bubbles generated at Q_W= 10 L/min is almost the same as that at Q_W=12 L/min although the pressure drop at Q_W= 10 L/min was greater that at Q_W=12 L/min.

On the other hand, the removal efficiency increases very slightly with the increase of air flow rate Q_A, which indicates the capacity of the improved method (b) is decided by the water flow rate, in another word, the pressure drop through the generator.

④ Effect of recycle ratio

Fig. 3-15 shows the effect of recycle ratio on the particle removal efficiency. The removal efficiency increases with the increase of recycle ratio, but 15% is enough to remove over 95% of the kaolin particles for Q_W of 12 L/min by dosing 1.5 mg-Al/L PAC. The increase of recycle ratio leads to the increase of bubble number concentration, which can improve bubble-particle collisions. However, the surface area of floc limits the number of bubbles that can be attached (Matsui *et al*., 1998). Hence, much higher recycle ratios cannot improve the performance further, but just increase the running cost.

3.4.3 Conclusions

The suitability of the one-cell IAF process developed with the improved microbubble generating system was examined in batch experiments. Results indicate that both coagulant dosage and flocculation time are vitally important. A slight overdose achieved better removal efficiency and no or less flocculation time performed very well. Water and air flow rates and recycle ratio were controlled to study the effects of bubble size and bubble concentration which have a major impact on the bubble-floc collisions. Lower water flow rate achieved better removal efficiency due to the increase of bubble concentration and decrease of bubble size. Air flow rate shows little effect on the removal efficiency under the present experimental conditions.

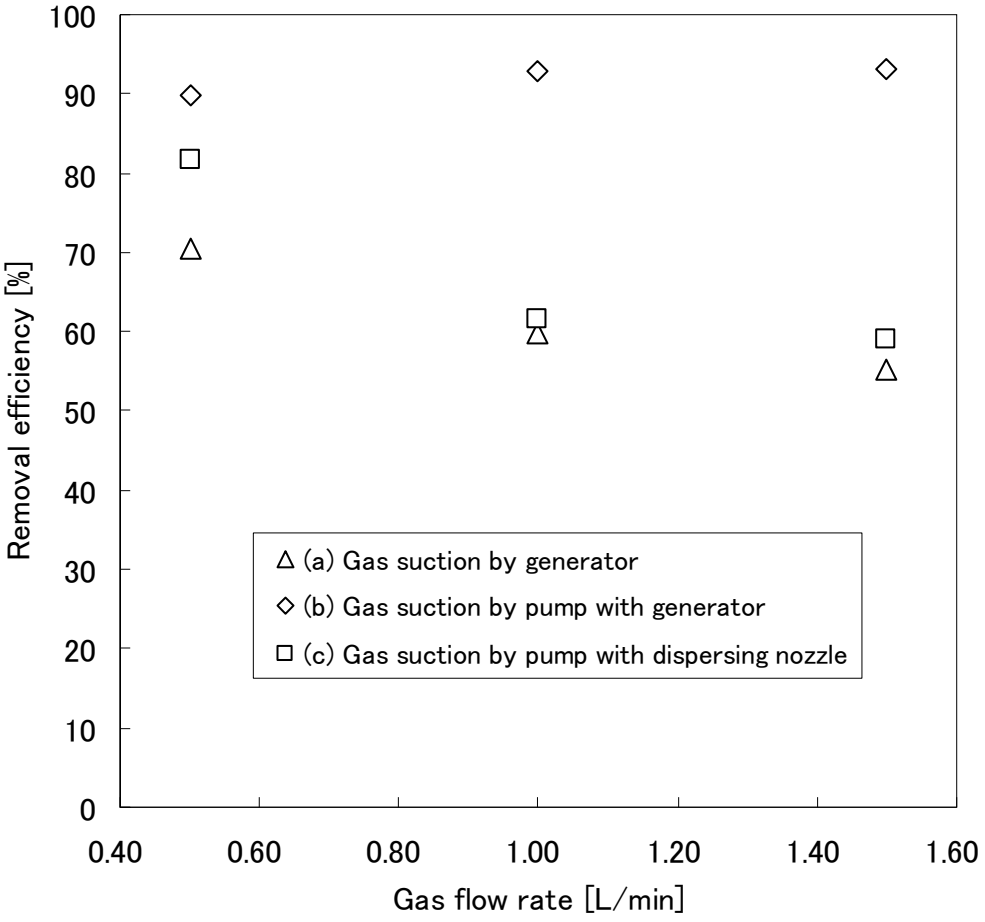

Fig. 3-11　Effect of microbubble generating method on removal efficiency (PAC dosage, 1.5 mg-Al/L; flocculation time, 10 min; r, 10%; Q_W, 12 L/min)

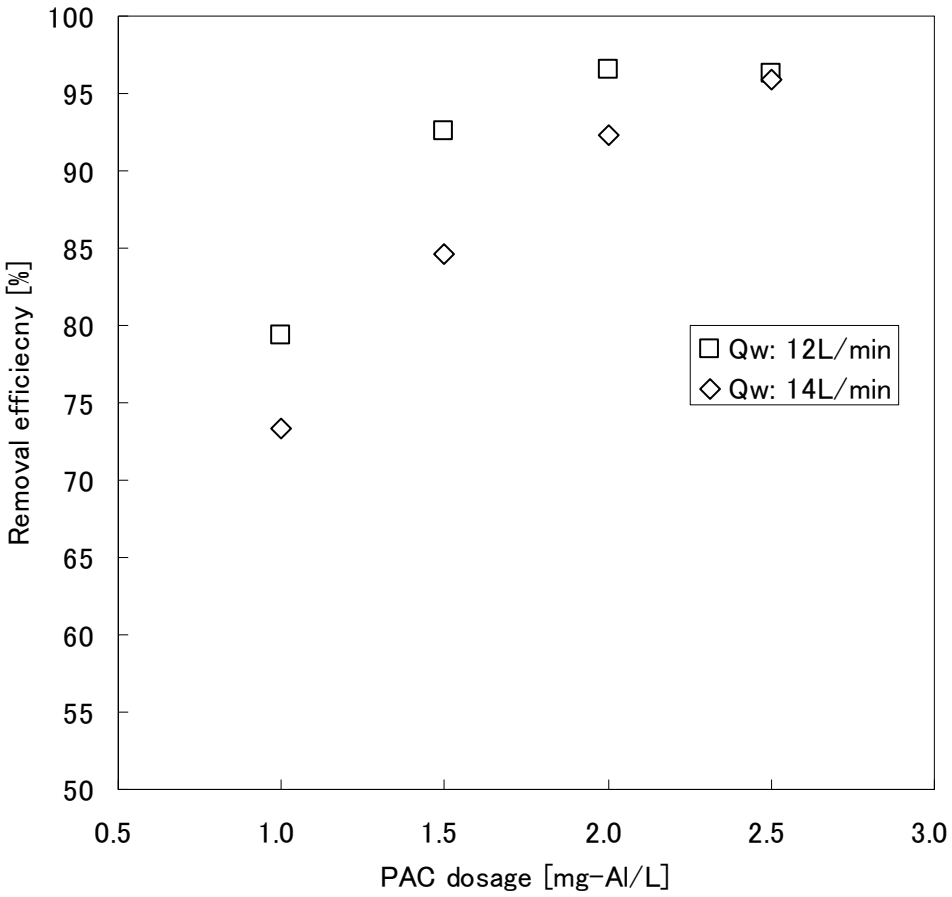

Fig. 3-12 Effect of PAC dosage on particle removal efficiency
(Flocculation time, 10 min; r, 10 %; Q_A, 0.5 L/min)

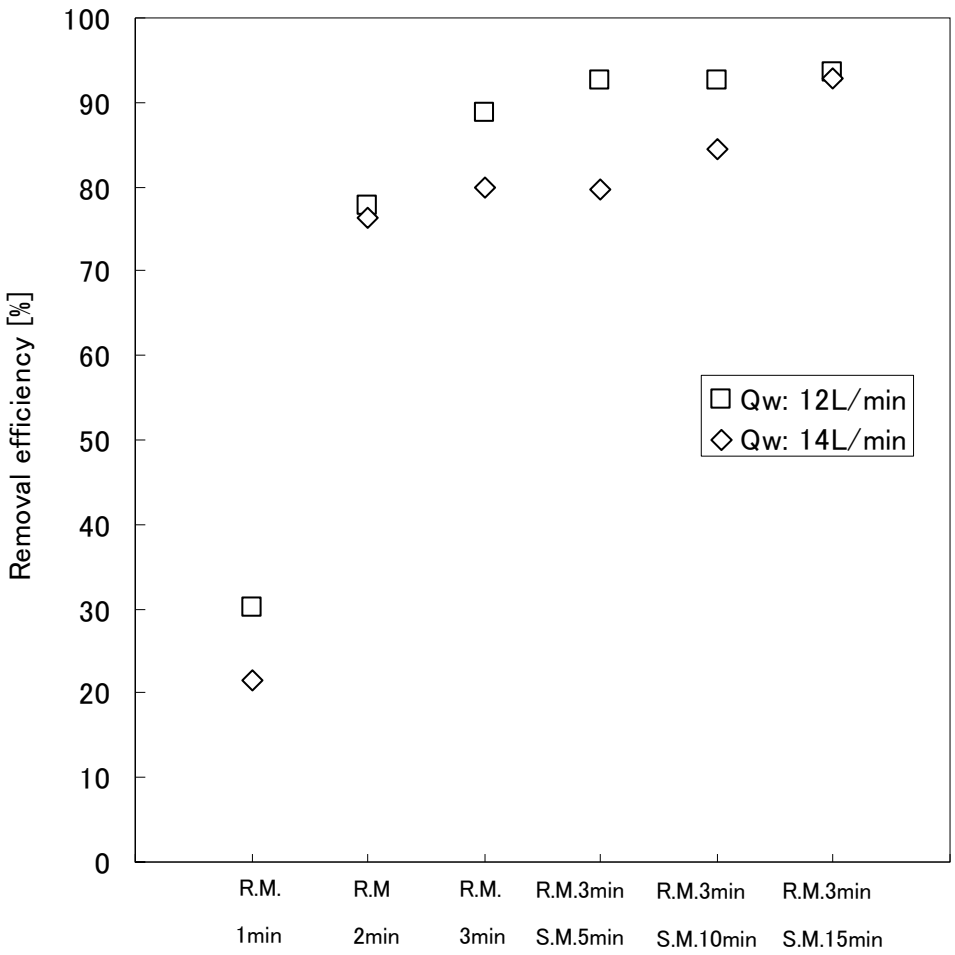

Fig. 3-13 Effect of mixing time on particle removal efficiency (R.M., rapid mixing; S.M., slow mixing; PAC dosage, 1.5 mg-Al/L; *r*, 10 %; Q_A, 0.5 L/min)

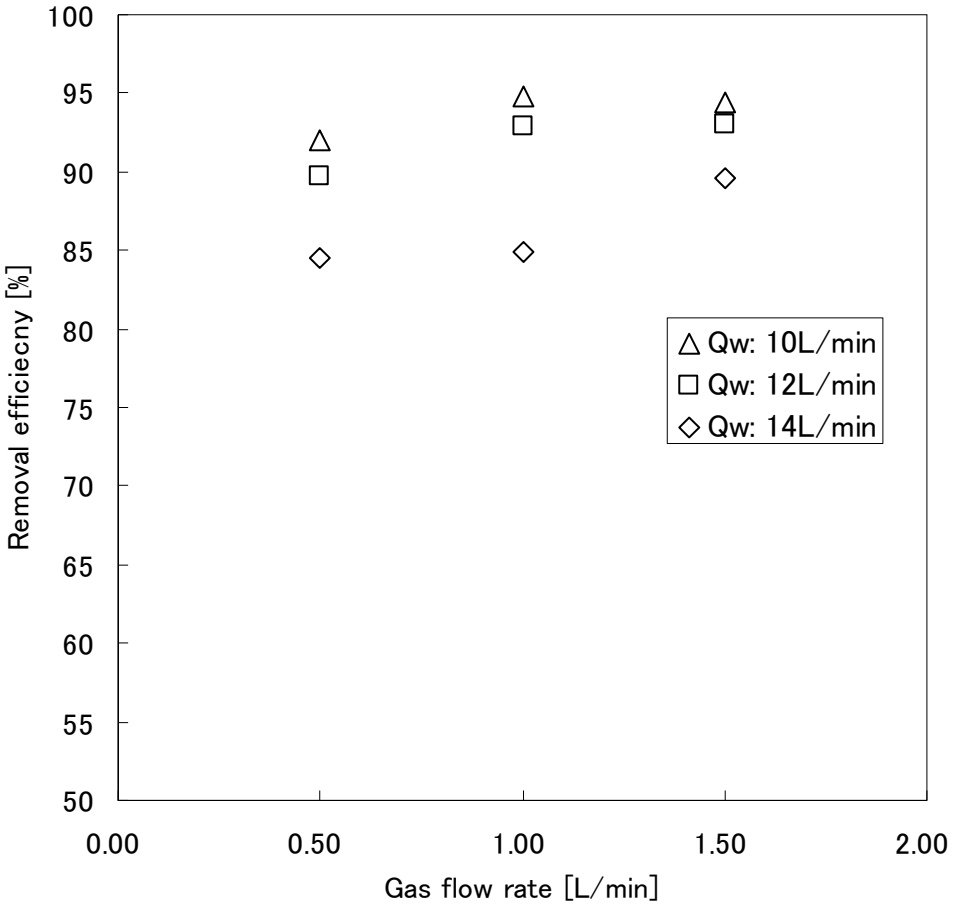

Fig. 3-14　Effect of gas and water flow rates on particle removal efficiency (PAC dosage, 1.5 mg-Al/L; Flocculation time, 10 min; *r*, 10 %)

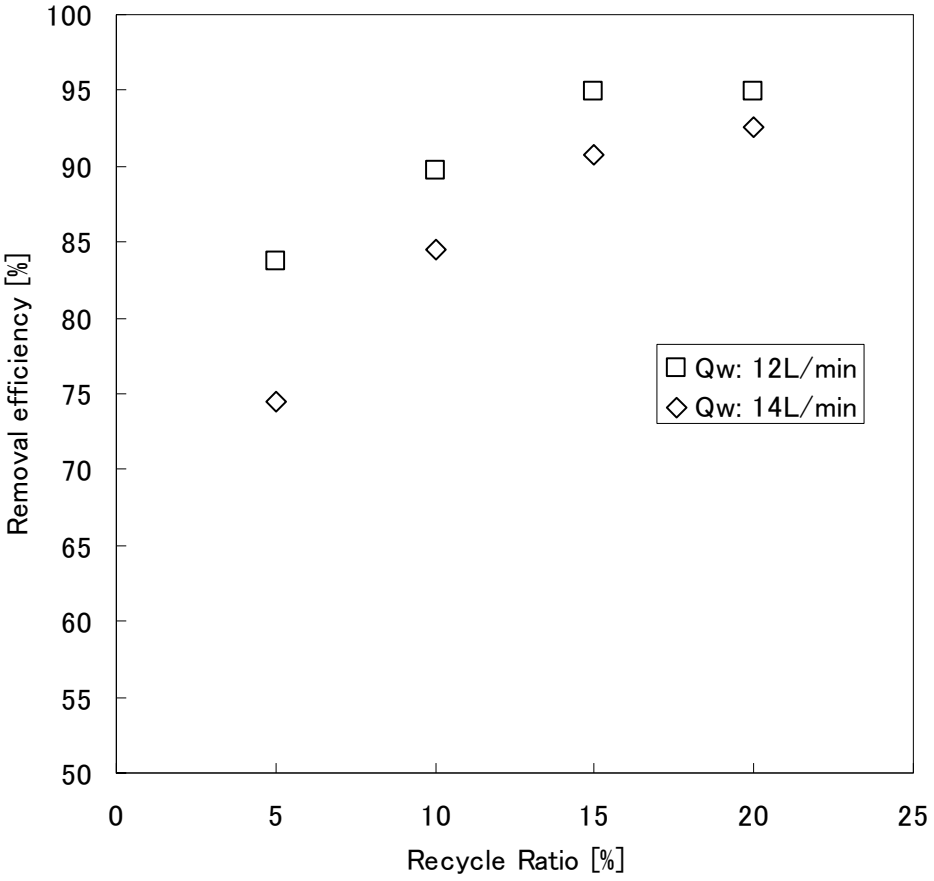

Fig. 3-15 Effect of recycle ratio on particle removal efficiency
(PAC dosage, 1.5 mg/L; Flocculation time, 10 min; Q_A, 0.5 L/min)

Table 3-2 Effect of water flow rate on bubble size and concentration

Q_W	Q_A	Pressure drop	Average diameter d_b	Standard deviation	ε_G	Bubble number concentration
L/min	L/min	MPa	μm	-	-	bubbles/mL
10	0.50	0.5	53	21	3.8×10^{-3}	4.9×10^{4}
12	0.50	0.4	52	20	3.4×10^{-3}	4.6×10^{4}
14	0.50	0.3	62	22	3.1×10^{-3}	2.5×10^{4}

Nomenclature

d_b	=	microbubble size	[μm]
d_p	=	particle size	[μm]
C_0	=	turbidity of raw kaolin suspension	[NTU]
C_0'	=	revised turbidity of raw kaolin suspension	[NTU]
C	=	turbidity of sample kaolin suspension	[NTU]
N_p	=	particle number concentration	[mL^{-1}]
r	=	dilution ratio or recycle ratio ($=V_r/V_0$)	[%]
R	=	particle removal efficiency defined by Eq. (3-3)	[%]
Q_W	=	water flow rate	[L/min]
Q_A	=	air flow rate	[L/min]
Q_{A1}	=	flow rate of air induced by pump	[L/min]
Q_{A2}	=	flow rate of air induced by generator	[L/min]
V_0	=	volume of raw kaolin suspension	[L]
V_r	=	volume of bubbly water	[L]
α_{pb}	=	particle-bubble collision efficiency	[—]
η_T	=	total single collector efficiency	[—]
φ_b	=	microbubble volume concentration	[—]

Literature cited

Edzwald, J. K., D. Q. Bunker, Jr. J. Dahlquist, L. Gillberg and T. Hedberg; "Dissolved Air Flotation: Pretreatment and Comparisons to Sedimentation," Chemical Water and Wastewater Treatment III, Springer-Verlag Berlin Heidelberg, pp.3-18 (1994)

Edzwald J.; "Principles and Applications of Dissolved Air Flotation," *Water Science & Technology*, **31**, 1-23 (1995)

Evans G.M., G. J. Jameson, and B.W. Atkinson; "Prediction of the Bubble Size Generated by A Plunging Jet Bubble Column," *Chemical Engineering Science*, **47**, 3265-3272 (1992)

Gregory, J. and L. Rossi; "Dynamic Testing of Water Treatment Coagulants," *Water Sci. Technol.: Water Supply*, **1**, 65-72 (2001)

Haarhoff J., and J. K. Edzwald; "Dissolved Air Flotation Modelling: Insights and Shortcomings," *J. of Water Supply: Research & Technology-AQUA*, **53**, 127-150 (2004)

Han M. Y., and S. Dockko; "Zeta Potential Measurement of Bubbles in DAF Process and Its Effect on The Removal Efficiency," *Water Supply*, **17**, 177-182(1999)

Han M., W. Kim and S. Dockko; "Collision Efficiency Factor of Bubble and Particle (α_{bp}) in DAF: Theory and Experimental Verification," *Water Science Technology*, **43**, 139-144(2001)

Han M.Y.; "Modeling of DAF: the Effect of Particle and Bubble Characteristics," *J. Water Supply: Research & Technology-AQUA*, **51**, 27-34 (2002a)

Han M., Y. Park, J. Lee and J. Shim; "Effect of Pressure on Bubble Size in Dissolved Air Flotation," *Water Sci. & Tech.: Water Supply*, **2**, 41-46 (2002b)

Heindel T. J., and F. Bloom; "Theory of Dispersed Air Flotation," *Encyclopedia of Surface and Colloid Science, Marcel Dekker, Inc.* 5298-5311 (2002)

Jameson G. J.; "Hydrophobicity and Floc Density in Induced-Air Flotation for water treatment," *Colloids Sufaces A: Physicochem. Eng. Aspects,* **151**, 269-281 (1999)

Li P. and H. Tsuge; "Water Treatment by Induced Air Flotation Using Microbubbles,"

Japanese Society for Multiphase Flow Annual Meeting, Tokyo, Japan, August 1-3, 2005

Kempeneers S., F. V. Menxel and L. Gille; "A Decade of Large Scale Experience in Dissolved Air Flotation. *Water Science & Technology*, **43**, 27-34 (2001)

Kiuru H. J.; "Development of Dissolved Air Flotation Technology from the First Generation to the Newest (Third) One (DAF in Turbulent Flow Conditions)," *Water Science & Technology*, 43, 1-7 (2001)

Matsui Y., K. Fukushi and N. Tambo; "Modeling, Simulation and Operational Parameters of Dissolved Air Flotation,*" J. Water SRT-Aqua*, **47**, 9-20 (1998)

McCurdy K., Carlson K. and Gregory D.; "Floc morphology and cyclic shearing recovery: comparison of alum and polyaluminum chloride coagulants," *Water Research*, **38**, 486-494 (2004)

Okada K. and Y. Akagi; "Method and Apparatus to Measure the ξ-potential of Bubbles," *J. Chem. Eng. Japan*, **20**, 11-15(1987)

Okada K., Y. Akagi, M. Kogure and N. Yoshika; "Effect on Suface charges of Bubbles and Fine Particles on Air Flotation Process," *Canadian J. Chem. Eng.,* **68**, 393-399 (1990)

Okamoto, R., H. Takeda, H. Shakutsui and H. Ohnari; "Performance of Micro-Bubble Generators," *Japanese Society for Multiphase Flow Annual Meeting*, Tokyo, Japan, August 1-3, 2005 (in Japanese)

Ohnari, H.; "Waste Water Purification in Wide Water Area by Use of Micro-Bubble Techniques,*" Japanese J. Mutiphase Flow*, **11**, 263-266 (1997) (in Japanese)

Ohnari, H., T. Saga, K. Watanabe, K. Maeda, K. Matsuo; "High Functional Characteristics of Micro-bubbles and Water Purification," *Resources Processing*, 46, 238-244 (1999) (in Japanese)

Ohnari, H; "Swing Type Fine Air Bubble Generating Device,**"** Patent Number: WO0069550 (2000)

Ohnari, H.; "Water Purification of Ocean Environment and Revival of Fisheries Cultivation Using Micro Bubble Technology," The 21st Symposium on Multiphase Flow, Nagoya, Japan, July 29-31 (2002) (in Japanese)

Ohnari, H.; “MB Research Front Line,” http://www.nanoplanet.co.jp/NP_mnbresearch2.html (2006) (in Japanese)

Sato, U.; “Effects of factors on microbubble generation,” Bachelor’s thesis, Keio University, pp.35 (2005) (In Japanese)

Schofield, T.; “Dissolved Air Flotation in Drinking Water Production,” *Water Science & Technology*, **43**, 9-18 (2001)

Shawwa, A. R. and D.W. Smith, “Dissolved Air Flotation Model for Drinking Water Treatment,” *Can. J. Civ. Eng.*, **27**, 373-382 (2000)

Yan, Y., G. J. Jameson; “Application of the Jameson Cell Technology for Algae and Phosphorus Removal from Maturation Ponds,” *Int. J. Miner. Process*, **73**, 23-28 (2004)

Zabel, Th. F.; “Flotation in Water Treatment,” *Innovations in Flotation Technology*, Kluwer Academic Publishers, Netherlands, 431-454 (1992)

Zlokarnik, M.; “New Approached in Flotation Processing and Waste Water Treatment in the Chemical Industry,” *Ger. Chem. Eng*. **5**, 109-115 (1982)

Zlokarnik, M.; “Separation of Activated Sludge from Purified Wasted Water by Induced Air Flotation (IAF),” *Water Research*, **32**, 1095-1102 (1998)

Zouboulis, A. I. and Traskas G.; “Comparable evaluation of various commercially available aluminium-based coagulants for the treatment of surface water and for the post-treatment of urban wastewater,” *J. Chemical Technology and Biotechnology*, **80**, 1136-1147 (2005)

CHAPTER 4

Ozone mass transfer using microbubbles

4.1 Introduction

Ozonation is now gaining popularity in water and wastewater treatment due to its high efficiency for decomposition of refractory organic compounds. In drinking water treatment, ozone has been used as a pretreatment reagent, an oxidant and a disinfectant. For the wastewater treatment, the ozonation has been applied to the removal of soluble organic matters and decolorization.

However, the application of ozone to water and wastewater treatment has been limited by its low utilization efficiency, which mainly results from the low mass-transfer rate of ozone from the gas phase to the liquid phase because the ozone concentration in the carrier gas is relatively low.

For the most popular ozone mass transfer technique in water and wastewater treatment, gas diffusers are used due to the effective ozone transfer and simple construction. However, it is required that the contactor has relatively deep height and wide surface area to achieve effective ozone transfer. Moreover, the occurrence of diffuser clogging and bubble vertical channel can cause an efficiency decrease. Except for the conventional bubble diffuser contactor, there are many other techniques including turbine mixers, injectors, packed columns and spray chambers. They all have their own merits and demerits when employed in ozone contact reactor (Bruno *et al*., 1991). One similarity among all of these systems mentioned above is that bubbles all have diameters on the order of millimeter.

The mass transfer efficiency of ozone from the gas phase to the liquid phase is always evaluated by the overall volumetric mass transfer coefficient, K_La. It is the product of the overall mass transfer coefficient, K_L, and the specific interfacial area, a. In the most ozone contact reactor, the resistance is predominantly on the liquid side. Thus, K_L is considered to equal to the liquid phase mass transfer coefficient, k_L. The k_L depends on the mixing

characteristics of the gas-liquid contactor used and the kinetics of ozone reactions produced, while *a* is determined by the number and size of ozone bubbles produced. The smaller the bubble size is, the higher the specific interfacial area is. Additionally, smaller bubbles are associated with larger residence time and, therefore, higher gas volume fraction. Moreover, as introduced in Section 1.2.1, the gas pressure inside a bubble is greater than that of outside it which is due to the surface tension. The magnitude of the pressure difference can be predicted according to the Young-Laplace Equation (Eq. 1-4). The smaller the bubble is, the higher the pressure inside it is. For instance, the Laplace pressure of a 1 μm bubble is about 0.29 MPa at 25℃, about 3 times the atmospheric pressure. According to the Henry's law, the dissolved concentration of ozone in water at saturation, C_L*, is proportional to the partial pressure of ozone, P, at a given temperature. Therefore, the driving force for mass transfer increases with the decrease of bubble size. Moreover, as the ozone gas dissolves into the liquid phase, the bubble shrinks, further increasing the Laplace pressure. Therefore, it is inferred that the effectiveness of ozone as an oxidant can be increased by the employment of smaller bubbles.

In this chapter, the rotating-flow microbubble generator was introduced to ozone contactor in order to improve its mass transfer to the liquid to be treated. Although this kind of microbubble generator has been successfully applied in many fields such as closed water purification and marine cultivation (Onari *et al*., 1997, 1999 and 2002), there is no specific evaluation on the mass transfer properties of the generator. Therefore, in the first part of this chapter, its properties for mass transfer were investigated when oxygen was used as a model gas. Then the different handling method proposed in CHAPTER 2 was utilized and compared with the standard one to check whether it can improve mass transfer efficiency or not. In the last part of this chapter, the ozone absorption efficiency were examined in a semi-batch bubble column with the microbubble generator and compared with the reference data where milli-bubbles were used.

4.2 Experiment in mass transfer of oxygen

4.2.1 Experimental apparatus

A schematic diagram of the experimental apparatus is illustrated in **Fig. 4-1**. The bubble column is made of acrylic resin and has an inner diameter of 0.20m and a height of 1.20m. Microbubble generation system consists of a rotating-flow microbubble generator (M2-LM/PVC, Nanoplanet Research Institute Co.) and a centrifugal pump (20KED04S, Nikuni Co., Ltd.). The generator, which has an outer diameter of 50mm and a height of 100mm, was set in the lower part of the column.

(1) Gas suction way

The normal microbubble system using the rotating-flow microbubble generator is shown in Fig. 2-2(a)**.** During bubble generation, water is pumped into the generator, and a rotating flow is formed along the inner wall leading to a negative pressure zone along its axis. Then air is sucked by the negative pressure zone and sheared by the rotating flow. Microbubbles are generated when the mixture of water and air is spouted out with a very high rotating velocity. To increase the gas/liquid ratio, *G/L*, the author tried to combine it with a centrifugal pump and change the gas suction way shown in CHAPTER 2. In this case, air is induced by the centrifugal pump instead of by the generator as shown in Fig. 2-2(b). Then water and air are simultaneously aspirated and mixed by the pump. The pressurized mixture of air and water is then decompressed through the microbubble generator with a high rotating velocity. The mass transfer efficiencies of these two methods are compared by measuring the volumetric mass transfer coefficient of oxygen.

(2) Experimental method

A dynamic oxygen stripping method was used to determine the volumetric mass transfer coefficient of oxygen. Firstly, air was distributed until water was saturated by oxygen. And then, oxygen microbubbles were allowed to disengage. After that, nitrogen microbubbles were produced and the change of dissolved oxygen concentration, C_{O_2}, with time, *t*, was measured with a DO sensor (DO-55, TOA Electronics Co., Ltd.) which

was set 0.70m from the bottom, nearly in the radial and axial center of the bubble column.

With the assumption that the liquid in the bubble column is completely mixed, because it is circulated with a relatively high specific velocity. Then the mass transfer rate can be given by the following equation,

$$\ln\left(\frac{C_{O_2}}{C_{0,O2}}\right) = -\frac{k_{L,O_2}a}{1-\varepsilon_G}t \qquad \textbf{(4- 1)}$$

where C_{0,O_2} is the dissolved oxygen concentration at the initial time [mg/L]; ε_G is the gas holdup [-]. If the gas holdup, ε_G, is known, the volumetric mass transfer coefficient, $k_{L,O_2}a$ [s^{-1}], can be obtained from the slope when plotting $\ln\left(C_{O_2}/C_{0,O_2}\right)$ against t. One example was shown in Fig. 4-2. Oxygen concentration decreased with the injection of nitrogen microbubbles. There is a good linear relationship between $\ln\left(C_{O_2}/C_{0,O_2}\right)$ and t.

4.2.2 Results and discussion

The oxygen volumetric mass transfer coefficient, $k_{L,O_2}a$, and the gas holdup, ε_G, of two kinds of microbubble generation methods at different superficial velocity are shown in **Fig. 4-3**. Both $k_{L,O_2}a$ and ε_G in the method (b), where nitrogen gas is aspirated by the pump and dispersed by the microbubble generator as shown in Fig. 2-2 (b), are higher than those in the method (a), where the gas was induced by the generator as shown in Fig. 2-2 (a). Then it is proved that gas mass transfer efficiency of the method (b) is higher than that of the method (a). The method (b) will be used for ozone mass transfer in the next section.

4.3 Experiments in mass transfer of ozone

4.3.1 Experimental apparatus

Ozone was generated from oxygen by a corona-discharge ozone generator (SO-03UN03, Tokyu Car Co.). Ozone concentration in the gas phase was monitored using an UV-absorption ozone meter (EG-320, Ebara Jitsugyo Co., Ltd.). A vane pump was used to continuously sample water to a polarographic ozone meter (ELP-100, Ebara Jitsugyo Co., Ltd.) for the analysis of dissolved ozone concentration. The outlet gas was fed into an ozone destructor after being analyzed by the gaseous ozone meter. The measurement of ozone gas flow rate was made using a mass flow meter (Model-3340, Kofloc Co.), while the water flow rate was measured with a flow meter (SP-562, Tecflow International IR-Flow Co.). A transistor inverter (VF-nC12004P, Toshiba Co., Ltd) connected with the centrifugal pump was used to control the water flow rate. Unbuffered distilled water was used in all the experiments.

The ozone contactor was operated under a semi-batch condition, with water circulated by the centrifugal pump. The experimental system was started by switching on the centrifugal pump and the ozone generator simultaneously. But, air instead of ozone was induced until a stable ozone concentration and desired gas flow rate were achieved. The increase of ozone concentrations in water and off-gas with time was monitored during 30 minutes' ozone absorption experiment.

The following parameters were varied during the experimental program: Inlet ozone gas concentration $C_{G,in}$: 10.8-28.2 g-O_3/Nm^3, water flow rate Q_W: 15.0~19.5 L/min, induced gas flow rate Q_G: 0.25~1.50 NL/min and water surface height h: 0.76-1.16m.

4.3.2 Analytical method

The volumetric mass transfer coefficient of ozone, $k_{L,O_3}a$ was determined from the Boltzmann fit as referred to Bin's method (Bin, 2004). Bin (2004) proposed that the changes of dissolved ozone concentration with time could be successfully approximated by the Boltzmann fit, which is based on the following expression,

$$C(t) = \frac{A_1 - A_2}{1 + \exp\left(\frac{t - t_0}{D}\right)} + A_2 \qquad \textbf{(4- 2)}$$

where A_1, A_2, t_0 and D are the fitting parameters, $C(t)$ is the fitted concentration [mg/L]

and t is time [s]. When the differentiation of $C(t)$ with respect to t and some arrangement are performed, the following equation is obtained from Eq. (4-2),

$$\frac{dC}{dt} = \frac{1}{D(A_2 - A_1)}[-A_1 A_2 + (A_1 + A_2)C - C^2] \quad \textbf{(4- 3)}$$

The mass balance of ozone in the liquid phase can be expressed by the following equation,

$$\frac{dC_{\mathrm{L}}}{dt} = k_{\mathrm{L},\mathrm{O}_3} a(C_{\mathrm{L}}^* - C_{\mathrm{L}}) + (k_2 C_{\mathrm{L}} - k_3 C_{\mathrm{L}}^2) = k_{\mathrm{L},\mathrm{O}_3} a C_{\mathrm{L}}^* + (k_2 - k_{\mathrm{L},\mathrm{O}_3} a) C_{\mathrm{L}} - k_3 C_{\mathrm{L}}^2 \quad \textbf{(4- 4)}$$

where C_{L} is the dissolved ozone concentration in the liquid phase [mg/L], C_{L}^* is the equilibrium ozone concentration in the liquid phase, $k_{\mathrm{L},\mathrm{O}_3} a$ is volumetric mass transfer coefficient of ozone [s^{-1}], k_2 and k_3 are the ozone decomposition rate constant, [s^{-1}] and [L/mg·s], respectively. The similarity between Eq. (4-3) and Eq. (4-4) reveals that Boltzmann equation Eq. (4-2) is one of solutions to Eq. (4-4), and the corresponding terms have the same value as shown in the following equations,

$$k_{L,O_3} a \cdot C_L^* = -\frac{A_1 A_2}{D(A_2 - A_1)} \quad \textbf{(4- 5)}$$

$$k_2 - k_{L,O_3} a = \frac{A_1 + A_2}{D(A_2 - A_1)} \quad \textbf{(4- 6)}$$

$$k_3 = \frac{1}{D(A_2 - A_1)} \quad \textbf{(4- 7)}$$

The fitting parameters A_1, A_2, t_0 and D are obtained by fitting Eq. (4-2) to the experimental data with the minimum value of the sum of squares of deviations.

The equilibrium ozone concentration, C_L^*, is given by the Henry's law,

$$C_{\mathrm{L}}^* = \frac{\rho RT}{M}\frac{C_{\mathrm{G}}}{H} \quad \textbf{(4- 8)}$$

where ρ is the water density [kg/m^3], R is the gas constant [0.08206L·atm/K·mol], T is temperature [K], M is water molecular weight [18 g/mol], C_{G} is ozone concentration in gas phase and H is the Henry's constant [atm/mol fraction] which can be calculated by means of the correlation proposed by Roth and Sullivan (1981):

$$H = 3.84 \times 10^7 [\mathrm{OH}^-]^{0.035} \exp(-2428/T) \quad \textbf{(4- 9)}$$

By assuming that the inlet and outlet ozone gas has the same flow rate ($Q_{\mathrm{G,in}}$=$Q_{\mathrm{G,out}}$),

we define the ozone transfer ratio, η [%], in the semi-batch ozone contactor as follows (Hsu and Huang, 1996),

$$\begin{aligned}\eta(t) &= \frac{W_{\text{in}} - W_{\text{out}}}{W_{out}} \times 100 \\ &= \frac{Q_{\text{in}} C_{\text{in}} t - \int_0^t Q_{\text{out}} C_{\text{out}} dt}{Q_{\text{in}} C_{\text{in}} t} \times 100 \\ &= (1 - \frac{1}{C_{\text{in}} t} \int_0^t C_{\text{out}} dt) \times 100\end{aligned} \quad \textbf{(4- 10)}$$

where W_{in} and W_{out} are the total input and output amounts of ozone measured in the gas phase, respectively [g]; C_{out} is the ozone concentration in off-gas from the top of the bubble column [mg/L]. Because C_{out} varied with time, the amount of ozone output during a period of t can be calculated through integrating the time-depending equation of C_{out} which was obtained by approximating the measured C_{out}.

4.3.3 Results and discussion

(1) Effect of gas flow rate on the ozone mass transfer

The dissolved ozone concentration in water is plotted against time for different induced-gas flow rates in **Fig. 4-4.** The Boltzmann fit results are also illustrated as solid lines in Fig. 4-4. The dissolved ozone concentration increases with time and reaches a equilibrium state at last. For a constant water flow rate, the dissolved ozone concentration gets constant more quickly as the gas flow rate increases. There is a little deviation in the equilibrium concentration, which results from the difference of temperature in these experiments. The change of dissolved ozone concentration with time can be expressed by the Boltzmann fit (Eq. 4-2) very well.

The volumetric mass transfer coefficient of ozone, $k_{\text{L,O}_3}a$, obtained in the present study, is compared to those from other researchers in **Fig. 4-5**. When microbubbles are used, the $k_{\text{L,O}_3}a$ reaches a similar value at lower gas flow rate as compared to milli-bubbles.

Fig. 4-6 shows the effect of gas flow rate on the ozone transfer ratio obtained by Eq. (4-10). As the driving force decreases with time owing to the increase of dissolved ozone concentration, the ozone transfer ratio also decreases with time. We can also find that the highest ozone transfer ratio was achieved at the lowest gas flow rate, 0.25L/min.

The curve fitting results of $k_{L,O_3}a$ and experimental results of ε_G are listed in **Table 4-1**. The average of squares of deviations R^2 is over 0.999, which indicates that experimental data on ozone dissolution with its simultaneous decomposition can be well fitted with the Boltzmann fit. The volumetric mass transfer coefficient of ozone, $k_{L,O_3}a$, increases with the feed gas flow rate due to the increase of specific area, a, which is proportional to the gas holdup, ε_G, and inversely proportional to the bubble diameter, d.

(2) Effect of water flow rate

The effect of water flow rates on the dissolved ozone concentration in water is shown in **Fig. 4-7.** The solid lines shown in Fig. 4-7 are the Boltzmann fit results which agree with the experimental results very well. For a constant gas flow rate and inlet ozone gas concentration, the equilibrium ozone concentration increases slightly with the increase of water flow rate. As the water flow rate increased from 15.0 L/min to 19.5 L/min, the head pressure also increased from 0.22 MPa to 0.38 MPa, which results in the slight increase in the equilibrium concentration.

The $k_{L,O_3}a$ increases with increasing the water flow rate, although the values of ε_G keep almost constant as shown in **Table 4-1**. The reason is that the increase of turbulent at high water flow rate decreases the thickness of the liquid film, leading to the increase of $k_{L.}$

(3) Effect of inlet ozone concentration

Fig. 4-8(a) shows the variation of dissolved ozone concentration in water with time at different inlet ozone concentrations using the same flow rates of water and gas. The

increase of inlet ozone concentration, $C_{G,in}$, greatly increases the dissolved ozone concentration in water. The reason is inferred as follows. Because the gas flow rate was constant, the increase of $C_{G,in}$ led to the increase of ozone mass input. The increase in $C_{G,in}$ means the increase of ozone partial pressure in the gas phase. With the partial pressure of ozone in the gas phase increasing, the driving force for gas mass transfer increases, which explains why high concentrations of dissolved ozone are obtained at the same value of $C_{G,in} \cdot t$ as shown in **Fig. 4-8(b).**

Fig. 4-9 shows the equilibrium ozone concentration in the liquid phase at different inlet ozone gas concentration. Along with the increase of inlet ozone concentrations, the concentrations of dissolved ozone in water at steady state also increased due to the increase of the partial pressure of ozone in the gas phase.

(4) Effect of water surface height

Water surface height, namely liquid volume in the reactor was varied from 0.76 m to 1.16 m, while water and gas flow rates, and inlet ozone concentration were kept constant. Variation with time of dissolved ozone concentration in the middle of the reactor for different water surface heights is illustrated in **Fig. 4-10(a).** It is shown that concentration of dissolved ozone decreases with increasing water surface height. Generally speaking, the circulation pathway of microbubbles and gas/liquid contact time increase with water surface, which lead to higher dissolved concentration for a continuous system. However, in the semi-batch reactor, ozone dosage of unit volume increases with decreasing water surface height, which causes the reverse trend shown in **Fig. 4-10(a).** So, when the dissolved concentration in water is plotted against time/water surface height as shown in **Fig. 4-10(b),** the difference found in **Fig. 4-10(b)** became very little.

Volumetric mass transfer coefficients, $k_{L,O_3}a$, obtained from Boltzmann fitting are listed in Table 4-1. The $k_{L,O_3}a$ has a little increase with decreasing the water surface height. One reason is that the low liquid volume leads to high gas holdup, and the other is that better turbulence is provided by the rotating flow at lower liquid level.

4.4 Conclusions

In this chapter, we developed a new gas-induced ozone contactor with the proposed microbubble generating method. The characteristics of the gas-induced ozone contactor with microbubbles were investigated by measuring the volumetric mass transfer coefficient and gas holdup.

Gas induction by the centrifugal pump shows better mass transfer ratio, due to its higher efficiency of microbubble generation. The value of $k_{L,O_3}a$ increases with increasing the induced gas flow rate and liquid flow rate, but decreasing the working liquid level. High ozone transfer ratio was achieved at low gas flow rate, which indicates that the gas-induced ozone contactor is a desirable device for the dissolution of high concentration ozone gas.

Nomenclature

a	=	specific interfacial area	[m^{-1}]
A_1, A_2, t_0 and D	=	fitting parameters in Eq. (4-2)	[-]
C_G	=	ozone concentration in gas phase	[mg/L]
$C_{G,in}$	=	inlet ozone gas concentration	[mg/L]
C_L	=	dissolved ozone concentration in the liquid phase	[mg/L]
C_L^*	=	equilibrium ozone concentration in the liquid phase	[mg/L]
C_{out}	=	ozone concentration in off-gas	[mg/L]
C_{O_2}	=	dissolved oxygen concentration	[mg/L]
C_{0,O_2}	=	dissolved oxygen concentration at initial time	[mg/L]
d	=	diameter of a bubble	[m]
G/L	=	Q_G/Q_W, Gas/liquid ratio,	[-]
H	=	Henry's constant	[atm/mol fraction]
k_2 and k_3	=	ozone decomposition rate constant	[s^{-1}] and [L/mg·s]
k_L	=	liquid phase mass transfer coefficient	[m/s]
$k_{L,O_2}a$	=	overall volumetric mass transfer coefficient of oxygen	[s^{-1}]
$k_{L,O_3}a$	=	overall volumetric mass transfer coefficient of ozone	[s^{-1}]
M	=	water molecular weight	[g/mol]
Q_W	=	water flow rate	[L/min]
Q_G	=	gas flow rate	[L/min]
$Q_{G,in}$	=	inlet gas flow rate	[L/min]
$Q_{G,out}$	=	outlet gas flow rate	[L/min]
R	=	gas constant	[L·atm/K·mol]
R^2	=	average of squares of deviations during curve fitting	[-]
T	=	temperature	[K]

t	=	time	[s]
W_{in} and W_{out}	=	total input and output amounts of ozone measured in the gas phase, respectively	[g]
ε_G	=	gas holdup	[-]
ρ	=	water density	[kg/m^3]
η	=	ozone transfer ratio	[%]

Literature cited

Bińi, A. K., B. Duczmal, P. Machniewski; " Hydrodynamics and Ozone Mass Transfer in a Tall Bubble Column," *Chem. Eng. Sci.*, **56**, 6233-6240 (2001)

Bińi, A. K.; "Ozone Dissolution in Aqueous Systems Treatment of the Experimental Data," *Experimental Thermal and Fluid Science*, **28**, 395-405 (2004)

Bruno L., A. R. David and R. B. Deborah; "Ozone in Water Treatment-Application and Engineering," Lewis Publishers, pp.120-121 (1991)

Hsu, Y. C. and C. J. Huang; "Characteristics of a New Gas-Induced Reactor," *AIChE J.*, **42,** 3146, (1996)

Okamoto, R., H. Takeda, H., Shakutsui and H. Ohnari; "Performance of Micro-Bubble Generators," Japanese Society for Multiphase Flow Annual Meeting, Tokyo, Japan, August (2005)

Ohnari H.; "Waste Water Purification in Wide Water Area by Use of Micro-Bubble Techniques," *Japanese J. Mutiphase Flow*, **11**, 263-266 (1997)

Ohnari H., T., Saga, K. Watanabe, K. Maeda and K. Matsuo; "High Functional Characteristics of Micro-bubbles and Water Purification," *Resources Processing*, **46**, 238-244 (1999)

Ohnari H.; Water Purification of Ocean Environment and Revival of Fisheries Cultivation Using Micro Bubble Technology," The 21st Symposium on Multiphase Flow, Nagoya, Japan, July 29-31 (2002)

Ohnari H.; "MB Research Front Line," http://www.nanoplanet.co.jp/NP_mnbresearch2.html (2006) (in Japanese)

Roth J. A. and D. E. Sullivan; "Solubility of Ozone in Water," *Ind. Eng. Chem. Fundam.* **20**, 137-140 (1981)

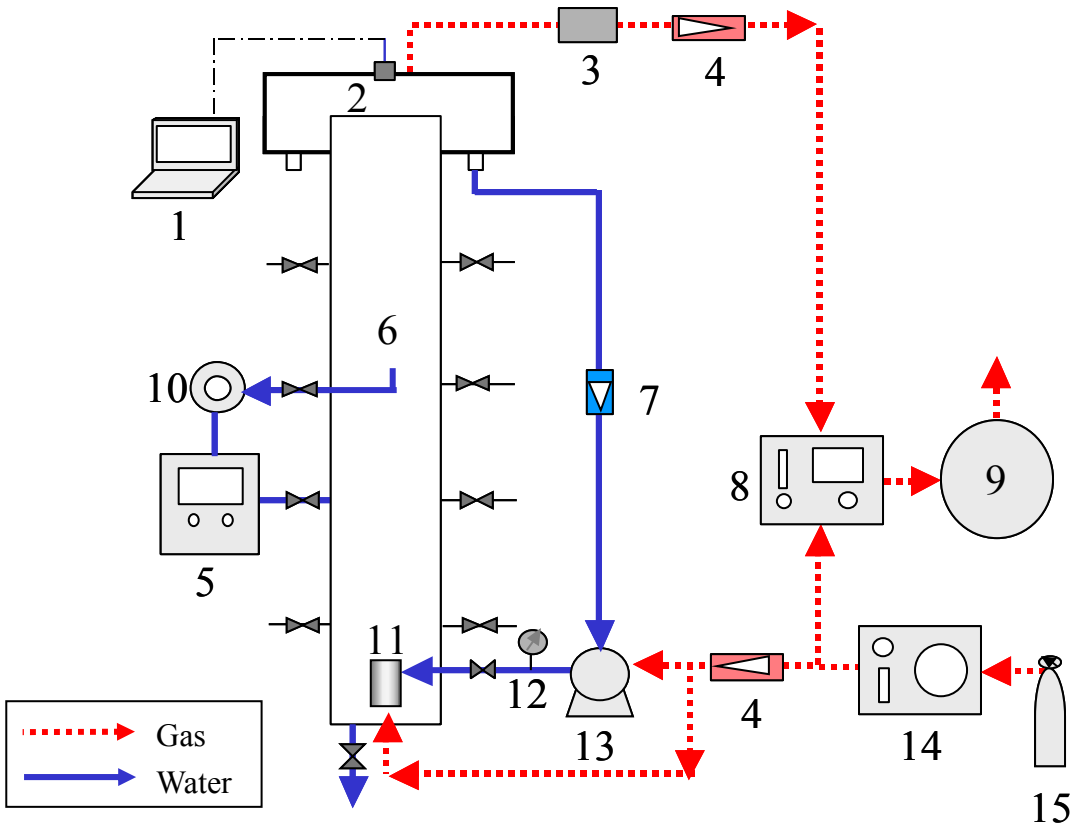

1. PC
2. Ultrasonic displacement sensor
3. Dehumidifier
4. Gas flow meter
5. Dissolved ozone monitor
6. Bubble column
7. Water flow rate
8. Gas ozone monitor
9. Ozone destructor
10. Vane pump
11. Rotating-flow microbubble generator
12. Pressure gauge
13. Centrifugal pump
14. Ozone generator
15. Oxygen cylinder

Fig. 4-1 Schematic diagram of experimental setup

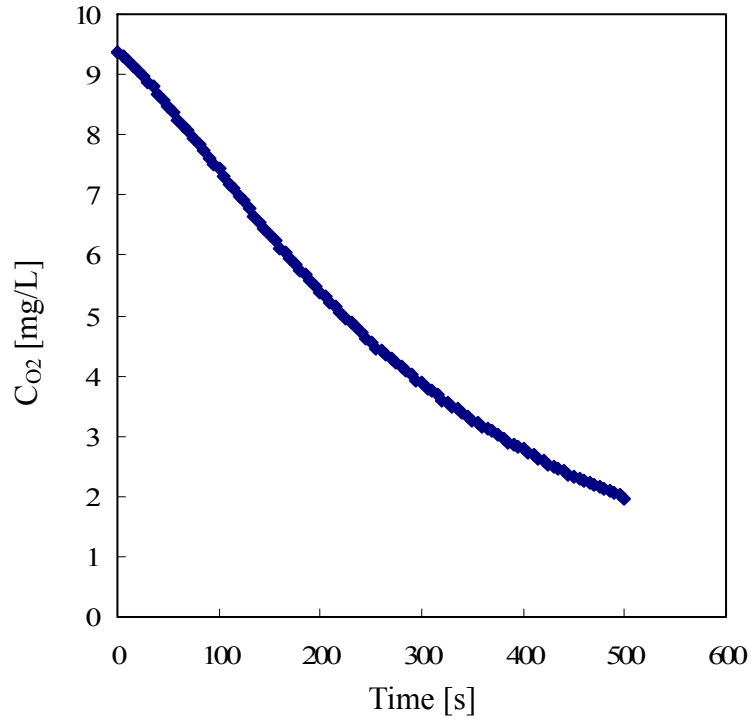

(a)

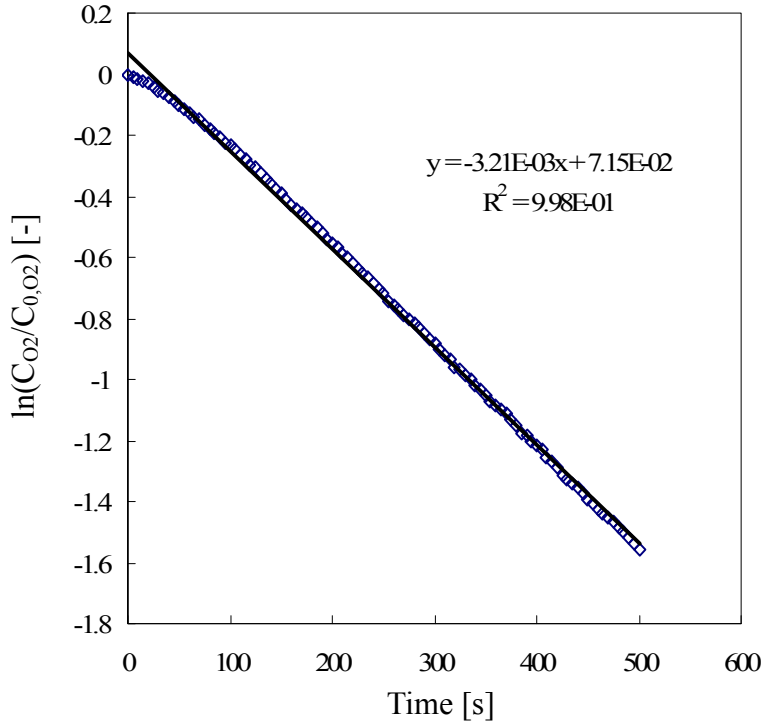

(b)

Fig. 4-2 Determination of the volumetric mass transfer coefficient of oxygen (Q_W, 15L/min; Q_G, 0.5L/min; Microbubble generation method (b))

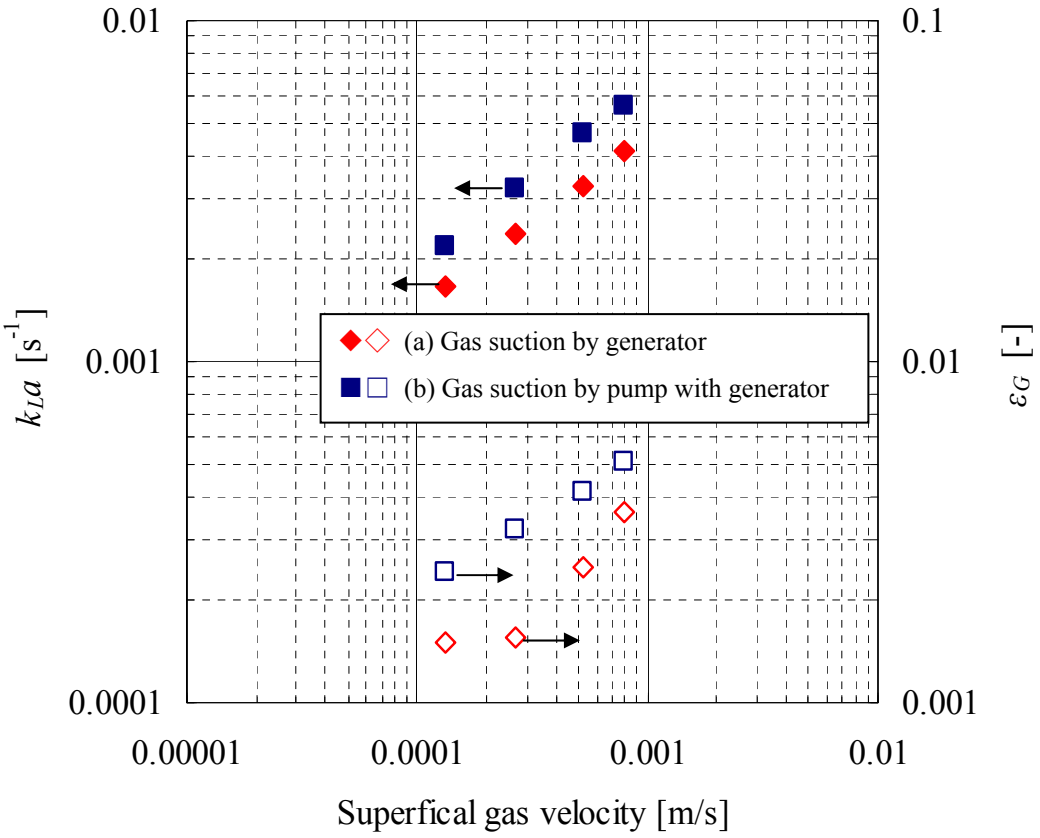

Fig. 4-3 Comparison of $k_{L,O_2}a$ and ε_G in different microbubble generation methods

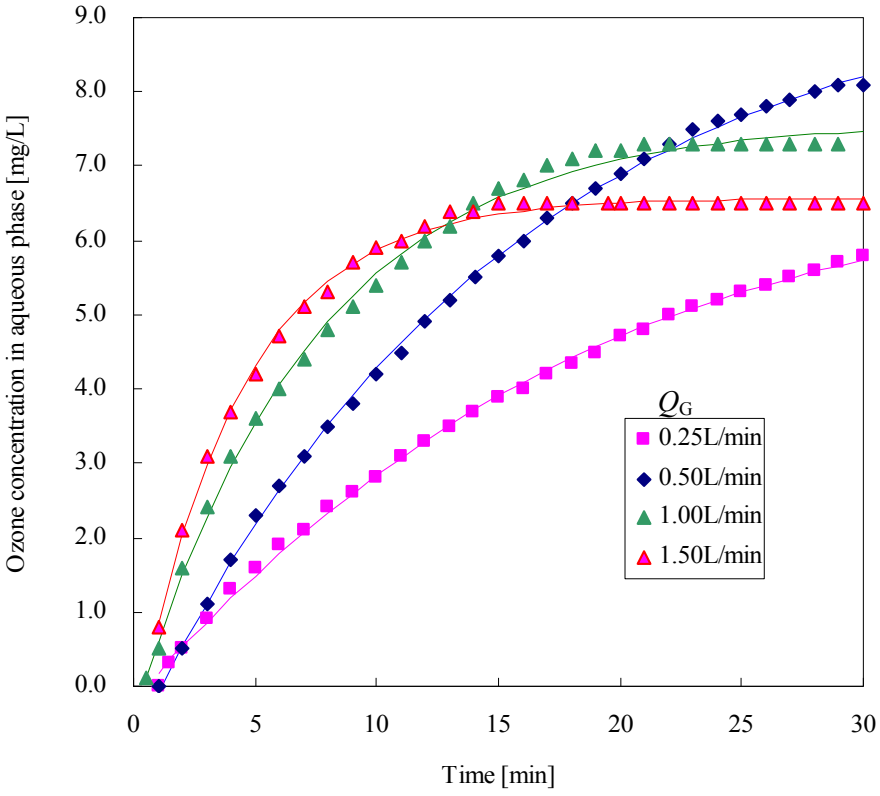

Fig. 4-4 Effect of gas flow rate on the dissolved ozone concentration in liquid phase (pH, 7.0±0.3; Temp., 23±2℃; $C_{G,in}$, 28.2 g-O_3/Nm^3; Q_W, 15L/min; lines, Boltzmann fit)

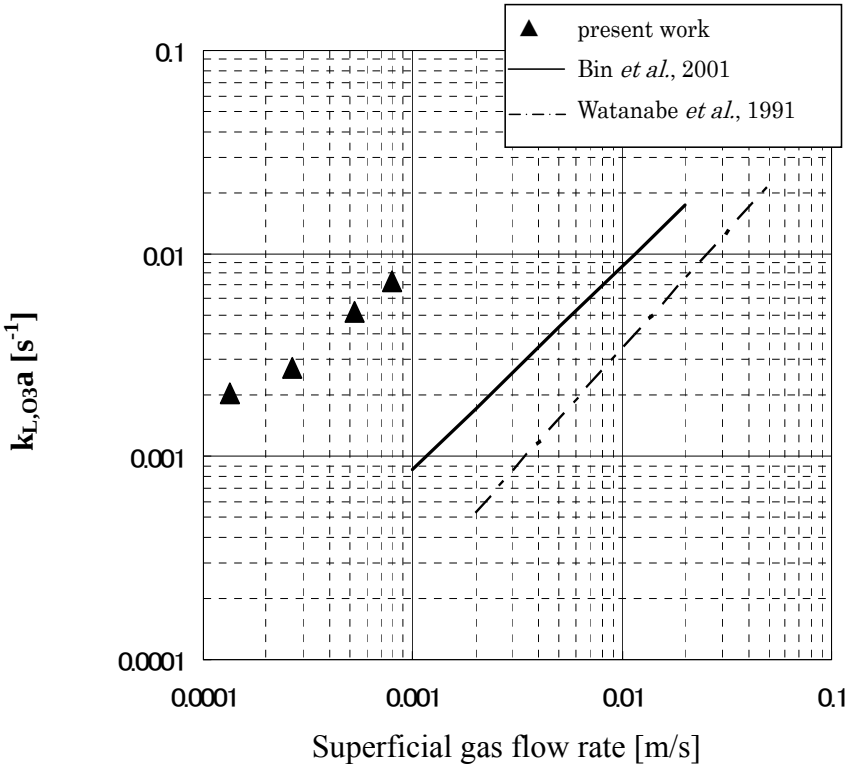

Fig. 4-5 Comparison of $k_{L,O3}a$ in the improved ozone reactor with reference data (pH,7.0±0.3; Temp., 23±2℃; $C_{G,in}$, 28.2 g-O_3/Nm^3; Q_W, 15L/min)

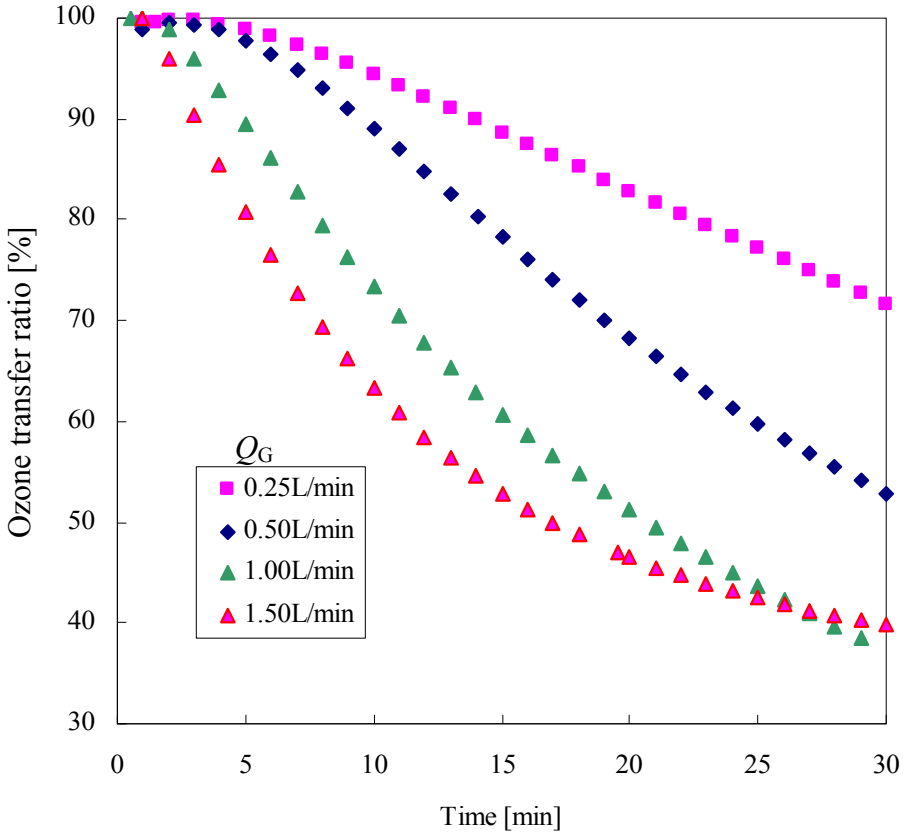

Fig. 4-6 Effect of gas flow rate on the ozone transfer ratio
(pH, 7.0±0.3; Temp., 23±2 ℃; $C_{G,in}$, 28.2 g-O_3/Nm^3; Q_W, 15 L/min)

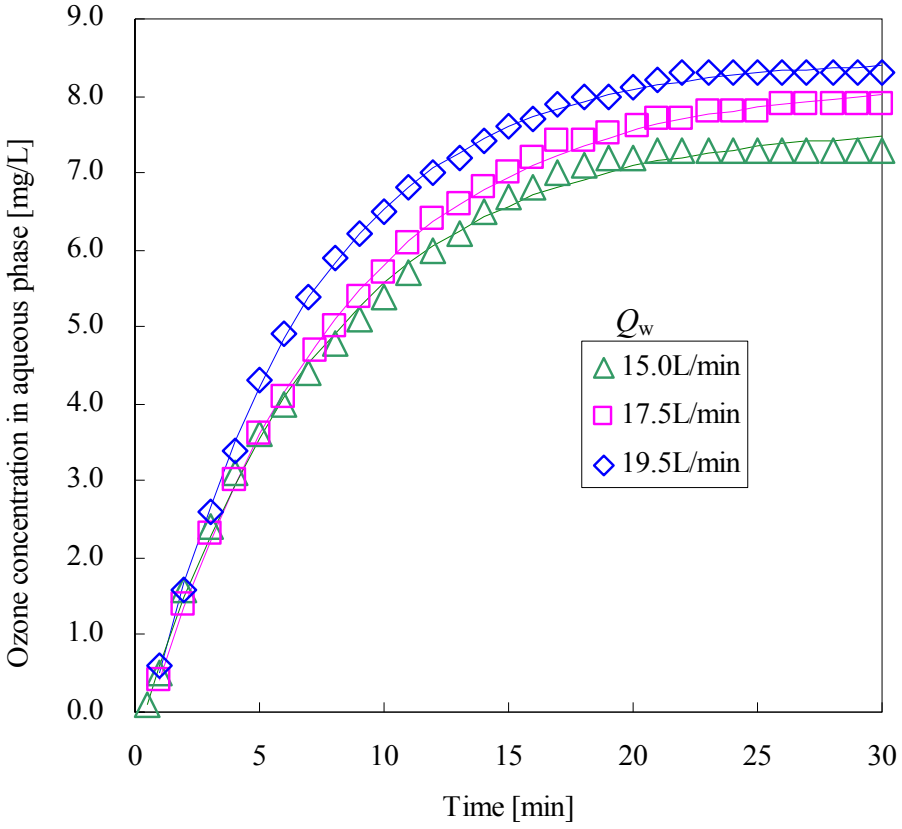

Fig. 4-7 Effect of water flow rate on the dissolved ozone concentration in liquid phase (pH, 7.0±0.3; Temp., 23.5±2 ℃; $C_{G,in}$, 28.2 g-O_3/Nm^3; Q_G, 1.0 NL/min; h, 1.16 m; lines, Boltzmann fit)

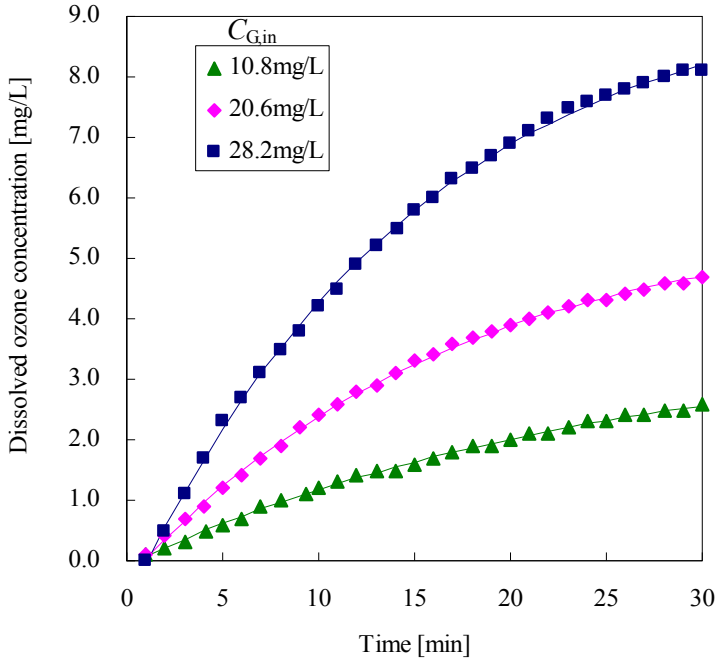

(a)

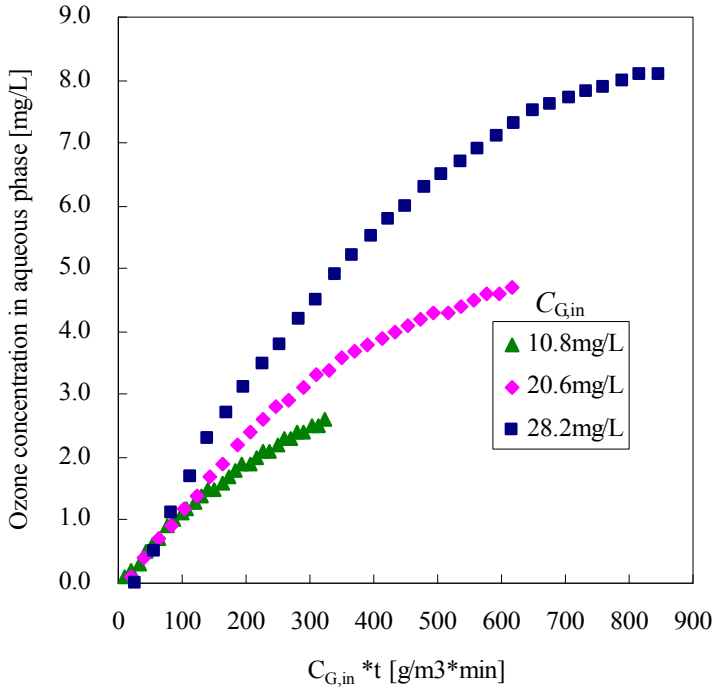

(b)

Fig. 4-8 Effect of inlet ozone concentration on the dissolved ozone concentration (pH, 4.9±0.6, Temp., 23.6±2.4℃; Q_G, 0.5 NL/min; Q_W, 15.0L/min; h, 1.16m; lines in (a), Boltzmann fit)

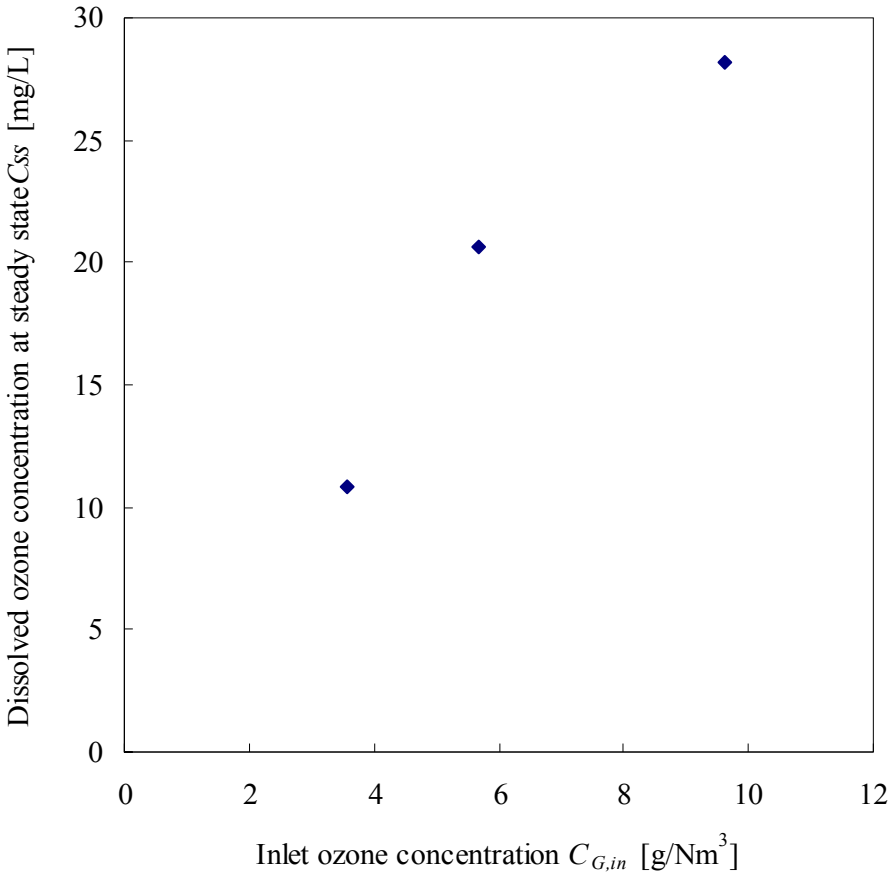

Fig. 4-9 Effect of inlet ozone concentration on the dissolved ozone concentration at steady state

(pH, 4.9±0.6; Temp., 23.6±2.4 ℃; Q_G, 0.5 NL/min; Q_W, 15.0 L/min; h, 1.16 m)

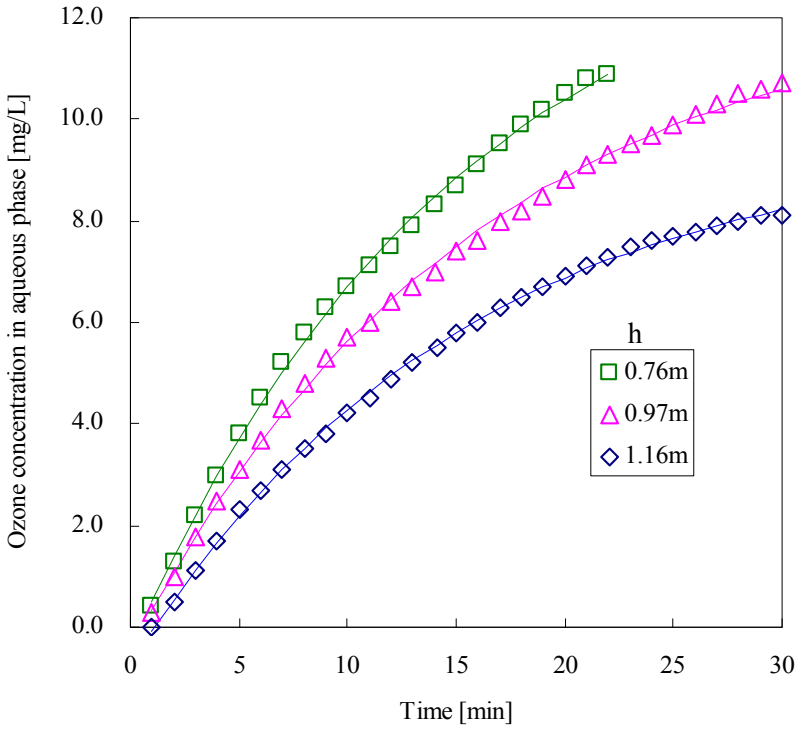

(a)

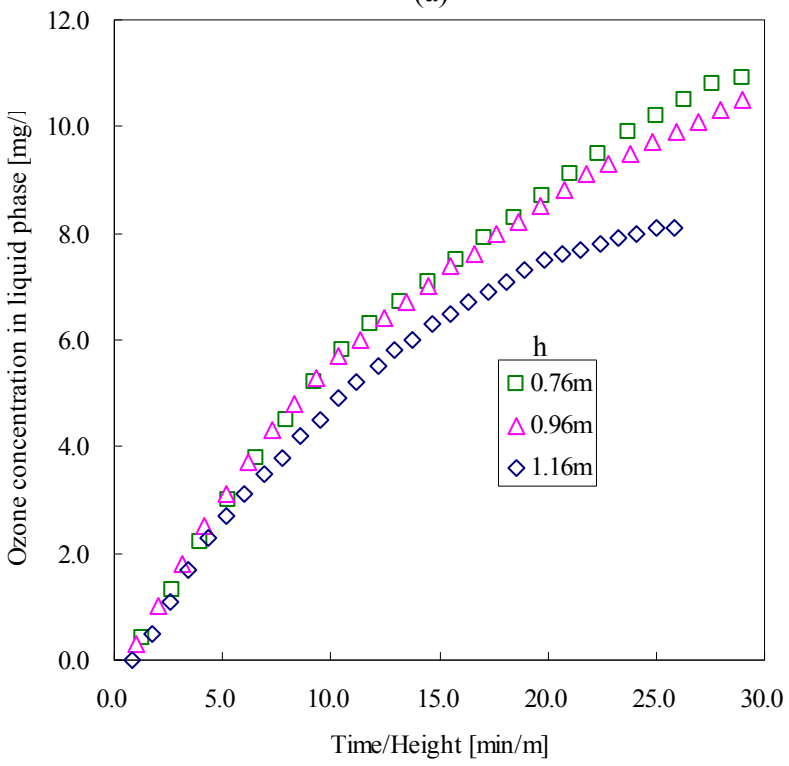

(b)

Fig. 4-10 Effect of water surface height on the dissolved ozone concentration (pH, 4.8±0.3; Temp., 21.6±2.3℃; $C_{G,in}$, 28.2 g-O_3/Nm^3; Q_G, 0.5NL/min; Q_W, 15.0L/min; lines, Boltzmann fit)

Table 4-1 Effects of gas and water flow rates on $k_{L,O_3}a$ and ε_G

$C_{G,in}$	Q_G	Q_W	G/L	h	$k_{L,O_3}a$	R^2	ε_G
[g-O_3/Nm^3]	[L/min]	[L/min]	[-]	[m]	[s^{-1}]	[-]	[-]
28.2	0.25	15.0	0.017	1.16	0.00207	0.99976	0.0024
	0.50		0.033		0.00274	0.99986	0.0032
	1.00		0.067		0.00521	0.99962	0.0041
	1.50		0.100		0.00728	0.99982	0.0051
	1.00	15.0	0.067		0.00521	0.99962	0.0040
		17.5	0.057		0.00550	0.99990	0.0039
		19.5	0.051		0.00688	0.99993	0.0041
20.6	0.50	15.0	0.033		0.00192	0.99985	0.0032
10.8					0.00134	0.99969	0.0032
28.2	0.50	15.0	0.033	0.96	0.00357	0.99980	-
				0.76	0.00402	0.99977	-

CHAPTER 5

Ozonation of dimethyl sulfoxide in aqueous solution using microbubbles

5.1 Introduction

Dimethyl sulfoxide ($(CH_3)_2SO$, DMSO), an organosulfur compound having two C-S bonds in its molecular structure as shown in **Fig. 5-1**, is colorless, thermally and chemically stable, and has excellent solvency for many organic and inorganic substances. It is widely utilized in numerous process and product applications. For example, in the manufacture of semiconductors and liquid crystal displays (LCD), it is used as a detergent or a photoresist stripping solvent in the washing and rinsing processes. Then there is a large quantity of wastewater containing DMSO produced from these processes. The annual production of wastewater containing DMSO from industries is about 5,000 tons in Japan (Murakami *et al.*, 2002). However, DMSO has toxic effects on many organisms due to its high osmolarity. Discharge of DMSO to the natural water body has led to serious environmental pollution. It is reported that DMSO plays an important role in the formation of marine troposphere aerosol and cloud condensation nuclei (Charlson *et al*., 1987; Park *et al*., 2001).

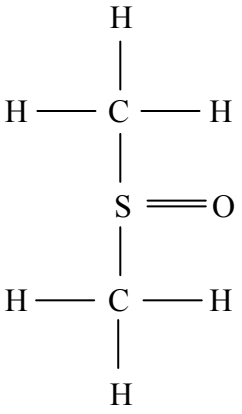

Fig. 5-1 Molecular structure of DMSO

Wastewater containing DMSO can be classified into two types according to DMSO concentration. The first type contains DMSO at high concentrations, usually more than 1,000 mg/L, and it is mainly discharged from the photoresist stripping solvent. Generally, this kind of wastewater is concentrated and combusted for the removal of DMSO. The other type contains DMSO at low concentrations ranging from 10 to 1000 mg/L, and it is mainly derived from the rinsing process in the manufacture of semiconductors and LCDs. The amount of the second type of wastewater is large as compared with that of the first type, and its low concentration results in low removal efficiency (Murakami *et al.*, 2002).

Biological treatment is the most popular method for the removal of DMSO from wastewater at a low level of concentration. Microorganisms in sewage and activated sludge can use DMSO as a carbon and energy source and degrade it to formaldehyde and sulfide by a pathway as shown in **Fig. 5-2(a)**. The breakdown of 1 mole of DMSO produces 2 moles of formaldehyde which is finally converted to carbon dioxide or used for cell synthesis, and 1 mole of sulfide which is oxidized to sulfide in the end. Intermediate products such as dimethyl sulfide (DMS), methyl mercaptan and hydrogen sulfide cause odor problems, and are toxic to humans (Park *et al*., 2001). Glindemann *et al.* (2006) carried out a field study at a sewage treatment plant of Philadelphia and found that overlooked mg/L concentration of industrial DMSO waste residues in sewage could cause “rotten cabbage” odor problems in conventional municipal wastewater treatment. They also reported that formation of odorant DMS from DMSO often occurred under anoxic and anaerobic conditions, such as in poorly conveyed zones in the sewers, primary sedimentation tanks, selector zones in activated sludge systems, zones with poor mixing performance in aeration tanks, and in secondary sedimentation.

Recently, advanced oxidation processes (AOPs) are applied to the biological treatment of DMSO as a pretreatment process to overcome the odor problem. Combinations of ozone (O_3) and hydrogen peroxide (H_2O_2) or UV are often utilized in the AOPs. Park *et al.* (2001) suggested fenton treatment (Fe^{2+}/H_2O_2) as a useful pretreatment method for biological treatment in the case of highly concentrated DMSO. But the production of fenton sludge is one big problem. Koito *et al.* (1988) showed that UV/H_2O_2 process could efficiently oxidize DMSO into methansulfonic acid (MSA, $CHSO_3H$)

which was biodegradable without producing any reduced and harmful sulfur-containing by-products. Shigeta (1999) proposed a treatment method concluding two steps: oxidation of DMSO to dimethyl sulfone ($DMSO_2$) with hydrogen peroxide (H_2O_2) and ozone, and biodegradation of $DMSO_2$ by activated sludge. In these AOPs, hydroxyl radical ·OH is assumed to be the main oxidant responsible for the decomposition of DMSO. A proposed oxidation pathway of DMSO is shown in **Fig. 5-2(b).** DMSO is firstly degraded into dimethyl sulfone ($DMSO_2$). Secondly, $DMSO_2$ is oxidized into MSA, and further to sulfuric acid. Although AOPs can efficiently control formation of odorant substances, the high costs of equipment, chemicals and electricity diminish their advantages to some extent. Shigeta (1999) demonstrated that the further oxidation of $DMSO_2$ to MAS was not recommended because that would increase the consumption of oxidizers which were always expensive.

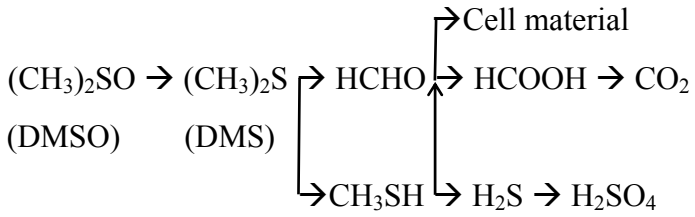

(a) Biological degradation (Park *et al*., 2001)

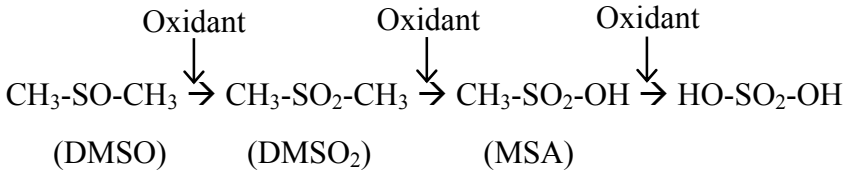

(b) Oxidation by O_3/H_2O_2

Fig. 5-2 Proposed pathways of DMSO during the degradation

In the first part of experiments in CHAPTER 5, the author tried to search for a non-chemical method to remove DMSO with microbubbles. Static pressure intensively increases and decreases after during microbubble generation, which may result in bubble collapse. As well known in the sonoluminescence phenomenon, the collapse of bubbles

produced by cavitation creates short-lived, localized hot spots (Gaitan *et al.*, 1992). In clouds of cavitating bubbles, these hot spots have equivalent temperatures of roughly 5000 K, pressures of about 1000 atmospheres, and heating and cooling rates about 10^{10} K/s (Suslick *et al.*, 1999). Such a high-temperature and high-pressure zone can make water molecules abound it decomposed, yielding hydroxyl radical ·OH. If hot spots occur during microbubble generation in the proposed system of this study, the produced ·OH can degrade DMSO to $DMSO_2$. This hypothesis will be verified through air microbubble generation under different conditions.

In the second part of CHAPTER 5, some experimental work on ozone oxidation of DMSO is shown. It has been verified in CHAPTER 4 that ozone mass transfer can be improved by the application of microbubbles. Consequently, the reaction between ozone and organic substance is supposed to be accelerated by using microbubbles.

5.2 Experimental

The raw water was prepared by diluting DMSO reagent with distilled water. The concentration of DMSO was kept about 10 mg/L in all experiments. 0.1M hydrochloric acid (HCl) solution and 0.05M sodium hydroxide (NaOH) solution are used to adjust pH of DMSO solution. Ionic strength of DMSO solution was varied by adding sodium chloride (NaCl). Salt concentration was changed from 0 to 1 wt%, while pH was varied in the range of 4.3~9.5.

The experimental apparatus was the same as that used in CHAPTER 4 as shown in Fig. 4-1. All the experiments were carried out in semi-batch mode. For the experiments in free radical verification, air microbubbles were generated at air and water flow rates of 0.5L/min and 15.0 L/min, respectively. Samples were taken from the sampling tap in the middle of the reactor every 5 minutes. For the experiments in ozone oxidation, ozone microbubbles are generated at different gas and water flow rates. Ozone concentrations in solution and inlet and outlet gases were online monitored during the whole reaction process.

DMSO and $DMSO_2$ concentrations in aqueous samples were determined by GC-FID (GC-2010, Shimazu Co.). The analysis conditions in GC method are as follows: the

initial temperature in DB-WAX column was 100 ˚C and kept for 1 minute; then the temperature was increased to 230 ˚C at a rate of 30 ˚C/min and maintained at the final temperature for 6 minutes; the temperature in FID was 250 ˚C. The detection time was 3.9 min for DMSO measurement and 5.3 min for $DMSO_2$. Carrier gas, helium, was fed at a flow rate of 15 mL/min.

TOC (total organic carbon) of aqueous samples was measured with SHIMAZU TOC-5000. A pH meter (HM-40S, DKK-TOA Co.) was used to measure pH of samples.

5.3 Theoretical

In a gas-liquid system where gas dissolution is followed by a chemical reaction, two steps control the overall reaction rate: the mass transfer from gas phase to the liquid phase and the chemical reaction in the liquid phase (Rice and Browning, 1981; Gould and Ulirsch, 1992). The ozone oxidation can be considered to be a mass-transfer controlled reaction owing to the low solubility of ozone (Hsu and Huang, 1996). In such a mass-transfer controlled reaction, the resistance of gas film diffusion is negligible as compared with that of liquid film diffusion, and the rate of mass transfer of ozone from gas phase into liquid phase is limited by liquid film diffusion (Kuo *et al*., 1977; Sotelo *et al*., 1989; Gould and Ulirsch, 1992; Munter *et al*., 1993).

It is assumed that the ozonation of DMSO can be presented by Eq. (5-1) with a stoichiometric ratio of *b*.

$$DMSO + bO_3 + H_2O \rightarrow DMSO_2 + \text{other products} \qquad (5\text{-}1)$$

By referring to Hsu and Huang (1996) and Saunders *et al.* (1983), the rate of reaction can be defined by Eq. (5-2) with assuming that the reaction is a first-order.

$$-\frac{dC_D}{dt} = k_D \cdot C_D = \frac{(k_{L,O_3}a)D_{L,D}}{D_{L,O_3}} \cdot C_D \qquad (5\text{-}2)$$

The terms in Eq. (5-2) are defined as follows: C_D [mg/L] is the concentration of DMSO, k_D [s^{-1}] is the reaction constant, $k_{L,O3}a$ [s^{-1}] is the mass transfer coefficient of ozone, $D_{L,D}$ and $D_{L,O3}$ [m^2/s] are the molecular diffusivity of DMSO and ozone. Assuming that the diffusivities of ozone and DMSO in water and the quantity of $k_{L,O3}a$ remain constant during the reaction, Eq. (5-3) can be obtained by integrating Eq.(5-2).

$$\ln \frac{C_{D0}}{C_D} = \frac{(k_{L,O_3}a)D_{L,D}}{D_{L,O_3}} t \qquad (5\text{-}3)$$

The value of $\ln(C_{D,0}/C_D)$ in a reaction can be plotted against with the reaction time. If there is a linear relationship between them, the assumption of firs-order ozonation kinetics of DMSO is correct and the slope of the line represents $(k_{L,O3}a)\ D_{L,D}/\ D_{L,O3}$.

5.4 Results and discussion

5.4.1 Air microbubbles

It has been reported in many literatures that high concentration of a solute could prevent bubble coalescence and cause small bubbles to be formed (Hofmeir *et al*., 1995; Walker *et al*., 2001). In this work, NaCl was added to the raw water containing DMSO. **Fig. 5-3** shows the variation of DMSO concentration, TOC and pH at different NaCl concentrations. DMSO concentration did not decrease but slightly increased when no salt was added. However, a little decrease in DMSO concentration was observed at salt concentrations of both 4.0 g/L and 9.4 g/L. TOC kept almost constant at all the salt concentrations. Changes of pH shows similar trend with that of DMSO concentration. However, $DMSO_2$, the expected product from DMSO oxidation by hydroxyl radicals, was not detected at all conditions, which suggested that no free radicals were generated during microbubble generation.

The initial pH of raw water without any adjustment was neutral. With the addition of NaOH or HCl solutions, the initial pH was changed to basic or acid, respectively. DMSO concentration, TOC and pH were plotted with time in **Fig. 5-4**. There are not any marked tendency shown in the variation of DMSO concentration, TOC and pH. Analysis results for $DMSO_2$ concentration were zero at each initial pH value. Then, it is believed that there were not free radicals produced during microbubble generation under the present conditions.

5.4.2 Ozone microbubbles

(1) Effect of ozone gas flow rate on DMSO oxidation

Gas flow rate of input ozone was varied from 0.25 L/min to 1.50 L/min, while water flow rate and ozone concentration was kept 15.0 L/min and 28.2 g-O_3/Nm^3, respectively. **Fig. 5-5** shows the changes of TOC, DMSO and $DMSO_2$ concentrations, and pH with reaction time. TOC remained constant as the gas flow rate was changed. DMSO concentrations and pH of solution decreased while the oxidation product, DMSO2, increased with time proceeding. The oxidation rate, that is, the decrease rate of DMSO or the increase rate of DMSO2, also increased with increasing the ozone gas flow rate. This can be explained by the difference in aqueous ozone concentrations as shown in **Fig. 5-6(a)**. When the input gas flow rate was increased, the concentration of ozone dissolved in water also increased, which resulted in the increase of oxidation rate.

The change of ozone concentration in off-gas with time as shown in **Fig. 5-6(b)** was used to calculate the ozone transfer ratio, η [%], through the Eq. (4-10). The calculation results are illustrated in **Fig. 5-7(b).** The ozone transfer ratio decreased with the increase of ozone gas flow rate, which agrees with the results shown in Fig. 4-6.

To examine the effect of gas flow rate on the ozone utilization ratio, we divided the quantity of ozone supplied into that of DMSO removed and plot them with gas flow rates in **Fig. 5-8(a).** The amount of ozone supplied, $W_{O3,S}$, and that of DMSO removed, $W_{D,R}$ during a time of t are calculated by the following equations,

$$W_{O3,S} = Q_{in} \times C_{in} \times t;\ W_{D,R} = (C_{D0}\text{-}C_D) \times V \times t \qquad \textbf{(5- 4)}$$

where V [L] is the volume of raw water in the ozone reactor. The ratio of $W_{D,R}/W_{O3,S}$ decreased with reaction time. When the ozone gas flow rate was varied from 0.25L/min to 1.50 L/min, the value of $W_{D,R}/W_{O3,S}$ at the end of reaction decreased from 0.72 to 0.31.

A part of ozone supplied into the reactor dissolved into water while the rest flowed out with the off-gas as shown in **Fig. 5-7(a)**. The amount of ozone dissolved into water, $W_{O3,D}$, can be calculated though the following equation,

$$W_{O_3,D} = W_{O_3,S} - W_{O_3,out} = Q_{in}C_{in}t - \int_0^t Q_{out}C_{out}dt \qquad \textbf{(5- 5)}$$

Therefore, it is also necessary to check how efficiently the part of ozone dissolved in water was utilized by DMSO. Then, we divided the amount of ozone dissolved in water into the corresponding amount of DMSO removed and illustrated the results in **Fig. 5-8(b).** The mass ratio of $W_{D,R}/W_{O3,D}$ decreased from 0.8 to 0.4 when the gas flow rate was varied from 0.25L/min to 1.00 L/min, but it slightly increased to 0.57 with the further increase of gas flow rate to 1.50 L/min. However, the highest ozone utilization ratio was obtained at the lowest gas flow rate for the present experimental conditions.

The linear relationship between $ln(C_{D,0}/C_D)$ and reaction time as shown in **Fig. 5-9** indicates that the ozonation of DMSO is a first-order mass-transfer controlled reaction. The reaction rate constants obtained from the slopes were listed in **Fig. 5-9Table 5-1**. k_D increased from 6.97×10^{-4} s^{-1} to 1.94×10^{-3} s^{-1} with the increase of gas flow rate from 0.25 L/min to 1.50 L/min.

(2) Effect of water flow rate on DMSO oxidation

The flow rate of water circulated by the centrifugal pump was changed from 15.0 L/min to 19.5 L/min, while gas flow rate and ozone concentration was kept 1.0 L/min and 28.2 g-O_3/Nm^3, respectively. **Fig. 5-10 (a), (b)** and **(c)** show the effect of water flow rate on the changes of TOC and DMSO concentrations, $DMSO_2$ concentration, and pH with reaction time, respectively. TOC kept constant with time as water flow rate was varied. DMSO concentration and pH of solution decreased and $DMSO_2$ concentration increased with reaction time proceeding. The effect of water flow rate on the oxidation rate was very small as compared with that of gas flow rate.

The ozone concentrations in water and off-gas were measured in the process of ozonation and the results are shown in **Fig. 5-11 (a)** and **(b).** Both the dissolved ozone concentration and the off-gas ozone concentration slightly increased as the water flow rated increased. Based on the data shown in Fig. 5-11, the ozone transfer ratio was calculated and illustrated in **Fig. 5-12 (a)** and **(b).** Water flow rate had small effect on the ozone transfer which is of great importance for a mass-transfer controlled reaction.

5.5 Conclusions

In the present chapter, the author verified whether hydroxyl radical can be generated by microbubbles or not. There were no ·OH detected when salt concentration and pH were changed for wide ranges. Much more intensive changes in static pressure are necessary to make microbubbles collapse and generate free radicals.

The oxidation of DMSO by ozone using microbubbls was investigated under different gas and water flow rates. Experimental results indicate that the ozonation of DMSO is a first-order mass-transfer controlled reaction. Ozone utilization ratio increases with decrease in gas flow rate. The ratio of DMSO removed to ozone dissolved can be raised to as high as 0.8 or higher with proper gas and water flow rates.

Nomenclature

b	=	stoichiometric ratio in Eq. (5-1)	[-]
C_D	=	DMSO concentration	[mg/L]
C_{D0}	=	DMSO concentration in raw water (at t=0min)	[mg/L]
C_{in}	=	inlet ozone gas concentration	[mg/L]
C_{out}	=	ozone concentration in off-gas	[mg/L]
$D_{L,D}$	=	molecular diffusivity of DMSO	[m^2/s]
$D_{L,O3}$	=	molecular diffusivity of ozone	[m^2/s]
k_D	=	reaction constant of reaction in Eq. (5-1)	[s^{-1}]
$k_{L,O3}a$	=	overall mass transfer coefficient of ozone	[s^{-1}]
Q_W	=	water flow rate	[L/min]
Q_G	=	gas flow rate	[L/min]
t	=	time	[min]
$W_{D,R}$	=	amount of DMSO removed	[mol]
$W_{O3,D}$	=	amount of ozone dissolved into water	[mol]
$W_{O3,S}$	=	amount of ozone supplied	[mol]
t	=	time	[min]
η	=	ozone transfer ratio	[%]

Literature cited

Charlson R. J., J. E. Lovelock, M. O. Andreae *et al.*; " Atomosphere Sulphur, Cloud Albedo and Climate." *Nature*, **61**, 326-655 (1987)

Gaitan, D. F., Crum L. A., Church C. C. et al.; "Sonoluminescence and Bubble Dynamics for A Single, Stable, Cavitation Bubble," *J. The Acoustical Society of America*, **91,** 3166-3183 (1992)

Glindemann, D.; J. Novak and J. Witherspoon; "Dimethyl Sulfoxide (DMSO) Waste Residues and Municipal Waste Water Odor by Dimethyl Sulfide (DMS): the North-East WPCP Plant of Philadelphia," *Environ. Sci. Technol.*, **40**, 202-207 (2006)

Gould, J. P., and G. V. Ulirsch; "Kinetics of the Heterogeneous Ozonation of Nitrated Phenols," *Wat. Sci. Technol.,* **26**, 169 (1992)

Hsu, Y. C. and C. J. Huang; "Characteristics of a New Gas-Induced Reactor," *AIChE*, **42**, 3146-3152 (1996)

Koito T., M. Tekawa and A. Toyoda; "A Novel Treatment Technique for DMSO wasterwater," *IEEE Transactions on Semiconductor Manufacturing*, **11**, (1988) 3-8

Kuo, C. H., K.Y. Li, C. P. Wen *et al.*; "Absorption and Decomposition of Ozone in Aqueous Solutions," *AIChE Symp. Ser.,* **73**, 230 (1977)

Murakami, N. T., H. Kurimura, K. Kirimura *et al.*; "Continuous Degradation of Dimethyl Sulfoxide to Sulfate Ion by Hyphomicrobium denitrificans WU-K217," *J. Bioscience & Bioengineering*, **94**, (2002) 52-56

Munter, R., S. Preis and S. Kamenev *et al.*, "Methodology of Ozone Introduction into Water and Wastewater Treatment," *Ozone Sci. Eng.*, **15**, 149 (1993)

Park S. J., T. I.Yoon, J. H. Bae *et al.*; "Biological Treatment of Wastewater Containing Dimethyl Sulphoxide from the Semi-Conductor Industry," *Process Biochemistry*, **36**, 579-589 (2001)

Rice, R. G., and M. E. Browning; "Ozone Treatment of Industrial Wastewater," *Noyes Data Corp., NJ* (1981)

Saunders, F. M., J. P. Gould and C. R. Southerland; “The Effect of Solute Competition on Ozonolysis of Industrial Dyes,” *Water Research*, **17**, 1407 (1983)

Shigeta, K.; “Method and Apparatus for Treatment Wastewater Containing Dimethyl Sulfoxide,” *Patent of Japan*, P2000-263069

Sotelo, J. L., F. J. Beltran, F. J. Benitez *et al*.; “Henry’s Las Constant for the Ozone-Water system,” *Water Res.*, **23**, 1239 (1989)

Suslick, K. S., W. B. Mcnamara III and Y. Didenko, “Hot Spot Conditions During Multi-Bubble Cavitation,” Sonochemistry and Sonoluminescence, Kluwer Publishers, Dordrecht, Netherlands, pp. 191-204 (1999)

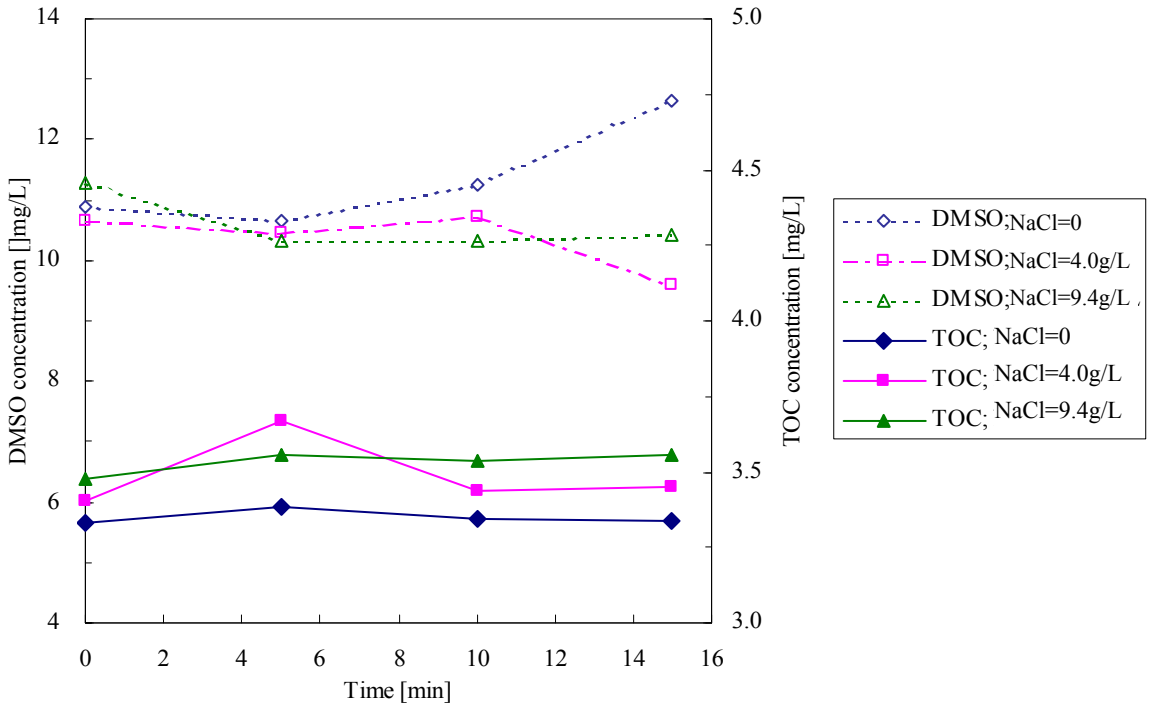

(a)

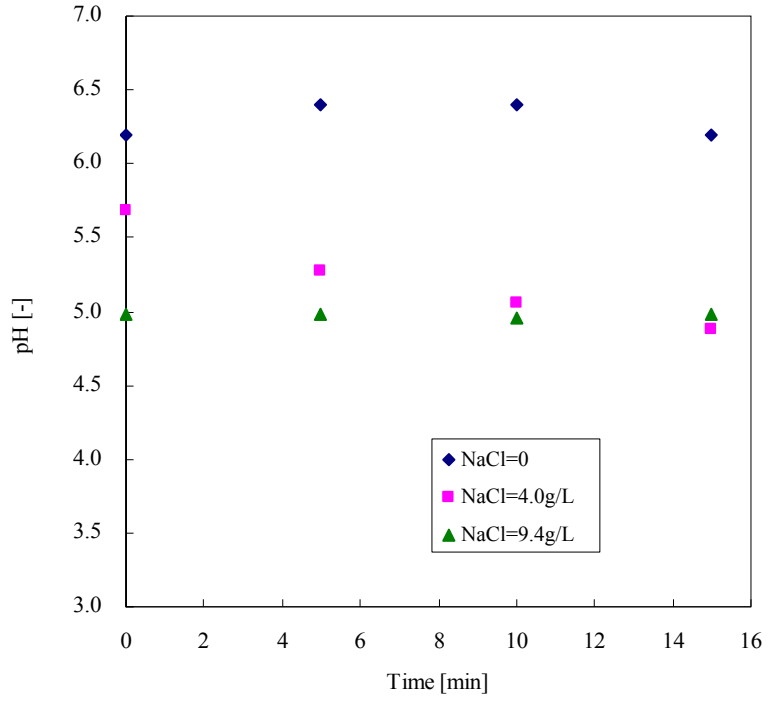

(b)

Fig. 5-3 Effect of salt concentration

(Q_A: 0.50~0.54 L/min; Qw: 15.0 L/min; T: 24~25 ℃)

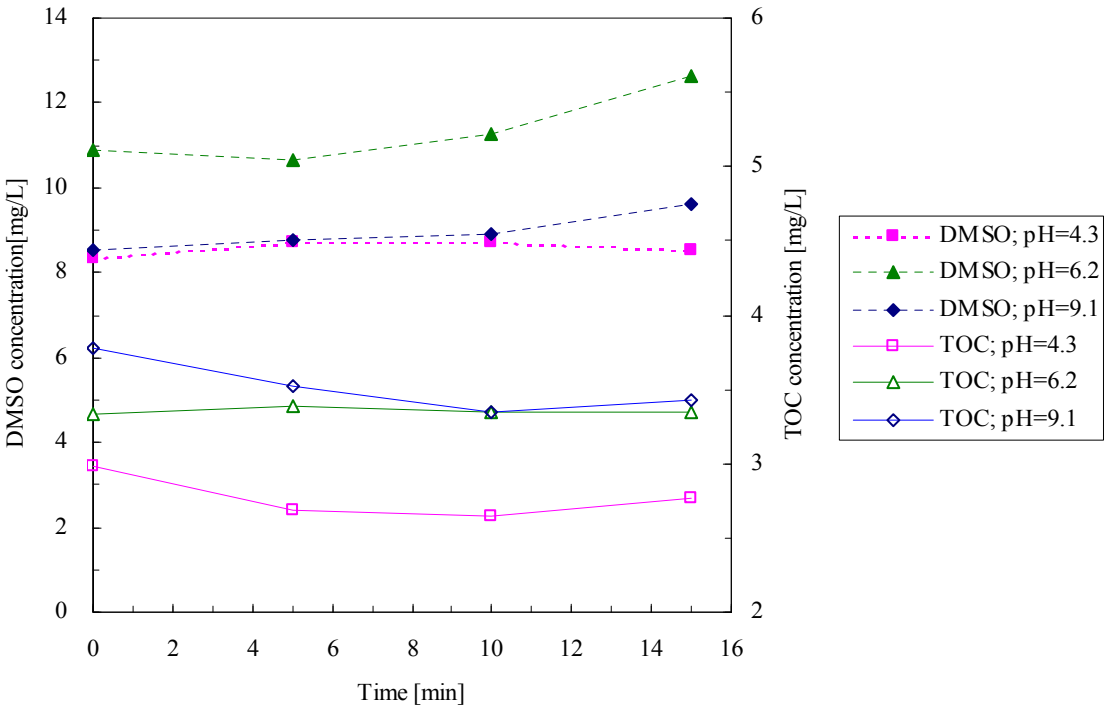

(a)

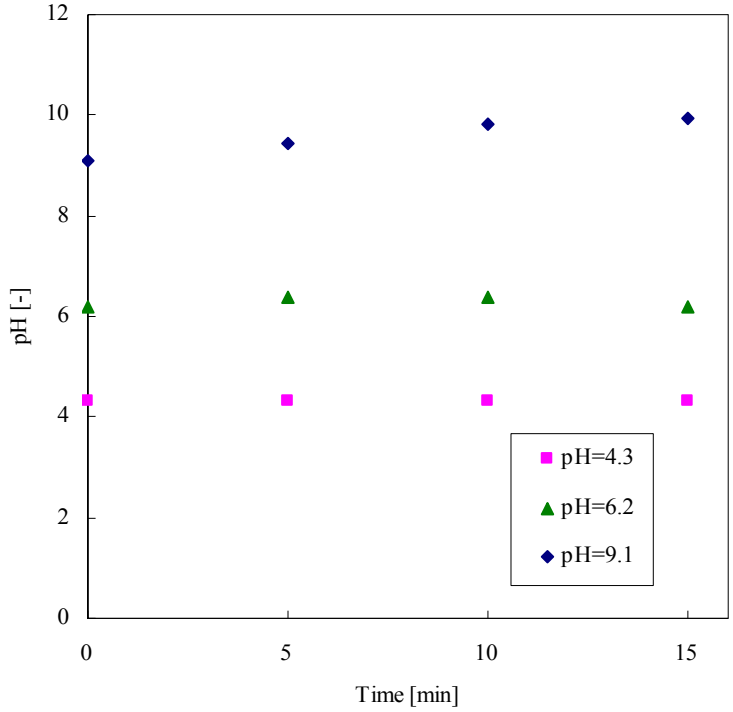

(b)

Fig. 5-4 Effect of initial pH

(Q_A: 0.5 L/min; Qw: 15.0 L/min)

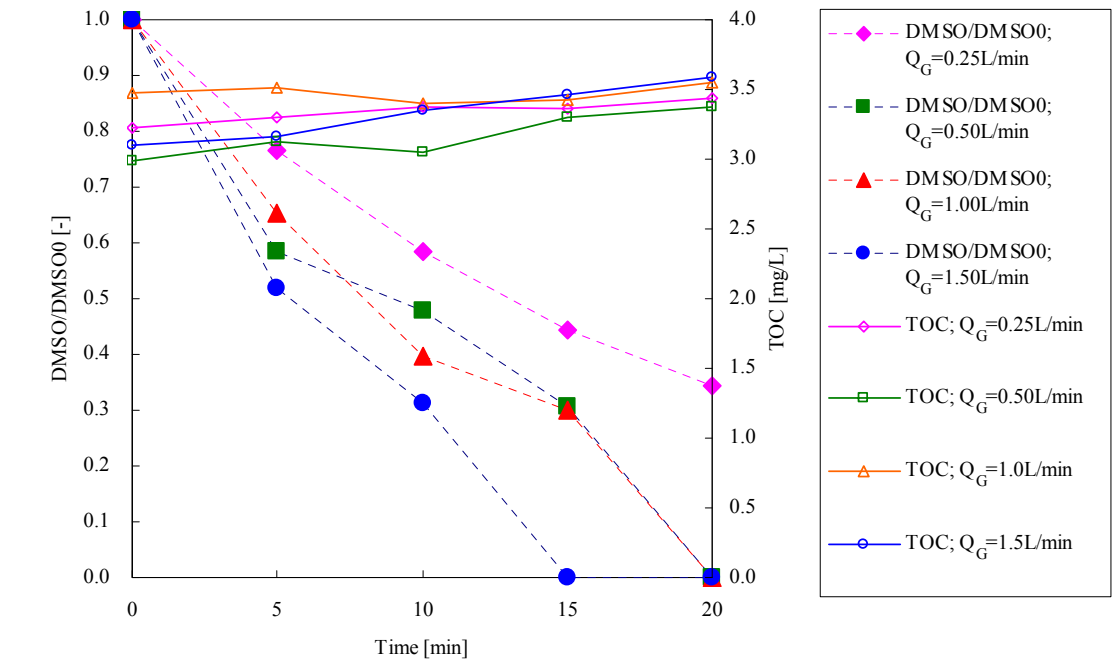

(a)

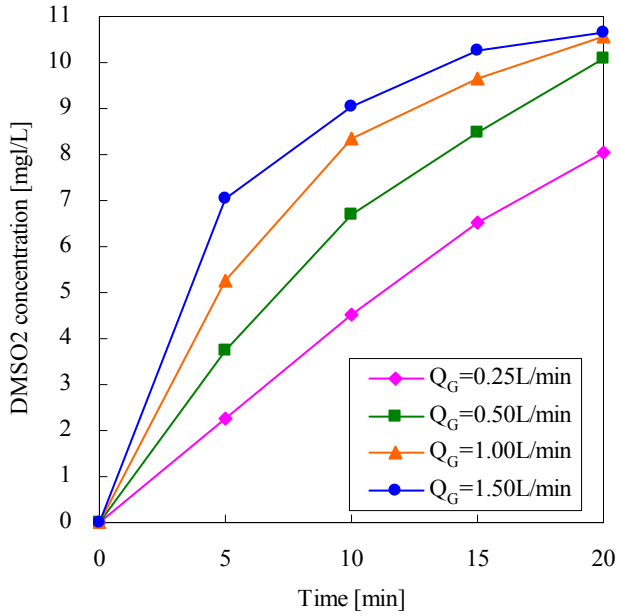

(b)

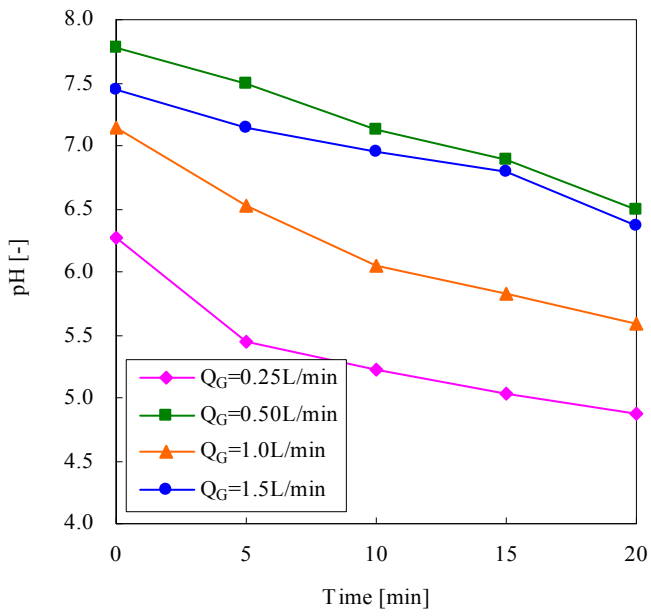

(c)

Fig. 5-5 Effect of gas flow rate on ozonation of DMSO

(Q_W, 15.0L/min; $C_{G,in}$, 28.2 g-O_3/m^3; T, 22~26 ºC; pH, 5.6-7.8 (unbuffered))

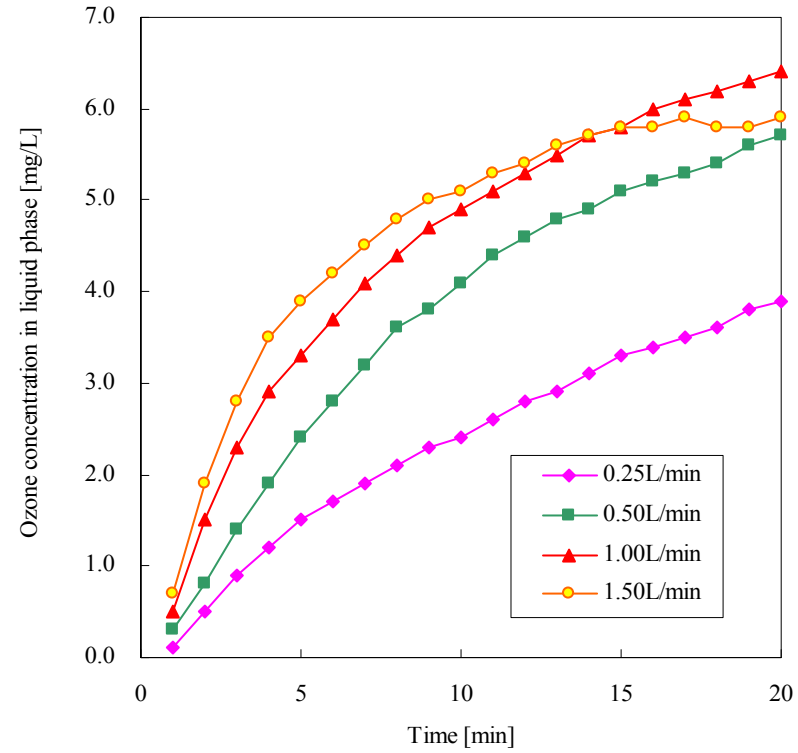

(a)

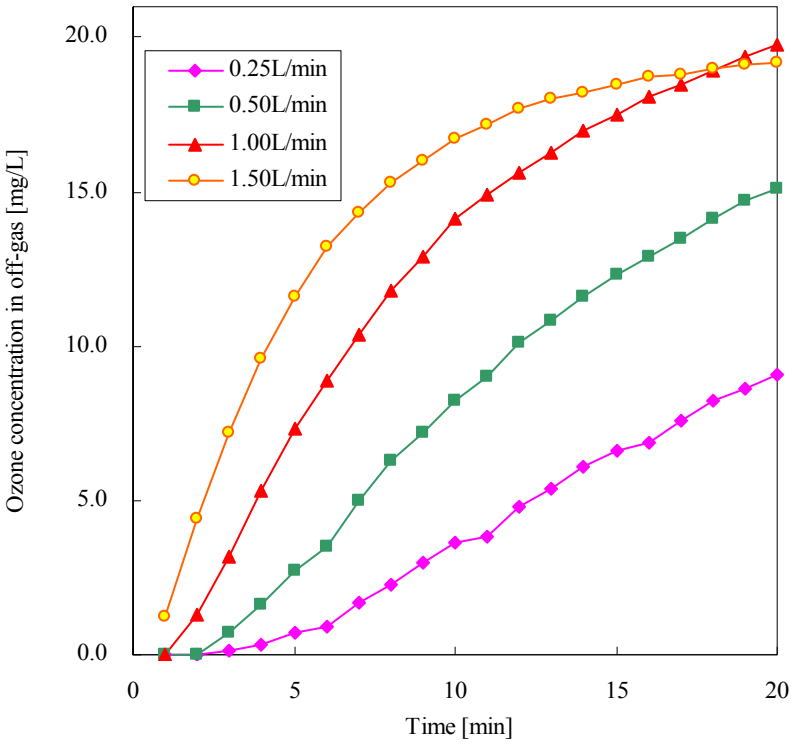

(b)

Fig. 5-6 Effect of gas flow rate on ozone concentrations in liquid and off-gas

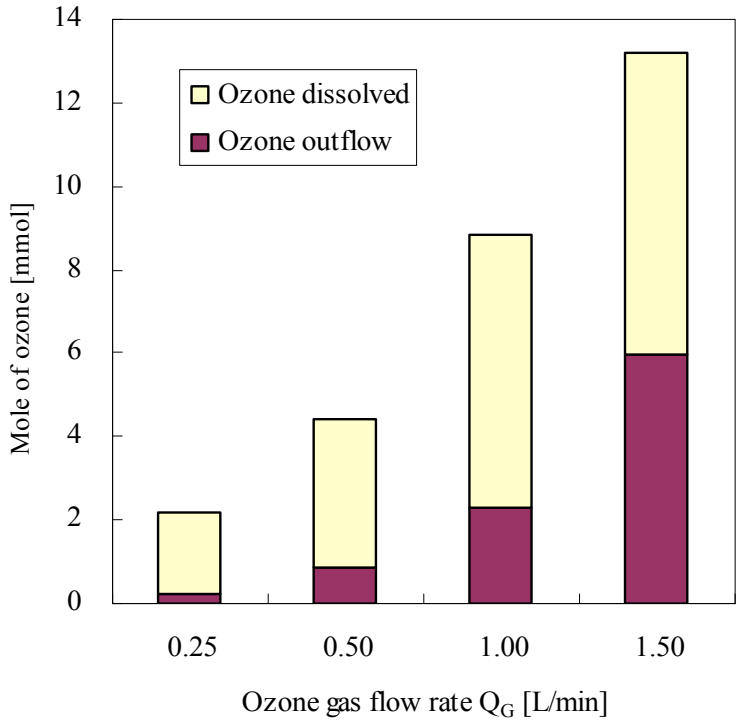

(a) at t = 15 min

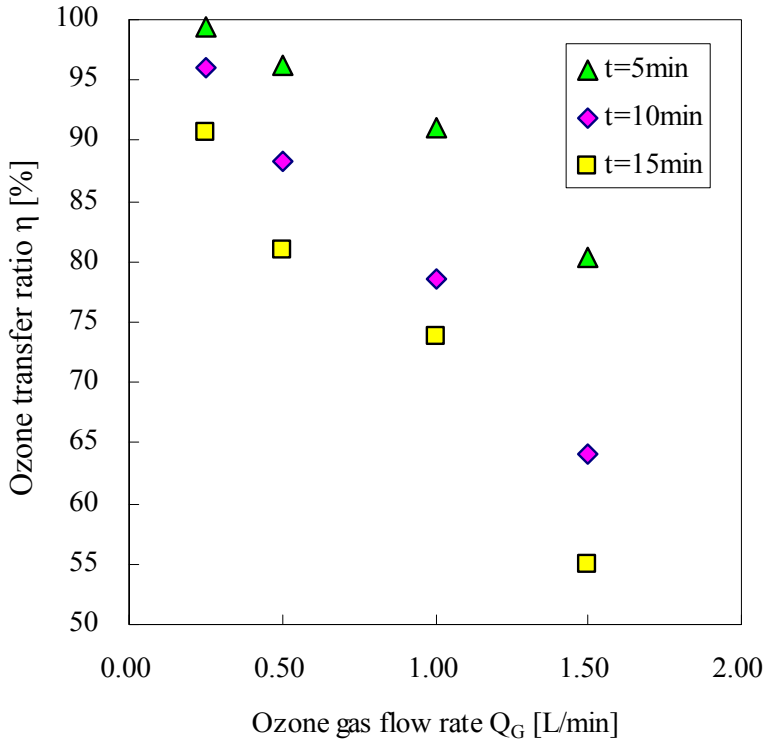

(b)

Fig. 5-7 Effect of gas flow rate on ozone transfer ratio

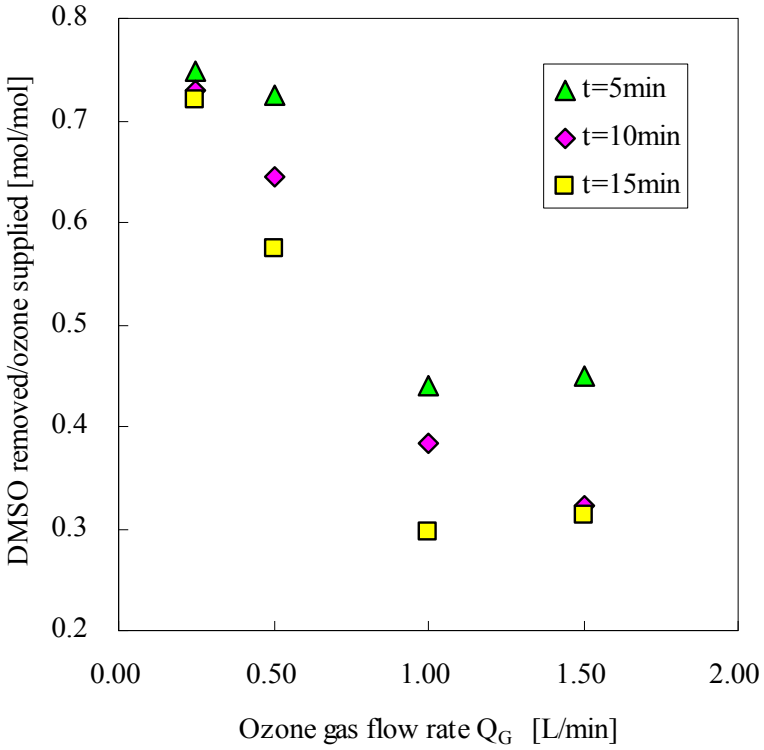

(a)

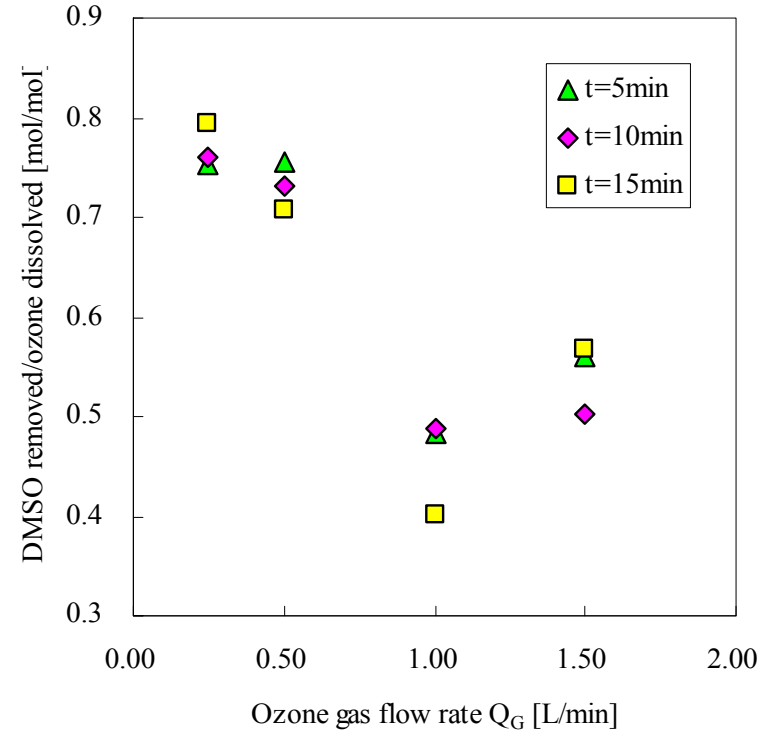

(b)

Fig. 5-8 Effect of gas flow rate on the DMSO oxidation by ozone

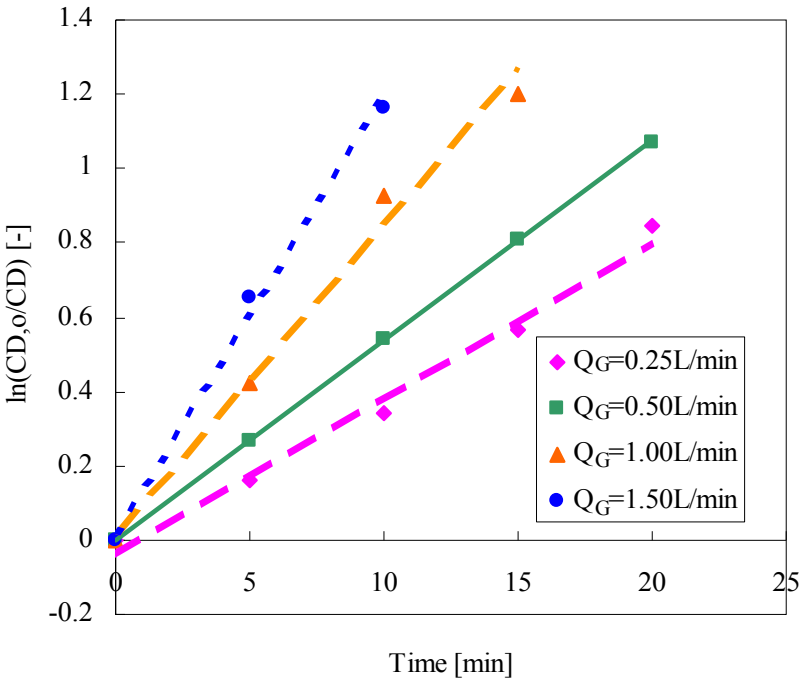

Fig. 5-9 Relationship between $\ln(C_{D,0}/C_D)$ and time in Eq.(5-3)

Table 5-1. Effect of gas flow rate on the reaction constant of DMSO Ozonation

Gas flow rate Q_G	Reaction constant k_D		R^2
L/min	min^{-1}	s^{-1}	-
0.25	0.0418	6.97×10^{-4}	0.987
0.50	0.0750	1.25×10^{-3}	0.973
1.00	0.0822	1.37×10^{-3}	0.989
1.50	0.1163	1.94×10^{-3}	0.995

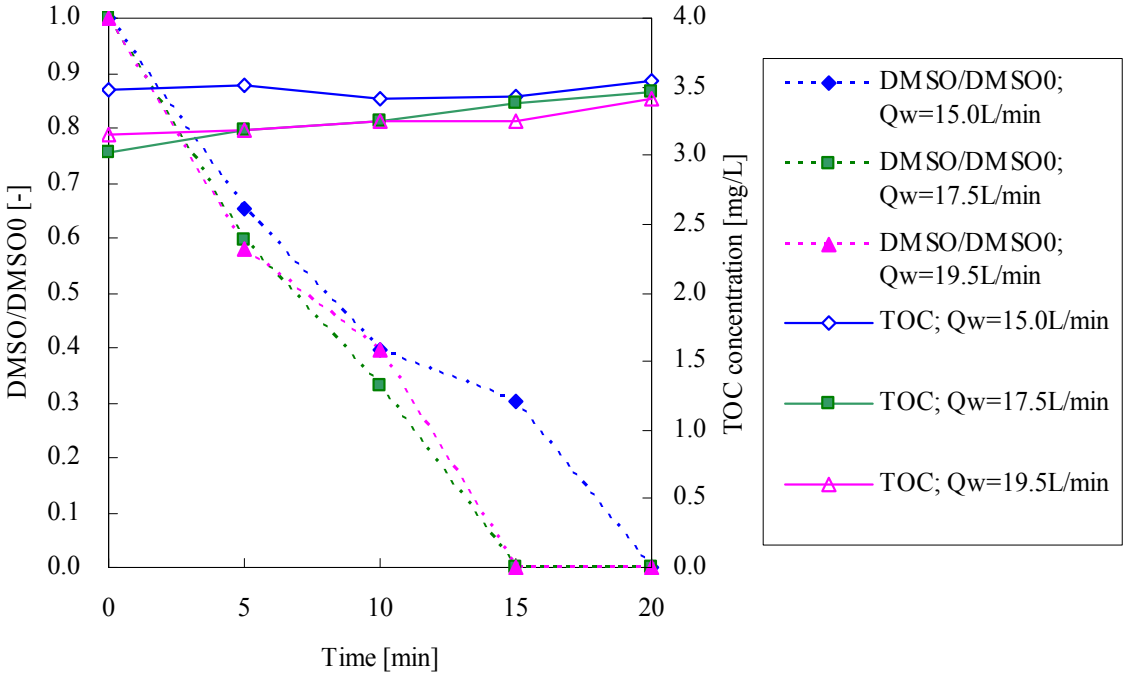

(a)

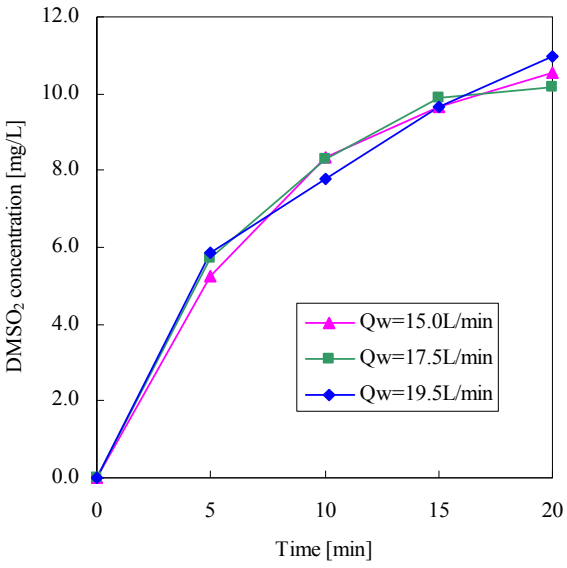

(b)

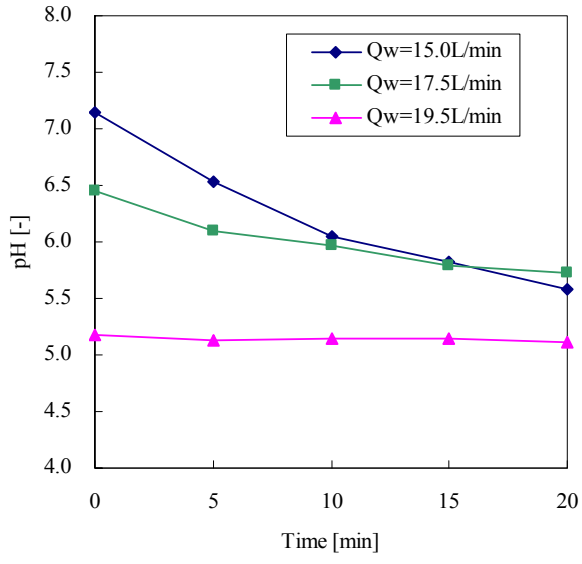

(c)

Fig. 5-10 Effect of water flow rate on DMSO oxidation

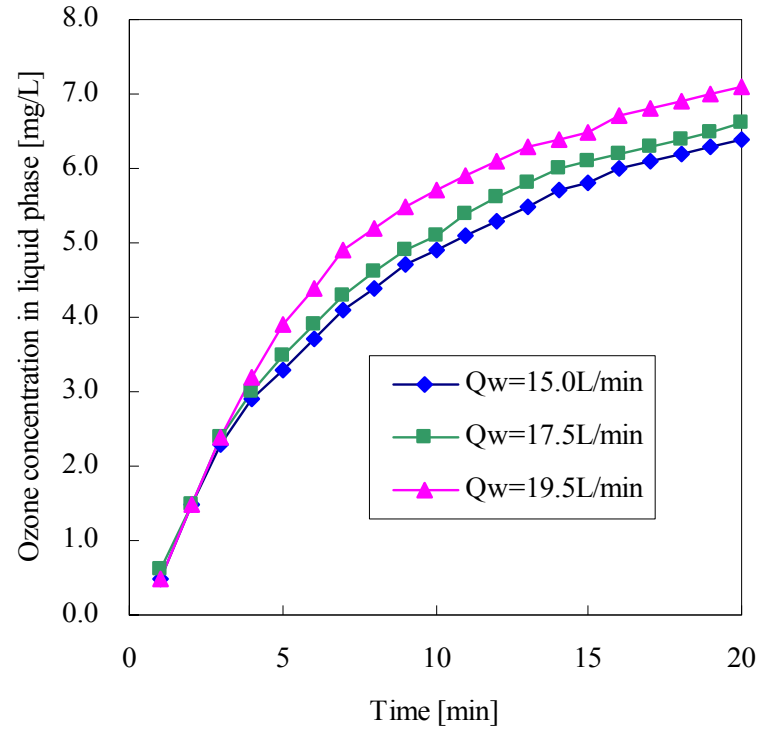

(a)

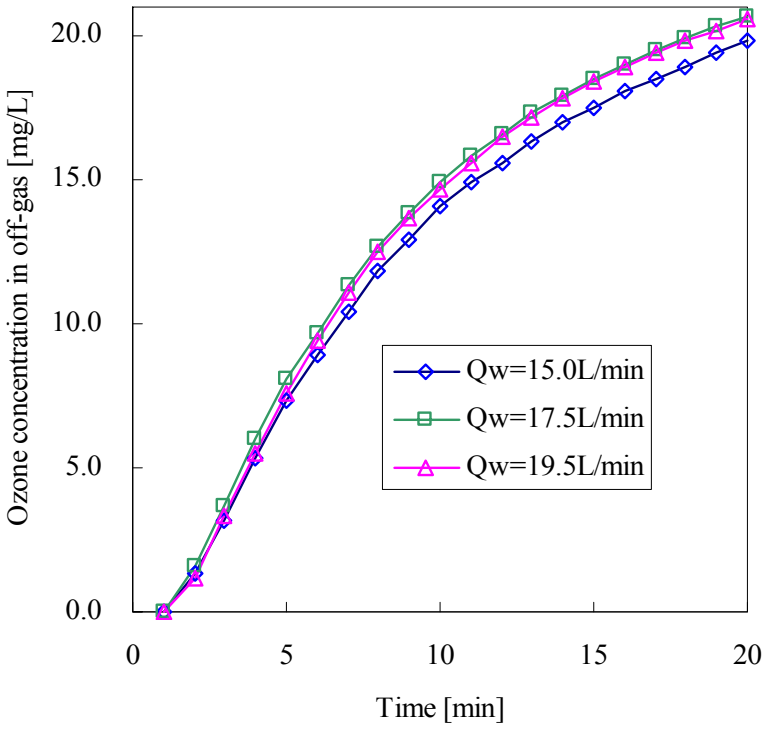

(b)

Fig. 5-11 Effect of water flow rate on ozone concentrations in water and off-gas

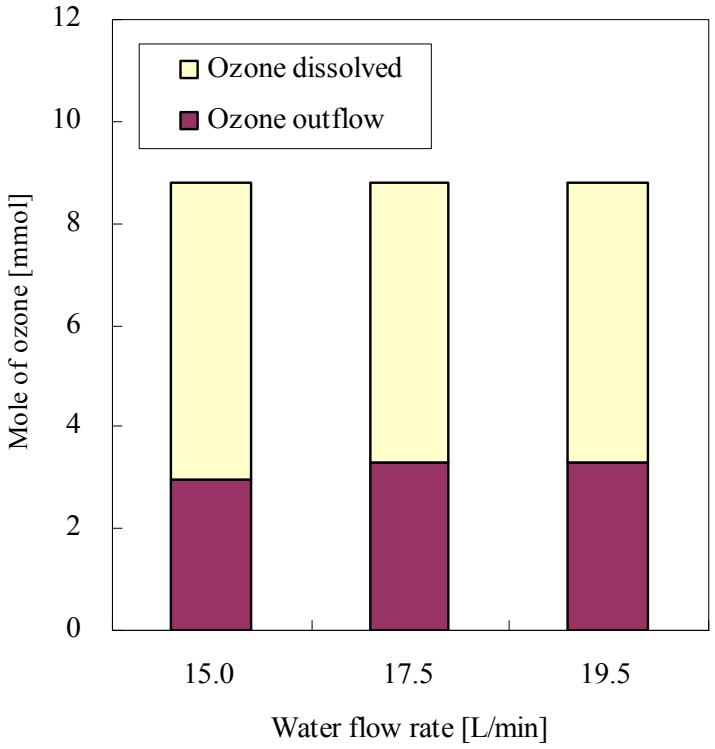

(a)

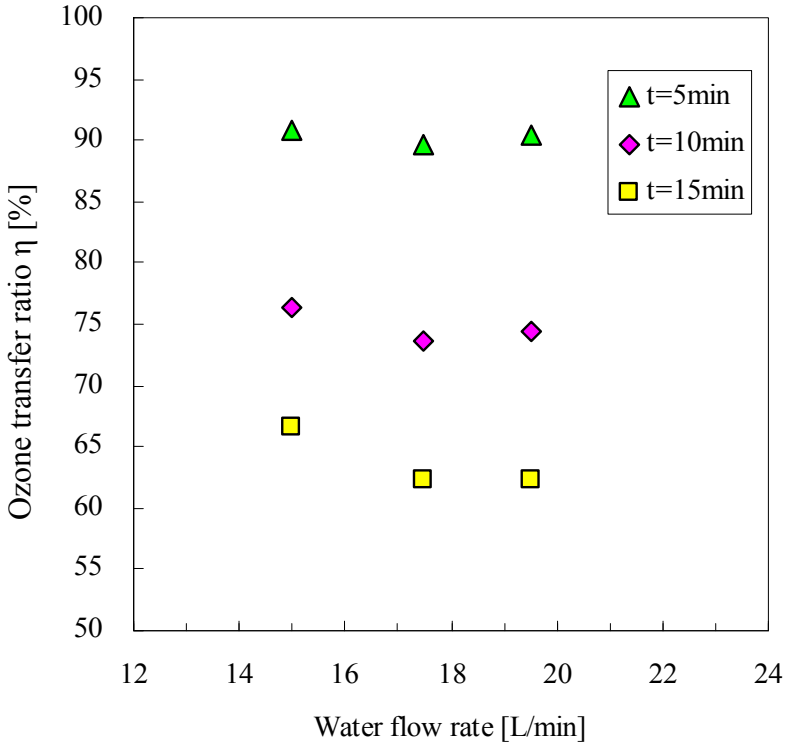

(b)

Fig. 5-12 Effect of water flow rate on ozone transfer ratio

CHAPTER 6

Summary

6.1 Microbubble generation

In this study, a newly-developed microbubble generator was applied and developed in CHAPTER 2. The author proposed combining the cavitation pump with the rotating-flow microbubble generator and changing the gas suction point to the pump's influx line. Observation for microbubble generation conditions and measurements for size distribution and gas holdup measurement showed that the combination of the cavitation pump with the microbubble generator greatly increased the microbubble generation efficiency (larger capacity, smaller size, higher gas holdup). In most cases of their applications, microbubbles are expected to have smaller sizes and a large quantity. Therefore, the improvement of microbubble generation efficiency afforded a high potential possibility to microbubble technology when applied to water and wastewater treatment.

6.2 Development of air Flotation using microbubbles

Along with its high efficiency for particle separation, air flotation has been widely used in water and wastewater treatment as an alternative of sedimentation, especially when particles have too low density or too small size to settle down. In the type of dissolved air flotation (DAF), microbubbles have enough quantity and suitable size in most cases. However, its high electrical power requirement and complex system diminished its advantages to a degree. On the other hand, the type of induced air flotation (IAF) is much simpler and more cost-efficient as compared to DAF. But it is often found that bubbles in IAF are too large and not enough to catch all the particles in water to be treated. It is necessary to search for a simple and energy-saving method which can successfully generate numerous microbubbles, and meanwhile will avoid high shear rates to obviate

the destruction of the aggregates. We made some efforts to approach this objective via improving the microbubble generation efficiency of the rotating-flow microbubble generator and strengthening the floc particles.

In CHAPTER 3, we firstly proposed a **separated flotation system** in which the high-shear region in the liquid where microbubbles are produced is separated from the relatively quiescent zone where flotation takes place. The results from batch flotation experiments showed that the separated flotation system achieved particle removal efficiency as high as 80-90% when treating water with kaolin particles at the concentration of 10 mg/L.

However, the operation in the separated system is relatively complicated, and therefore the author made an attempt to develop a much simpler system, **one-cell flotation system** where microbubbles were directly generated in the flotation tank. Much effort was made both to search for an appropriate polymeric flocculant and to increase the microbubble concentration. At last, particle removal efficiency of over 90% was achieved via applying polyaluminum chloride as the flocculant and the improved microbubble generation system proposed in CHAPTER 2. Results of batch experiments of the one-cell flotation also indicated that both coagulant dosage and flocculation time are vitally important. A slight overdose achieved better removal efficiency. No or less flocculation time performed very well. Water and air flow rates and recycle ratio were controlled to study the effects of bubble size and bubble concentration which have a major impact on the bubble-floc collisions. Lower water flow rate achieved better removal efficiency due to the increase of bubble concentration and decrease of bubble size. Air flow rate showed little effect on the removal efficiency under the present experimental conditions.

6.3 Development of ozonation using microbubbles

Microbubbles are expected to improve the ozone mass transfer from the gas phase to the liquid phase due to its slow rise velocity, high specific surface area and inner pressure. In CHAPTER 4, the author evaluated the mass transfer efficiency of microbubbles in a semi-batch ozone reactor. Firstly, the overall mass transfer coefficient of oxygen, $k_{L,O_2}a$,

was measured to compare the improved microbubble generation system with the normal one. Experimental results indicated that the improved one had better mass transfer ability because of its higher efficiency in microbubble generation. And then, the overall mass transfer coefficients of ozone, $k_{L,O_3}a$, were measured when the induced gas flow rate, liquid flow rate, ozone gas concentration and working liquid level were varied. The increases of $k_{L,O_3}a$ were investigated when the induced gas flow rate and liquid flow rate were increased. However, $k_{L,O_3}a$ decreased with the increase of working liquid levels. High ozone transfer ratio was also achieved at low gas flow rate, which indicates that the gas-induced ozone contactor is a desirable device for the dissolution of high concentration ozone gas.

The ozonation of dimethyl sulfoxide in aqueous solution using microbubbles was examined in CHAPTER 5. Experimental results indicate that the ozonation of DMSO is a first-order mass-transfer controlled reaction. Ozone utilization ratio increases with a decrease in gas flow rate. The ratio of DMSO removed to ozone dissolved can be raised to as high as 0.8 or higher with proper gas and water flow rates. It was also proved that no free radicals were yield by air microbubbles in the microbubble generation system in this study.

6.4 Remarks on applications of microbubbles on advanced water treatment

A rotating-flow microbubble generator (RFMG) was evaluated regarding microbubble size and number concentration in CHAPTER 2, which provides very valuable data for its application design. Moreover, the author developed a microbubble generation system with the RFMG in this study, and it showed much better performance in microbubble generation.

An induced air floatation system with microbubbles was developed in CHAPTER 3. It has been proved that IAF using our improved microbubble generation system had the ability to alternative the traditional dissolved air flotation.

Microbubble technology was applied in the ozonation process in CHAPTER 4. The ozone reactor using the improved microbubble generation system also showed excellent capacity for gas mass transfer. The evaluation of ozone mass transfer under various conditions provides basics of ozone system design which were utilized in CHAPTER 5 for the design of a DMSO wastewater treatment process with ozone.

Publication list

Original papers (English)

1. Pan Li and Hideki Tsuge; **"**Water Treatment by Induced Air Flotation Using Microbubbles," *J. Chemical Engineering of Japan*, **39**, 896-903 (2006)

2. Pan Li and Hideki Tsuge; "Ozone transfer in a new gas-induced contactor with microbubbles," *J. Chemical Engineering of Japan* (In press)

Summary paper (Japanese)

1. 柘植秀樹，李攀；"マイクロバブルを利用した水質浄化技術,"*ECO Industry*, **11**, 53-57 (2006)

International conference

1. Hideki Tsuge, Pan Li, and Hirofumi Ohnari; "Application of Induced Air Flotation on Water Treatment," The 10th Asian Pacific Confederation of Chemical Engineering, Kitakyushu, Japan, 1P-06-030, October, 2004 (Poster)

2. Pan Li, Hideki Tsuge, and Hirofumi Ohnari; "Application of A New Kind of Micro-Bubble Generator on Water Treatment," The 9th Asian Conference on Fluidized-Bed and Three-Phase Reactors, Wanli, Taiwan, pp.355-360, November, 2004 (Oral presentation)

Domestic conference

1. Pan Li and Hideki Tsuge; "Water Treatment by Induced Air Flotation Using

Microbubbles," Japanese Society for Multiphase Flow Annual Meeting, Tokyo, Japan, pp. 343-344, August, 2005 (Oral presentation)

2. Pan Li and Hideki Tsuge; "Development of an ozone oxidation reactor using microbubbles," Society of Chemical Engineers Japan 71st Annual Meeting, Tokyo, D316, March, 2006 (Oral presentation)

3. 李攀*, 島村有紀, 島谷直孝, 柘植秀樹, 中田英夫, 大平美智男; "マイクロバブルによる殺菌効果の基礎研究," 日本混相流学会年会, pp. 282-283, 2006.8 (Oral presentation)

Acknowledgments

This dissertation and the related study were completed under the devoted guidance and supervision of Prof. Tsuge of Keio University in Japan. First of all, I would like to express my cordial gratitude to Prof. Tsuge for providing me the opportunity to conduct this research work, his valuable advice, helpful instruction, and warm encouragement.

My highest appreciations are due to the remaining members of the examination committee, Prof. Shikazono, Prof. Ueda and Prof. Hishida who have given peer reviews and valuable comments.

I really appreciate all the kind help and valuable advice from Associate Prof. Terasaka.

I gratefully acknowledge all the members in both Tsuge and Terasaka labs for their warm and kind help in my research work and daily life in Japan. I will never forget the happy time I spend with them.

This study is supported in part by Grant in Aid for the 21st century center of excellence for “System Design: Paradigm Shift from Intelligence to Life” from Ministry of Education, Culture, Sport, and Technology in Japan.

I also take this opportunity to extend my sincere gratitude to The Watanuki Scholarship Foundation for the very valuable financial support regarding my living here in Japan, my study and research in Keio University.

I also thank Prof. Ohnari for his kind offer of rotating-flow microbubble generators.

I acknowledge Organo Corporation for the financial support and providing me the ozone reactor apparatus. I really appreciate Mr. Yano and Mr. Meguro’s help in the analysis of DMSO and the direction of experiments.

Support from Ebara Corporation was overly generous. I would like to express my thanks to Mr. Ohira and Mr. Nakata for their kind help and valuable advice.

I will also thanks Mrs. Miura in Physic Japan Corporation for her financial support and apparatus providing.

Thank to Mr. Kato in Ota City Industrial Promotion Organization for providing us the

opportunity to get contact with Physic Japan Corporation, and for all the kind help in the experiments.

I would also like to thank Tokyo Nichigo Gakuin for offering me opportunities to learn Japanese language and culture.

I would like to give my special thanks to Mrs. Fujioka and her family. Without their kind help, I would not have been able to overcome the difficulties and continue my study in Japan.

I am grateful to my husband J. Wang for many years of full support and continuous encouragement.

Finally, I would like to delicate this dissertation to my parents, sister and brother for their love and support.